SAINT-PETERSBURG STATE UNIVERSITY

Elets Denis Igorevich

ACTIVATION MECHANISMS AND KINETICS OF HYDROGEN DESORPTION FROM MAGNESIUM HYDRIDE

Scientific speciality 1.3.8. Condensed Matter Physics

DISSERTATION

for a degree

candidate of physico-mathematical sciences

Translation from Russian

Supervisor:

Doctor of Physical and Mathematical Sciences,

professor Gabis I.E.

Saint-Petersburg

2024

Table of contents

Introduction

Research relevance

Finding solutions to the problems of storing and transporting hydrogen is an important part of the research into its use as an energy carrier. Unfortunately, there is no hydride that perfectly matches all the properties required for practical applications. These properties include:

1) High mass and volume concentrations of hydrogen;

2) Low cost of starting metals;

3) Technological simplicity of hydride synthesis and storage;

4) Low temperature of hydrogen sorption-desorption;

5) Sufficiently high rate of hydrogen extraction from hydrides;

6) Low toxicity and explosion hazard;

7) Possibility of large-scale application.

One of the most promising materials for solid state hydrogen storage is magnesium hydride. It is an ionic covalent hydride that can contain up to 7.6% by weight of hydrogen [1]. MgH_2 complies with the first three requirements. Its disadvantages are a high decomposition temperature (400 – 450 ºC), which is highly related to the method of MgH_2 production, and a low rate of hydrogen release [2].

To overcome these disadvantages, various methods are used to activate hydrogen desorption from MgH_2 during its thermal decomposition:

1) Thermal - preheating in an inert medium to lower the decomposition temperature (used in [3] for aluminium hydride).

2) Chemical - consists in adding to the metal hydride a substance-catalyst for the thermal release of hydrogen [4–6].

3) Mechanical - consists of applying mechanical stress to magnesium hydride or magnesium to activitate it (ball milling, cold rolling and forging) [7–10].

4) Mechanochemical - combination of the two previous methods [11].

In addition to practical results, it seems important to understand the physical mechanisms of the processes that lead to the activation of hydrogen desorption from metal hydrides. This may open the way to a meaningful search for the best results.

In this work, the mechanisms and changes in the kinetics of hydrogen evolution were studied using the following activation methods:

- Chemical activation by mixing with different catalysts.
- Mechanical activation by uniaxial pressing in air and vacuum.
- Mechanochemical activation by uniaxial pressing with addition of nickel catalyst.

Ball milling has not been considered in this work as it is a very complex process, the details of which are difficult to control. In addition, the reaction products obtained by ball milling are often prone to spontaneous combustion in air [12].

During the study of mechanochemical activation, we found that the synthesis of the hydride intermetallide Mg_2NiH_4 occurs in the temperature range of 400 - 475 °C and at hydrogen pressures exceeding the decomposition pressure of MgH_2. Previously, a similar synthesis had been observed, but under more difficult conditions. For example, in [13] the synthesis was carried out using a hydrostatic press at a pressure of 2 GPa and a temperature of 750 °C, which significantly exceeds our conditions in terms of both temperature and pressure.

Mg_2NiH_4 is of independent interest for potential applications in solid state hydrogen storage [14]. Its hydrogen content reaches 3.6 mass % [15]. Compared to MgH_2, Mg_2NiH_4 has a higher hydrogen sorption/desorption rate and a lower

temperature (223 °C) at equilibrium of the hydride with hydrogen at atmospheric pressure.

This was the motivation for a detailed study of the mechanisms and kinetics of the synthesis of the hydride intermetallide Mg_2NiH_4. The synthesis was studied in a planar configuration, where a layer of Mg_2NiH_4 grows on a nickel plate immersed in magnesium hydride in a hydrogen atmosphere. Here, the Mg_2NiH_4 film on the nickel feeder is synthesised in a single process cycle. This configuration may also be of practical interest for the likely use of this hydride as an electrode in lithium-ion batteries. The prospects for the use of metal hydrides as electrodes are indicated by recent studies. [16–21].

Goals and tasts

The aim of this work was to establish the physical mechanisms and construct models of:

- magnesium hydride decomposition with different activation methods.
- intermetallide hydride Mg_2NiH_4 synthesis.

In order to achieve the objective, the following tasks were carried out:

- Identify the mechanisms of magnesium hydride decomposition during uniaxial pressing and the influence of catalytic additives.
- Construction of an activation model for hydrogen desorption from MgH_2 by uniaxial pressing with a nickel catalyst.
- Construction of a formation model for Mg_2NiH_4 films on nickel substrate at moderate temperature and pressure.
- Determination of film synthesis kinetics.

Scientific novelty

In the works for the first time:

1. A mechanical method for activating the thermal decomposition of magnesium hydride - uniaxial pressing - has been developed. This method can be easily scaled up for the production of solid state hydrogen storage devices. It is shown experimentally that a higher pressing force results in a lower magnesium hydride decomposition temperature.
2. By experiments on pressing magnesium hydride in a vacuum have shown that hydrogen desorption occurs when a load is applied
3. The following causes of activation of thermal decomposition of magnesium hydride during pressing have been analysed and substantiated:

- formation of metallic magnesium, which serves as a channel for rapid dehydrogenation due to hydrogen desorption;
- due to cracking of hydride particles and opening of the surface of non-hydrogenated metal cores;
- the occurrence of structural defects that may facilitate the formation of metallic nuclei.

4. A model is proposed to describe the processes occurring during uniaxial pressing of magnesium hydride with and without nickel. The agreement of the kinetic parameters obtained for pressed and unpressed magnesium hydride is demonstrated.
5. The synthesis of a hydride film of Mg_2NiH_4 intermetallide on a nickel substrate in a hydrogen atmosphere has been carried out. A model has been developed which takes into account the thin sublayer of $MgNi_2$ intermetallide during film formation at the $MgNi_2$-Mg_2NiH_4 interface with a constant growth rate.

Practical significance

The established physical mechanisms of activation of the thermal decomposition of magnesium hydride by the addition of catalyst powders, with and without pressing, may be of interest in the large-scale synthesis of hydrogen storage materials.

The estimates of the kinetic parameters of the thermal decomposition of magnesium hydride obtained in this work may find application in the design of industrial hydrogen storage devices.

The procedure for the synthesis of the hydride intermetallide Mg_2NiH_4 and the possibility of obtaining a thin film material based on it may be of interest both for the design of hydrogen storage devices and for the production of a negative electrode consisting of a nickel feeder with deposited Mg_2NiH_4 as an active substance for the production of lithium-ion batteries.

Work approval

The main results of the work have been presented and discussed at the following conferences in Russia and at international conferences:

- The 10th A. A. Kurdyumov International School of Young Scientists and Specialists: Interaction of Hydrogen Isotopes with Structural Materials (IHISM´15 JUNIOR).
- The 11th A. A. Kurdyumov International School of Young Scientists and Specialists: Interaction of Hydrogen Isotopes with Structural Materials (IHISM´16 JUNIOR).
- The 7th Hydrogen Technology Convention together with Czech Hydrogen Days 2017 9-12 July 2017 Prague Czech Republic.

- The 13th A. A. Kurdyumov International School of Young Scientists and Specialists: Interaction of Hydrogen Isotopes with Structural Materials (IHISM´19 JUNIOR).
- Russian Conference on Natural Sciences and Humanities with International Participation "SPbSU Science - 2022", 21 November 2022.

Structure of the work

The thesis consists of an introduction, 4 chapters, a conclusion and a bibliography of 101 titles. The content of the thesis is presented in 99 pages, including 40 figures.

The introduction justifies the relevance of the topic of the thesis, the choice of the object of research and the main scientific results to be defended. The structure and content of the thesis chapters are considered. A list of the author's publications on the subject matter of the thesis is given.

The first chapter is a review and is devoted to the consideration of general issues related to sorption-desorption processes for metal hydrides, as well as relevant experimental data on the properties of magnesium hydride. A comparison with other hydrides of the ionic-covalent group is made. Methods for the preparation of magnesium hydride, its main structural and thermodynamic properties are briefly described. Analyses of studies devoted to the kinetics of magnesium hydride decomposition and methods of activating thermal desorption are carried out. Methods of synthesis and basic properties of hydrides of Mg-Ni intermetallides are considered.

The second chapter describes the magnesium hydride samples and the setup and conditions for the synthesis of MgH_2 used in this work. The technique and methodology of isothermal and linear heating experiments are described. The results of scanning electron microscopy studies of the synthesised magnesium hydride are

presented. Additional techniques used to characterise the magnesium hydride samples are described.

The third chapter is devoted to the results of studies on the chemical activation of magnesium hydride. The results of thermodesorption of mixtures of magnesium hydride with: magnesium, aluminium, nickel and activated carbon are presented. The results of studies of activation methods: mechanical and mechanochemical, including a new mechanical method of activation of thermal decomposition of magnesium hydride - uniaxial pressing in air, are described. The activation mechanisms associated with uniaxial pressing are discussed in detail, namely

1) Particle cracking and opening of the metallic core.

2) Increase in the defectiveness of the crystal lattice (hydrogen vacancies).

3) Release of some of the hydrogen, resulting in the appearance of metallic nuclei.

The results of experiments on uniaxial pressing in vacuum are described. It is shown that the amount of hydrogen released during pressing depends almost linearly on the pressure applied. Uniaxial pressing in air in the presence of nickel is compared with other mechanical and mechanochemical activation methods. The dependence of the decomposition of magnesium hydride activated by uniaxial pressing with nickel on the nickel concentration is presented. A model of hydrogen thermodesorption from the pressed mixture of magnesium hydride and nickel is constructed. It is shown that the decomposition temperature of magnesium hydride decreases with increasing nickel concentration in the mixture.

The fourth chapter is devoted to the synthesis of the intermetallide hydride Mg_2NiH_4 and the description of the mechanisms of formation of such a film on a nickel substrate. The films obtained were characterised by different methods: scanning electron microscopy with elemental analysis, X-ray diffraction and thermodesorption spectroscopy. A model considering a thin sublayer of $MgNi_2$

intermetallide and describing the mechanism of film formation at the $MgNi_2$-Mg_2NiH_4 interface with a constant growth rate has been constructed.

The conclusion summarises the main results of the thesis and the conclusions drawn by the author.

Financial and organisational support for the work

The work was supported by the RFBR grant № 16-08-01244. The research was supported by the SPbSU Resource Centres: MRC "Nanotechnologies", RC "X-ray diffraction methods of research" and RC "Thermogravimetric and calorimetric methods of research".

The most important scientific results

The main scientific results have been published in 10 printed works, including 5 articles in peer-reviewed journals and 5 abstracts.

In the work: Elets D., Chernov I., Voyt A, Shikin I., Dobrotvorskii M., Gabis I. Influence of uniaxial pressing and nickel catalytic additive on activation of thermal decomposition of magnesium hydride // Int. J. Hydrogen Energy. Elsevier Ltd, 2017. Vol. 42, № 39. P. 24877-24884, doi: 10.1016/j.ijhydene.2017.08.076, the following results are presented:

1. Activation of the thermal decomposition of magnesium hydride by the addition of catalyst powders with and without pressing. Hydrogen desorption starts through the metal channel of the foreign metal particles with subsequent expansion of the desorption channel.
2. A plausible mechanism of hydrogen thermodesorption from magnesium hydride pressed with nickel powder is proposed and confirmed by a valid mathematical model. The approximation results obtained are in good agreement with the experimental data.
3. During the uniaxial pressing of magnesium hydride, the following

processes take place which lead to the activation of thermodesorption:

1) The splitting of magnesium hydride particles reveals the metallic nucleus remaining from the direct synthesis;
2) Formation of a large number of defects in the crystal structure, which can be centres of accelerated formation of metallic phase nuclei;
3) At the moment of force application and release, some hydrogen is released, resulting in the appearance of metallic magnesium nuclei. At a force of 2400 kg/cm^2 the amount of hydrogen released is 1.4-10^{-3} wt.%. A separate article is devoted to this subparagraph: *Voyt A. P., Elets D. I., Denisov E. A., Gabis I. E. Hydrogen Release from Magnesium Hydride Subjected to Uniaxial Pressing // Mater. Sci. 2019. Vol. 54, № 6. P. 810–818., doi: 10.1007/s11003-019-00268-1.*

4. An efficient mechanical method of uniaxial pressing to activate the desorption of magnesium hydride has been developed and tested. The method is quite simple to use and comparable in efficiency to other known mechanical methods (ball mill grinding, cold forging and rolling), with the decomposition temperature reduced to 280 °C. The method and the results of its validation are presented in the paper: *Shikin I. V., Elets D. I., Voyt A. P., Gabis I. E. Activation of magnesium hydride by pressing with catalytic additives // Tech. Phys. Lett. 2017. Vol. 43, № 2. P. 190–193, doi: 10.1134/S1063785017020262.*

5. Разработана методика синтеза пленки Mg_2NiH_4 на поверхности никелевой пластины, окруженной гидридом магния в атмосфере водорода при давлении, превышающем давление разложения Mg_2NiH_4, которая представлена в статье: *Baraban A. P., Chernov I. A., Dmitriev V. A., Elets D. I., Gabis I. E., Kuznetsov V. G., Voyt A. P. The Mg_2NiH_4 film on nickel substrate: synthesis, properties and kinetics of formation // Thin Solid Films. Elsevier B.V., 2022. Vol. 762, № October. P. 139556., doi: 10.1016/j.tsf.2022.139556.* The synthesis technique described allowed the preparation of crystalline films with thicknesses ranging from 0.2 to 4 μm by increasing the synthesis time from 2 to 32 h. The film thickness growth rate was determined to be 0.13 μm/h.
6. The mechanism of film formation at the $MgNi_2$-Mg_2NiH_4 interface is

described. The limiting factor is the diffusion of nickel through a thin sublayer of $MgNi_2$ intermetallide. This mechanism is discussed in detail in the paper: *Baraban A.P., Voyt A. P., Gabis I. E., Elets D. I., Levin A. A., Zaytsev D. A. Synthesis of a Thin Metal Hydride Mg_2NiH_4 Film on a Nickel Substrate // Crystallography Reports, 2024, Vol. 69, No. 1, pp. 93–101., doi: 10.1134/S1063774523601259.*

In all five scientific publications referred to in the description of the main scientific results, the personal contribution of the co-researcher includes the preparation and execution of the experiments, the processing and discussion of the results obtained, the drafting of parts of the texts, and the preparation of figures and tables.

Defence related provisions

1. The physical mechanism of activation of the thermal decomposition of magnesium hydride by the addition of catalyst powders and/or pressing is the appearance of foreign metal or magnesium particles in contact with the hydride and the consequent formation of a rapid channel for the onset of hydrogen desorption.

2. The activation mechanism of the thermal decomposition of magnesium hydride by uniaxial pressing without catalyst is determined by:

1) the experimentally demonstrated release of hydrogen resulting in the appearance of metallic magnesium nuclei;

2) the splitting of magnesium hydride particles and the probable detection of metallic nuclei remaining from direct synthesis;

3) the formation of a large number of defects in the crystal structure, which could potentially be centres of accelerated formation of metallic phase nuclei.

3. The constant rate of formation of the Mg_2NiH_4 film on the Ni substrate is due to the flow of nickel atoms through the $MgNi_2$ sub-layer, which has a constant thickness, to the $MgNi_2$-Mg_2NiH_4 interface.

The flux density of nickel atoms through the $MgNi_2$ layer in the reaction of Ni and MgH_2 in the presence of a hydrogen atmosphere at 450 °C is $5 \cdot 10^{13}$ $1/(s \cdot cm_2)$ and determines the synthesis rate of Mg_2NiH_4 of 0.13 μm/h.

Chapter 1

Literature review

1.1 General information about metal hydrides

Metal hydrides are a class of chemical compounds with a crystal structure composed of metal and hydrogen atoms. These substances do not occur in nature and their study began with the discovery of the effect of hydrogen absorption by palladium with the formation of hydrides [22]. Later, the same behaviour was found in other metals and alloys, which became known as hydride formation. In general, almost any metal is capable of hydride formation at high temperatures and hydrogen pressures of several thousand atmospheres [23].

During the formation of stoichiometric hydride, hydrogen is adsorbed on the surface and penetrates further into the crystal lattice, where it dissolves intensively - and its atoms accumulate in the interstices and defects of the metal crystal lattice. When the dissolved hydrogen reaches a critical concentration, the system undergoes a phase transition involving a local change in the nature of the crystal lattice and the incorporation of hydrogen atoms into it. As a result, small regions of a new chemical compound, the metal hydride, are formed. Further absorption of hydrogen from the gas phase leads to an increase in the size of these regions until the hydride occupies the entire volume of the original sample. This process is usually accompanied by an increase in the volume of the material and, as a consequence, cracking of its particles due to the significant difference in density between the metal and the hydride formed on its basis. In detail, the processes of formation and decomposition of hydrides, as well as various models and experimental methods for determining the thermodynamic and kinetic parameters of hydrides using these models are discussed in the paper [24].

1.2 Metal hydrides properties

Many metals and alloys are capable of reversibly absorbing hydrogen by direct reaction of the metal with hydrogen gas or by electrochemical regeneration. The conditions under which a metal can accumulate hydrogen are determined by the PCT diagram shown in Figure 1.1(a). At a given hydrogen pressure, the metal initially dissolves some hydrogen as a solid solution (α-phase), and as the hydrogen concentration and pressure increase, a metal hydride phase (β-phase) nucleates and grows. When the two phases coexist, a plateau is observed whose concentration range determines the reversible hydrogen capacity of the metal.

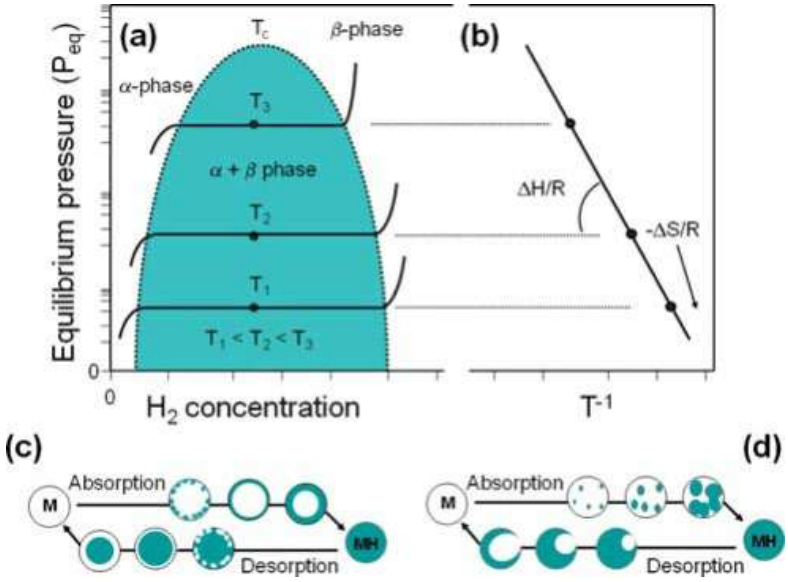

Figure 1.1 – (a) PCT diagram of the metal-hydrogen system; (b) Vant-Goff diagram; (c) Schematic process of hydrogen absorption/desorption in magnesium at high temperature and pressure and (d) at low pressure; M - metal, MH - metal hydride [25].

The equilibrium pressure is described by the Van 't Hoff equation (1.1) [26]:

$$ln\frac{P_{\text{равн}}}{P_0} = \frac{1}{R}\left(\frac{\Delta H^0}{T} - \Delta S^0\right) \quad (1.1).$$

At high temperatures and pressures, hydrogen is rapidly absorbed by the entire surface, forming a hydride surface layer that prevents hydrogen diffusion into the metal volume (M→MH in Fig. 1.1(c)). The diffusion coefficient of hydrogen in non-metals is much lower than that in metals. For example, in silicon the diffusion

coefficient of hydrogen is 3-6 orders of magnitude smaller than in metals [27]. The same applies to metallic and non-metallic metal hydrides.

A similar situation is observed for the rate of associative desorption of hydrogen from metals and non-metals. Figure 1.1(d) (MH→M) shows that desorption proceeds only from the metal surface, which occupies a small fraction of the surface area. This nature of the adsorption/desorption and hydrogen diffusion processes for nonmetals and metals is explained by the presence of free electrons in the latter [28,29].

The Van 't Hoff plot is shown in Figure 1.1(b), where the slope of the plot is related to the enthalpy of the reaction and the point of intersection with the ordinate is the entropy of the reaction [25]. Since the entropy corresponding to the transition of gaseous hydrogen molecules to chemisorbed hydrogen in the metal is similar for most metal-hydrogen systems (130 kJ/(mol·K)) [25], The thermodynamic properties of metal-hydrogen systems are usually characterised by the strength of the metal-hydrogen bond and hence by the enthalpy of the hydrogenation (dehydrogenation) reaction. For practical use of hydrogen storage materials in vehicles, the metal-hydrogen bond strength should correspond to an enthalpy of about 30 kJ/mol [30].

1.3 Magnesium hydride structure

The crystal structure of magnesium hydride (shown in Figure 1.2) has been determined and extensively studied using X-ray and neutron analysis techniques [31]. Magnesium forms stoichiometric MgH_2, which crystallises in two polymorphic forms. The stable form under ambient conditions is α-MgH_2, which has a tetragonal structure of the rutile TiO_2 type with the following unit cell parameters: a = 0.45168 nm, c = 0.30205 nm, corresponding to an X-ray density ρ = 1.419 g/cm^3. [32].

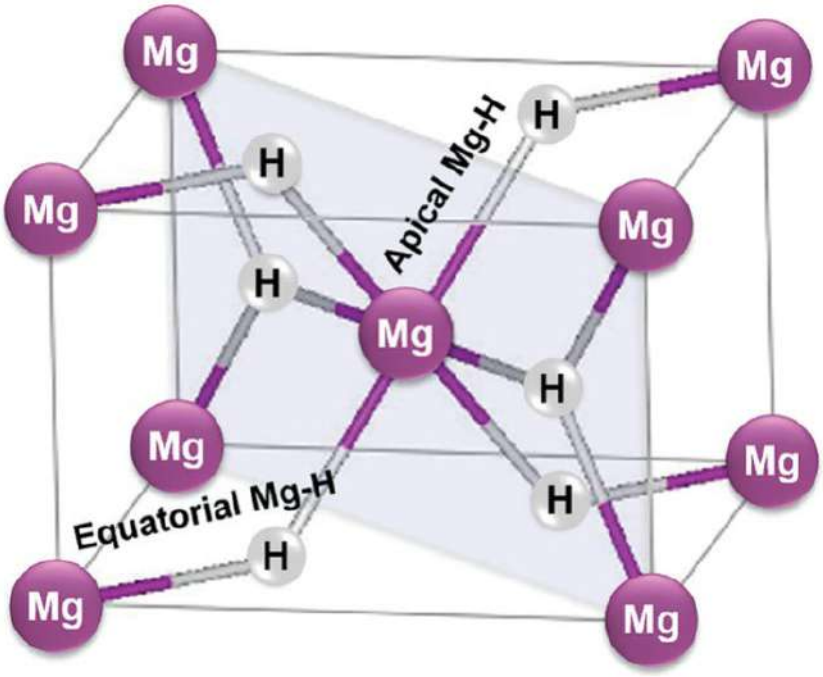

Figure 1.2 – Crystal structure of magnesium hydride, rutile type [33].

The two magnesium atoms and four hydrogen atoms in the unit cell are at positions (0, 0, 0), (1/2, 1/2, 1/2) and ±(x, x, 0), ±(x+1/2, 1/2-x, 1/2) respectively (x = 0.306) [34]. In this structure, each magnesium atom is surrounded by six hydrogen atoms, which in turn contain three magnesium atoms in their coordination sphere. The interatomic distances are respectively Mg-H - 0.195 nm, H-H - 0.249 nm and 0.276 nm, Mg-Mg - 0.353 nm. The increase of the distance Mg-Mg in the hydride compared to magnesium, where it is equal to 0.32 nm, characterises a significant expansion of the metal lattice upon the introduction of hydrogen and, consequently, a relative decrease of the density of the hydride (ρ_{Mg} = 1.738 g/cm^3).

1.4 Synthesis and properties of MgH_2

Magnesium hydride was first discovered in 1912 as a pyrolysis product of ethyl magnesium iodide [35]. Until 1951, all studies of this compound were related to the decomposition products of organomagnesium compounds. Only in [36] was the direct synthesis of magnesium hydride from elements reported for the first time:

$$Mg + H_2 \rightarrow MgH_2 \qquad (1.2)$$

Even with the use of catalysts (MgI_2), high pressure and temperature (20 MPa, 567 ºC), the authors were only able to achieve a yield of 69% of the product. Further research in this area is aimed at finding optimal catalysts to ensure the completeness of the reaction (1.2) [37, 38].

In the following work [39, 40], significant success was achieved in the catalytic-free synthesis of MgH_2. A temperature of at least 350-400 °C is required for hydrogen absorption and desorption, but even in this case the process takes several hours to complete. The equilibrium pressure of hydrogen for magnesium hydride is rather low, about 0.1 MPa at 280 °C. The formation of magnesium hydride should take place at room temperature, but the process is kinetically limited. [41].

As previously shown in [42, 43], the appearance of metallic magnesium nuclei facilitates hydrogen release due to the fact that the rate of associative desorption of hydrogen from the surface of the metal (Mg) radically exceeds that from the surface of MgH_2, which has dielectric properties.

Direct metal hydrogenation is a heterophase reaction in which hydrogen combines with a metal to form a hydride [44]. The direct hydrogenation reaction of magnesium is no exception and consists of several stages: transport of the hydrogen molecule (H_2) to the magnesium surface, chemisorption of hydrogen molecules, dissociation of the H_2 molecule into atoms (H), surface-to-volume migration, diffusion of the dissolved hydrogen in the solid phase, formation and growth of the hydride phase [45].

There are several factors that significantly reduce the rate of hydrogenation. One of these is the formation of oxide and hydroxide on the surface of the magnesium, which are readily formed when magnesium comes into contact with air. The MgO film formed in the air during hydrogenation prevents hydrogen from penetrating into the material [41]. To start the absorption process, the oxide layer on the surface of the magnesium particles must somehow be overcome. To destroy this layer, the surface must be activated. For example, annealing causes the oxide film to

break down and the clean metal surface becomes accessible to hydrogen. Another reason for the low hydrogenation rate is the slow dissociation of hydrogen molecules on the magnesium surface. The activation barrier of the surface can be reduced by adding catalysts such as palladium or nickel [46].

According to [47], the rate of formation of magnesium hydride nuclei is directly proportional to pressure. This dependence is maintained up to 3 MPa (400 ºC) and with further increase in pressure the rate of absorption decreases. This effect is observed when the initial hydrogenation is relatively rapid. Subsequently, the process of hydride formation at the surface blocks further hydrogen absorption. Further studies have shown that the growth of the hydride phase is controlled by the slow rate of the hydride-magnesium interface, and in particular by hydrogen diffusion through the hydride layer to the hydride-metal interface. In any case, it is almost impossible to completely hydrogenate magnesium, even at very high pressures and temperatures, because the rate of hydrogen uptake decreases as the hydride nuclei on the magnesium surface combine to form a continuous hydride layer.

According to [41] (Figure 1.3), hydrogenation of magnesium powder does not start immediately and the hydrogenation curve should have an incubation period. In addition, at low temperatures (300 ºC) there is absolutely no hydrogen uptake, and at higher temperatures (up to 350 ºC) the onset of hydrogenation is observed only after 0.5 hours. The speed at the beginning is not maximum, but increases for some time and then gradually slows down. At a temperature of 400 ºC for 1 hour of hydrogenation process of synthesis of magnesium hydride (MgH_2) passes on 25-30%. Thus, it can be concluded that the rate of hydrogenation depends largely on the size of the magnesium particles, since the authors of this work managed to obtain magnesium hydride powder with particles of different sizes.

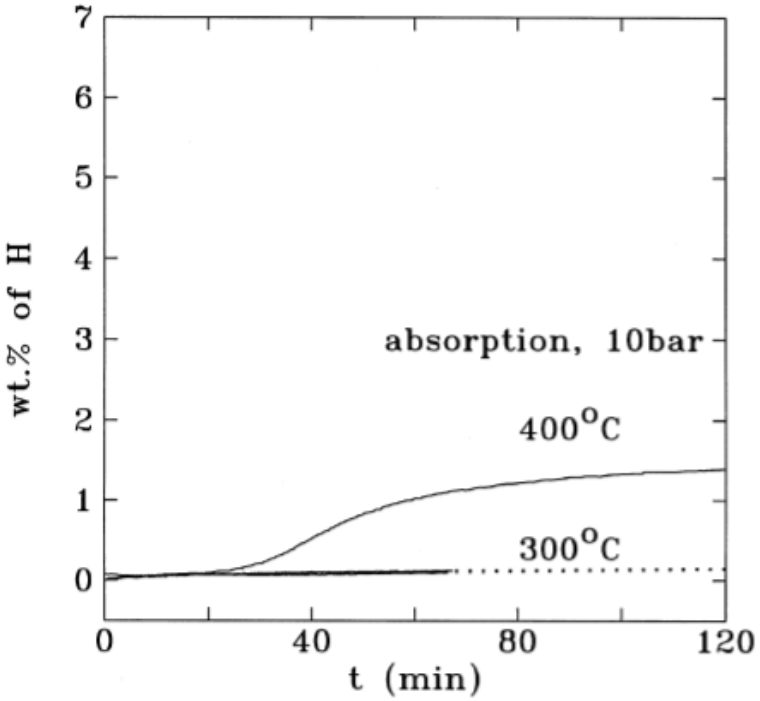

Figure 1.3 – Hydrogen uptake by magnesium powder [41]

Figure 1.4 shows the absorption rate of magnesium powders of different dispersities after heating in a vacuum to a temperature of 300 °C.

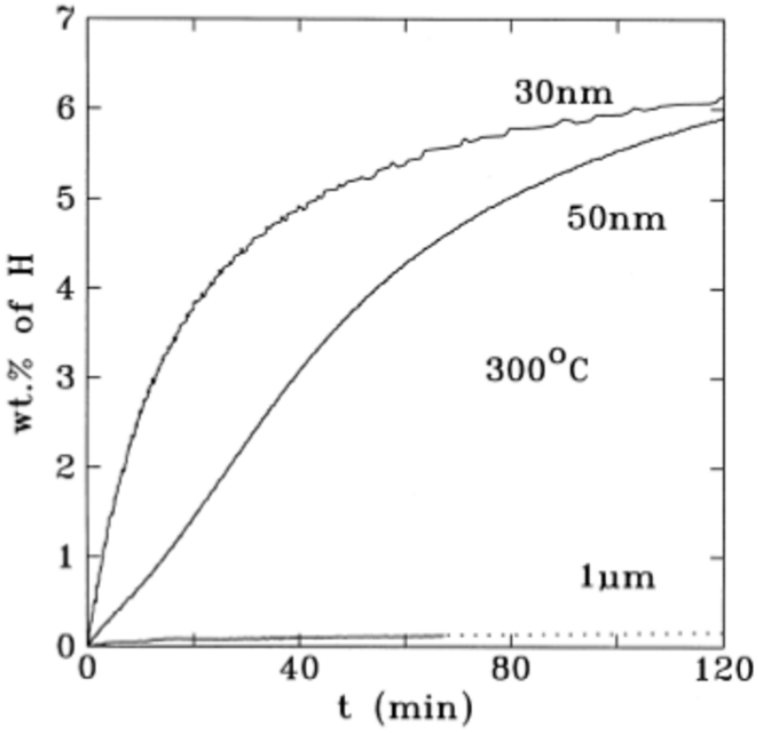

Figure 1.4 – Effect of particle size on hydrogen absorption of magnesium powder subjected to mechanochemical treatments of different durations [41]

Figure 1.4 shows that magnesium powder with a particle size of about 1 μm absorbs practically no hydrogen at 300 °C. Samples with a dispersity of about 30 nm showed the highest hydrogenation rate. A similar behaviour was observed for desorption. The increase in hydrogenation rate caused by grinding is a consequence of the occurrence of a high concentration of defects in the resulting nanocrystalline microstructure.

1.5 Hydrides decomposition

Metal hydride decomposition is usually understood as the transformation of a hydrogen-rich phase into a poorer phase [48]. Hydride decomposition can be described by several models.

According to [49], when the hydride decomposition rate is high, the hydrogen concentration in the metal at the hydride/metal interface is in equilibrium. Then the first order condition $c_m = \overline{c}_m(T)$ applies at the points at the interface, where the equilibrium concentration $\overline{c}_m$ depends only on temperature.

If the decomposition rate is limited, the concentration near the interface may be below the equilibrium concentration because the diffusion outflow is not compensated by decomposition. It is clear that the decomposition rate of the hydride depends on the hydrogen concentration near the interface, in particular at the equilibrium concentration the hydride does not decompose. It follows from the law of conservation of matter that the hydrogen flux densities for hydride decomposition and diffusion near the interface are the same. It is physically reasonable to assume a linear dependence between flux density and concentration, taking into account that there is no flux at $c_m = \overline{c}_m$; we obtain a linear boundary condition of the third kind at the interface:

$$D_m \frac{\partial c_m}{\partial r} = -k_m \cdot (1 - \frac{c_m}{\overline{c}_m}) \qquad (1.3)$$

The constant k_m has the meaning of the limiting flux density of hydride decay: it is reached at zero concentration. Note that for $k_m \to \infty$ ((fast decay) and for limited fluxes we get the first kind of condition. The law of conservation of the amount of matter at a moving (free) interface leads to a condition on the velocity of this

interface. Hydrogen atoms are diffusely removed from the site δS for time dt , released from the hydride in the process of its decay. Thus we obtain:

$$D_m \frac{\partial c_m}{\partial r} \delta S dt = (c_h - c_m)\delta V \quad (1.4)$$

where c_h is the hydrogen concentration in the hydride phase, c_m – is the hydrogen concentration in the metal phase, δV is the volume of hydride decomposed. For small volumes, the equality δV = δSδn, n – is approximately satisfied, where n is the normal displacement of the interphase boundary. Finally, we obtain the Stefan-type condition:

$$(c_h - c_m)\frac{dn}{dt} = D_m \frac{\partial c_m}{\partial r} \quad (1.5)$$

Generalizing formulae (1.4) and (1.5), it follows that $c_m = 0$: $\frac{dn}{dt} \to -\frac{k_m}{c_h}$.

This shows the relationship between k_m and the interfacial limit velocity. This is the velocity that occurs at the limit of the hydride decomposition reaction, i.e. when the released hydrogen is rapidly removed from the interface.

The symmetry assumptions allow us to simplify the model considerably. If the particle has the shape of a sphere of radius L, and the hydride phase occupies a concentric sphere of smaller radius ρ, then the metal phase occupies a layer of thickness L-ρ. n this case the direction of the normal coincides with the radius, in which case formula (1.5) will take the form:

$$(c_h - c_m)\frac{d\rho}{dt} = D_m \frac{\partial c_m}{\partial r} \quad (1.6)$$

Thus, the considered reactions of hydrogen transfer provide a basis for the construction of mathematical models of hydrogen extraction from metal hydrides during their decomposition.

Comparing the same reactions with respect to metals and non-metallic solids, it is clear that adsorption-desorption processes and diffusion proceed at a much higher rate in metals than in ionic-covalent materials. In the case of ionic-covalent hydrides, nucleation of the metallic phase can only occur after desorption of the first portions of hydrogen. In the case of non-metals, however, desorption takes place at low rates,

so that they are characterised by the appearance of a small number of nucleations. The nuclei of the metallic phase are a channel of faster desorption, so in the process of decomposition there is an increase in their volume. It is then possible for the nuclei to coalesce and form a continuous crust of metallic phase. Figure 1.5 shows optical photographs of magnesium hydride after partial hydrogen evolution (white areas are metallic magnesium). The initial magnesium powder, which consists of almost spherical particles, was specially prepared by arc melting [50]. However, the formation of metallic phase crusts during the decomposition of ionic covalent hydrides does not always occur.

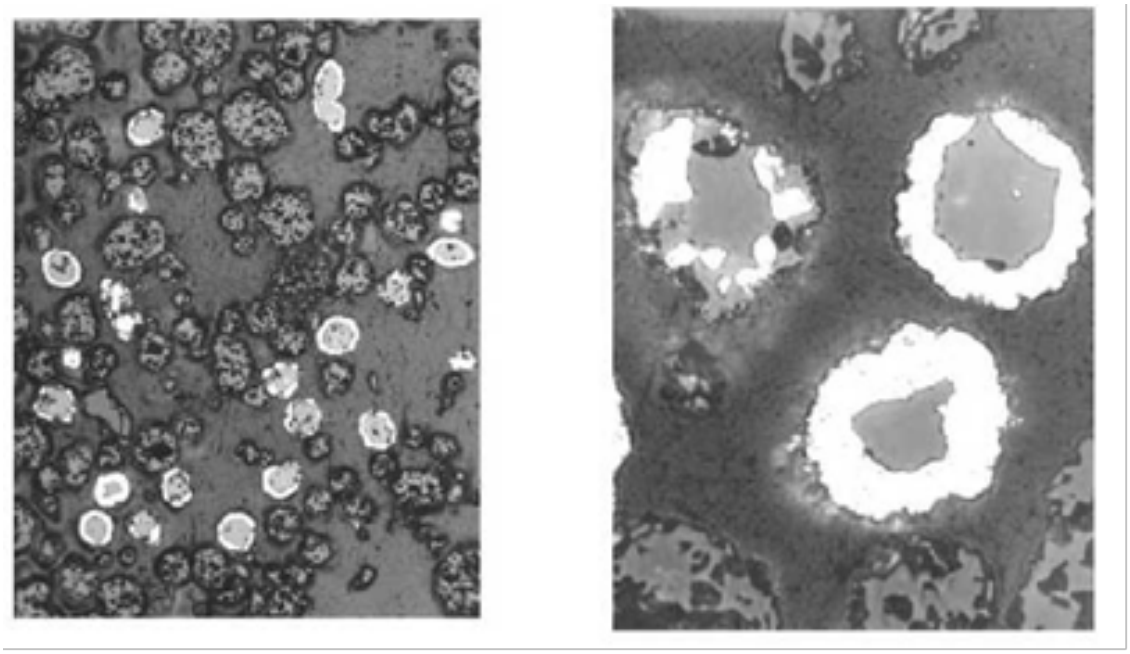

Figure 1.5 – Optical images of magnesium hydride obtained by arc melting after partial hydrogen evolution [50]

Figure 1.6 shows an optical image of magnesium hydride obtained by direct hydrogenation of magnesium chips after partial decomposition [43]. One can see the development of several metallic embryos that will not be able to coalesce into a continuous crust.

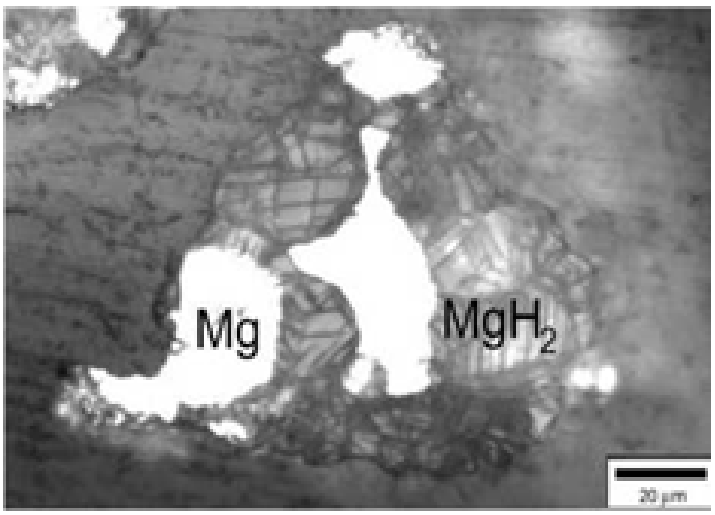

Figure 1.6 – Metallography of magnesium hydride after partial hydrogen evolution [43]

Hydrogen desorption from metal hydrides occurs at a high rate from the entire surface of each particle. This favours the formation of a crust of new phase, with the old phase forming the so-called 'shrinking core' [51]. Thus, differences in the morphology of new phase formation during metal hydride decomposition lead to different mathematical models: the 'shrinking core' model and the 'nucleation' model, which may later form a continuous crust of new phase. These models are described in some detail in [49]. The 'nucleation' model describes the decomposition of ionic covalent limiting hydrides, to which MgH_2 belongs.

In general, the following factors can influence the degradation (dehydrogenation) kinetics

1) probability of formation of metallic phase nuclei;
2) dissusion;
3) desorption;
4) interface velocity;
5) Particle dispersibility.

1.6 Incubation period

Depending on temperature and environmental parameters, nuclei of a new phase are formed. For many hydrides, the appearance of nucleation is preceded by an 'incubation period' during which hydrogen evolution is virtually absent. Figure 1.7

shows the hydrogen evolution curves at constant temperature for ionic covalent hydrides of magnesium and aluminium [43].

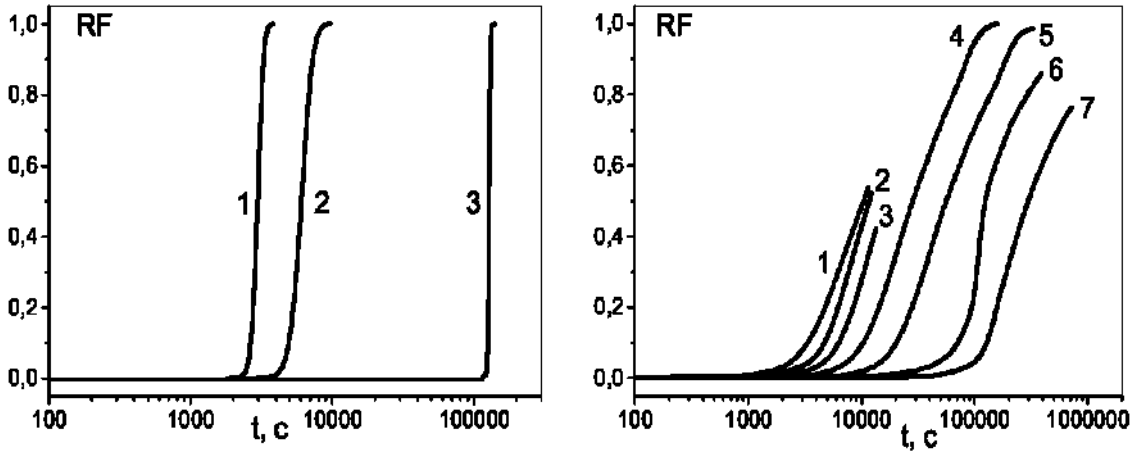

Figure 1.7 – Dehydrogenation at constant temperature MgH_2 (left, temperature: 1 - 400, 2 - 375, 3 - 350 °C), and AlH_3 (right, temperature: 1 - 125, 2 - 120, 3 - 115, 4 - 110, 5 - 100, 6 - 90, 7 – 80 °C)

It can be seen that time elapses from tens of minutes to hours and days before intensive hydrogen release begins. A fairly common view is that the surface of the hydride material is initially covered with a passivating film (e.g. oxide) which prevents hydrogen desorption. Under the influence of elevated temperature, the film is gradually destroyed and desorption begins. The time required for the film to break down is called the incubation time. Such a view is justified if we are talking about active hydrides with a metallic type of bonding. If the bond is ionic-covalent, as in the case of magnesium and aluminium hydrides, the material itself must be extremely passive in terms of hydrogen desorption. The presence of a film, such as an oxide film, cannot be excluded, but salt-like crystals, which include magnesium and aluminium hydrides, are much less prone to oxidation than metals. In addition, hydrogen itself plays the role of an oxidant in these crystals, attracting part of the charge from the aluminium or magnesium [52].

The properties accumulated in this process eventually lead to the onset of the active phase of hydrogen evolution [49]. Since the incubation processes proceed at considerable speed at elevated temperatures (compared to room temperature), we can

speak of thermal activation of hydrogen evolution. The incubation time is obviously dependent on the temperature of the hydride material. This indicates the progress of some latent reactions leading to the appearance of metallic nuclei.

Figure 1.7 shows the delay before the onset of active hydrogen evolution from MgH_2 and AlH_3 hydrides. A relationship can be seen between the forbidden band width of the material and the temperature to which it must be heated for hydrogen desorption to begin within a reasonable time. The forbidden band widths of AlH_3 and MgH_2 are 3.54 and 5.32 eV respectively [53].

The authors of the article [53] state that the density of electronic states near the top of the valence band is mainly represented by hydrogen states. This means that in the hydrides considered, hydrogen plays the role of an oxidant, pulling down part of the charge. As a result, the transfer of electrons from the valence band to the conduction band is mainly possible from hydrogen states.

In [54] the likely processes occurring during incubation were considered for AlH_3 and it was shown that at least one of these processes is the appearance of hydrogen vacancies which are the site of potential nucleation. By using UV light, the authors were able to reduce the incubation time. It is assumed that all the processes occurring during the isothermal decomposition of magnesium hydride are similar in nature and regularity to those occurring during the dehydrogenation of aluminium hydride.

The study of decomposition kinetics, incubation process and activation methods for the decomposition of MgH_2 is important for science and technology. Understanding the processes affecting the incubation time will provide a solution for the application of metal hydrides in the creation of a renewable energy source based on solid state hydrogen storage systems.

1.7 Activation techniques

Various methods of desorption activation are used to reduce the incubation time and increase the kinetics of hydrogen release during the decomposition of metal hydrides. The existing methods are listed in the 'Relevance of the research topic'

section. In this thesis, the following methods have been used for experiments with magnesium hydride: chemical, mechanical and mechanochemical. In the literature these methods are very closely related and are often combined. To illustrate the wide nomenclature of materials used to activate hydrogen desorption from $_{MgH2}$, the following few papers are reviewed.

Transition metals are known to promote hydrogen desorption. In cases where surface reactions are limiting, the rate of H_2 desorption can be improved by the addition of small amounts (typically 1-5 mol%) of such materials. In [55], grinding was carried out for 20 h in a mixture with MgH_2: Ti, V, Mn, Fe and Ni (5 mol%) to study the kinetics. It was found that the desorption time decreased significantly with the most effective addition of V, but the enthalpy and entropy remained unchanged. Non-transition metals Ca and Al and non-metals (including C) were also investigated in this work and were found to have no effect on the kinetics despite the reduction in grain size during the milling process.

In [56], a variety of metals including Pd, Fe, V, Zr, Ti and Mn, as well as combinations of these metals, were used as catalysts. Nanocrystalline magnesium with different grain sizes were obtained by grinding Mg in a ball mill in Ar mode with different additive concentrations for times ranging from 15 min to 20 h. The most effective combinations were V and Zr and a mixture of Mn and Zr.

Magnesium with 10 wt% Co, Ni or Fe was ball milled in hydrogen (and in Ar for Co mixtures) for various times from 0 to 10 h in [57]. It was found that the grain size decreased with increasing grinding time and that grinding in Ar reduced the grain size compared to grinding the same materials in hydrogen.

Much work has been done on the addition of various oxides. For example, in [58] Metal oxides were investigated as additives for the MgH_2 system using 5 mol% Sc_2O_3, TiO_2, V_2O_5, Cr_2O_3, Mn_2O_3, Fe_3O_4, CuO, Al_2O_3 and SiO_2 additives. MgH_2 milling was carried out for 20 h before additives and then for 100 h with additives. Authors' work [58] found that all oxides improved the kinetics, but the most effective

for desorption were V_2O_5 and Fe_3O_4, with all hydrogen desorbed from the samples in 5 minutes at 300 °C. The high efficiency of oxides can be explained by the fact that such additives act as abrasive particles, helping to pulverise MgH_2 during grinding.

Oxides are generally not chemically active, unlike metals such as Ni which, in addition to acting as a catalyst, can also react chemically with Mg and MgH_2 to form intermetallides and intermetallide hydrides.

1.8 Intermetallide hydride Mg_2NiH_4

Figure 1.8 shows the crystal structure of Mg_2NiH_4. Unit cell parameters: a = 1,4389 nm, b = 0,6415 nm, c = 0,6527 nm [59]. The X-ray density is ρ = 2,78 g/cm^3 [60]. At temperatures below 510 K Mg_2NiH_4 has a monoclinic low temperature modification (LT), which is shown in Figure 1.8. In the cubic high temperature phase (HT) Magnesium ions form a cube around the non-valent NiH_4 complexes in the antifluorite arrangement.

Mg_2NiH_4 in the NT monoclinic phase is an indirect bandgap semiconductor. Many theoretical calculations give different values of the bandgap width in the range from 1.36 to 1.65 eV [58–61]. In [61], an analogy between the electronic properties of silicon and Mg_2NiH_4 was shown. This fact can open the prospect of using them as solar cells for power generation.

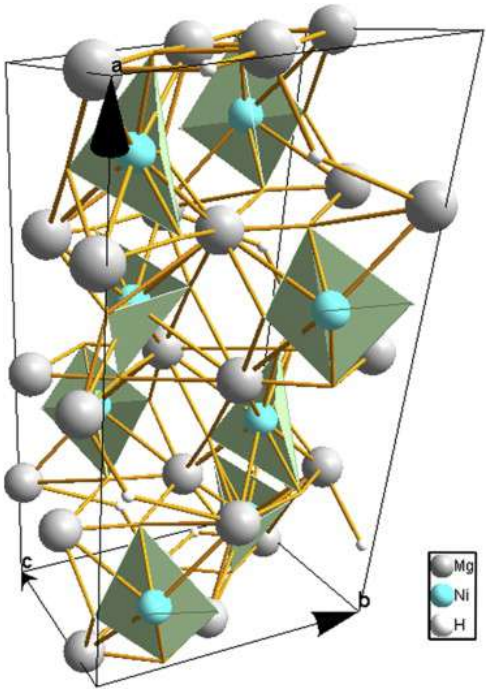

Figure 1.8 – Crystal structure of the intermetallide hydride Mg_2NiH_4 [13]

In the HT-phase, hydrogen atoms make a rapid reorientation around the central nickel atom [60]. In the LT-phase, this motion is 'frozen' and an ordered arrangement of slightly distorted tetrahedral NiH_4-complexes is observed by neutronography [61]. In addition to this, a frequently encountered packing defect or microvoining at the unit cell level is introduced into the crystal lattice [61, 62]. If micro twinning is suppressed, the stability of the hydride is reduced, making it more practical for hydrogen storage [62].

It is rather difficult to make an alloy of magnesium with nickel because, according to the Mg-Ni phase diagram, Mg and Ni are mutually insoluble [63], there are two intermetallic compounds, Mg_2Ni and $MgNi_2$, but only Mg_2Ni (mass capacity 3.62 wt%) reacts with hydrogen under relatively mild conditions in terms of temperature and pressure compared to the $MgNi_2$ [64]. In [65], succeeded in hydrogenating $MgNi_2$ by holding pre-pressed 590 MPa Mg_2Ni powder in hydrogen, which was atomised in a high-frequency plasma discharge. The authors also [65] MgNi2H3 was obtained at 300 °C and hydrogen (deuterium) pressures in the range 2.8 - 7.4 GPa. With the addition of Ni as a MgH_2 catalyst, there has been a significant decrease in the hydrogen desorption temperature [66]. By varying the parameters of

the high-energy ball milling and the composition of the powder mixture of Mg and Ni, solid state amorphisation occurs [67] or mechanochemical solid phase transformation reaction $Mg + Ni \rightarrow Mg_2Ni$ [68, 69].

Chapter 2

Methods of investigation and synthesis of magnesium hydride

2.1 Thermal desorption spectroscopy

The main method of investigation in this work was thermodesorption spectroscopy (TDS) in the barometric mode. In this mode, the analysis of desorption products is not important because the main product of thermal decomposition of metal hydrides is hydrogen. The content of various impurities (oxygen, carbon, water, etc.) is so insignificant that their amount can be neglected. Using TDS, the following dependencies can be obtained:

1) Variation of hydrogen pressure with temperature ΔP(T) during continuous linear heating of a sample at a given rate over the temperature range of interest - *linear heating*;
2) The change in hydrogen pressure from time ΔP(t) when the sample is held at a given temperature until the sample is completely decomposed - *desorption at constant temperature*.

The dependence ΔP(T) allows us to determine the temperature at which hydrogen desorption from the hydride sample begins, and the dependence ΔP(t) - the incubation time at a given holding temperature.

An experimental vacuum apparatus of the Siverts type was used to measure the amount of hydrogen released from the samples. A similar apparatus was used in the study of hydrogen thermodesorption from titanium hydride in [70]. The layout of the unit is shown in Figure 2.1. The unit is an all-metal high vacuum system comprising a pumping system, a hydrogen inlet system and a working chamber containing the sample to be tested.

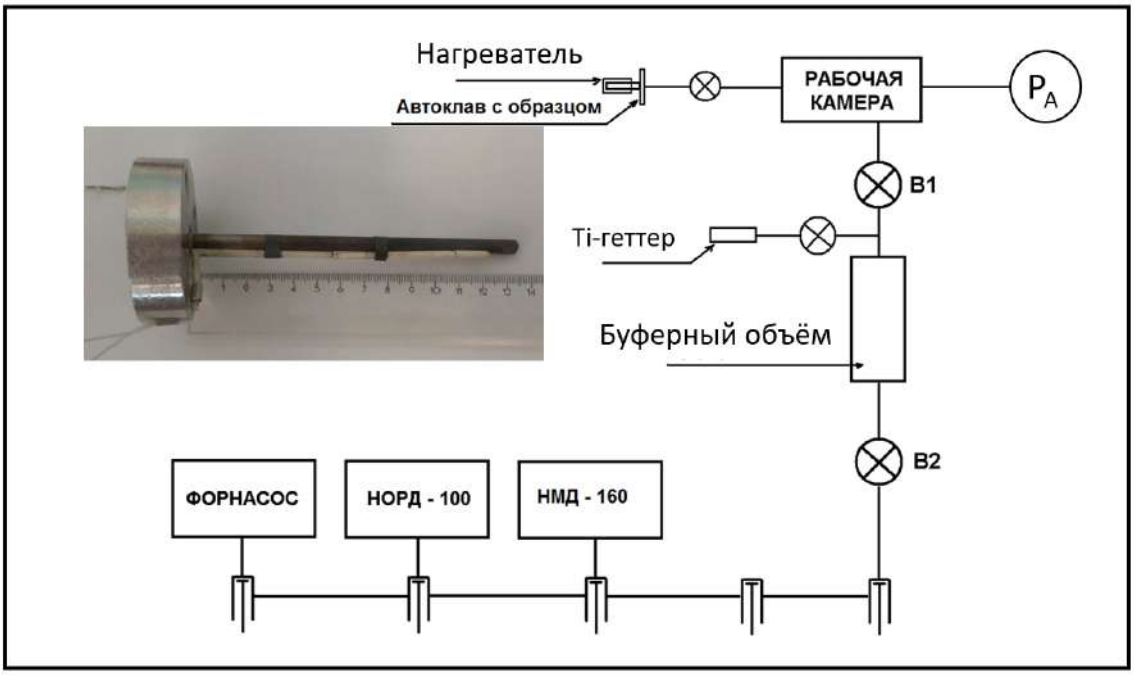

Figure 2.1 – Schematic diagram of the TDS plant

The pumping system consists of:

1. Vacuum pump - allows any chamber of the unit to be evacuated to a pressure of 10 mTorr.
2. Cooled magnetically discharged diode pump NORD-100 provides vacuum necessary for efficient operation of high vacuum pump, i.e. pump of ‘clean’ pumping.
3. The NMD-160 pump performs 'clean' pumping of the entire high vacuum section of the unit.

The entire pumping system provides a vacuum of the order of 10^{-8} Torr in the working part of the unit. The pressure of the hydrogen released during the hydride decomposition was monitored by two membrane pressure sensors from Varian Inc. Vacuum Technologies (Agilent Technologies) (ranges up to 10 and 1000 Torr, accuracy 0.5%), the measurement chamber of 1351 cm^3 was at room temperature, controlled to an accuracy of 0.1 ^oC. The volume of the autoclave containing the sample was of the order of 10 cm^3.

A sample of magnesium hydride (typical 15 mg sample) was placed in the autoclave and vacuumed to a pressure of 10^{-5} Torr. Prior to heating, hydrogen is injected into the autoclave at a pressure of P_0 ~ 50 Torr to improve heat transfer between the sample and the heated walls. The constant temperature TDS experiments were performed by heating at a rate of 0.2 °C/s to a set temperature, which was then held constant until the end of hydrogen release from the sample. The sample was then heated to 450 °C to ensure that all hydrogen had been released from the sample. After complete decomposition of the hydride, the pressure change in volume did not exceed 10 Torr, so the final pressure in the chamber was less than 60 Torr. The pressure change obtained over time allows us to estimate the reacted fraction (RF), which is calculated according to formula 2.1:

$$RF(t) = \frac{P(t)-P_0}{\Delta P} \quad \text{или} \quad RF(T) = \frac{P(T)-P_0}{\Delta P}, \quad (2.1)$$

where P is the actual hydrogen pressure in the measuring volume; ΔP is the difference between the final and initial hydrogen pressure; t is the time from the moment the set temperature is reached; T is the sample temperature. RF = 0 corresponds to magnesium hydride and RF = 1 corresponds to metallic magnesium. This gives the time dependence of RF(t) or the temperature dependence of RF(T). A typical result of an isothermal heating experiment is shown in Figure 2.2 (a).

In the linear heating experiments the sample was heated to 450 °C at different rates in the range 0.05 - 1 °C/s. During the heating time, all hydrogen is released from the sample. A typical result of such an experiment is shown in Figure 2.2 (b).

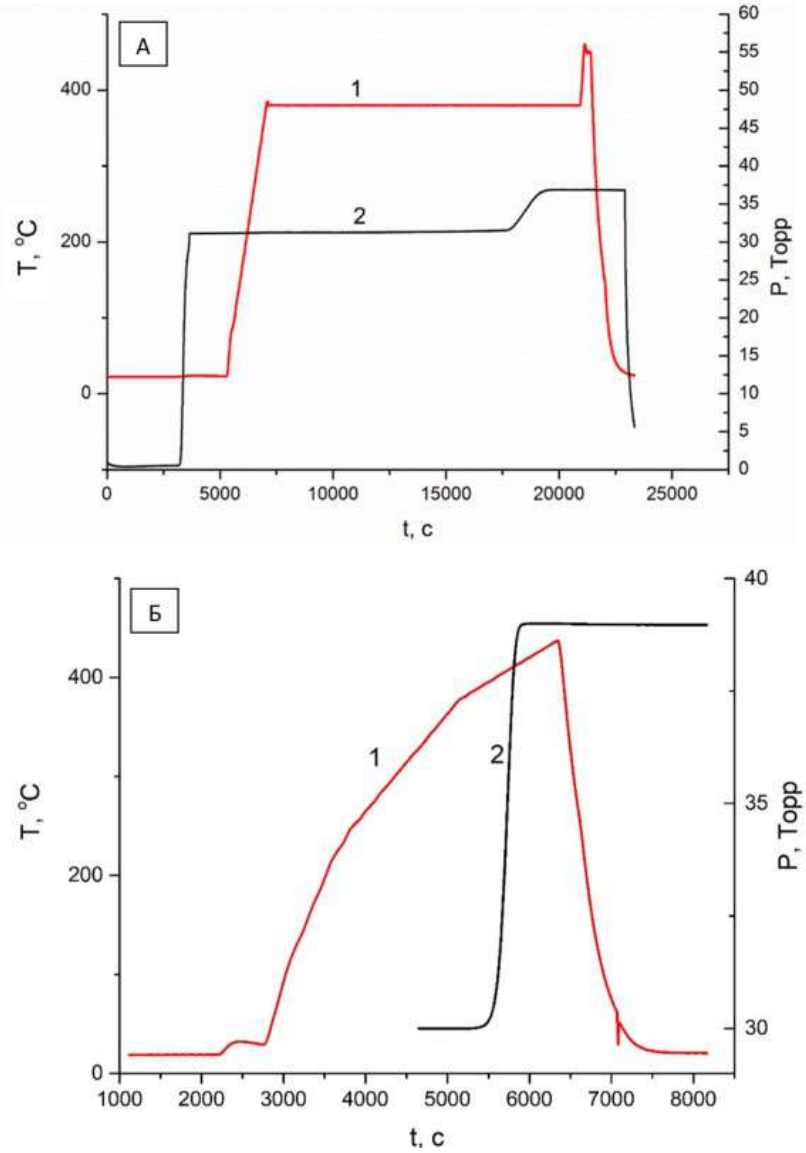

Figure 2.2 – Typical result of the experiment of hydrogen desorption from MgH_2 at constant temperature (A) and linear heating (B): 1 - temperature; 2 - pressure

2.2 Supporting techniques

In addition to TDS as the main method, auxiliary diagnostics were used to characterise the samples. The samples were analysed by X-ray diffraction (XRD), scanning electron microscopy (SEM) and differential scanning calorimetry (DSC). All participating Resource Centres (RCs) are located at the St. Petersburg State University.

Phase composition was analysed in the RC 'X-ray diffraction methods' using a Bruker 'D2 Phaser' powder diffractometer. A standard CuKα X-ray tube was used

as the anode material. Full profile analysis of the diffractograms and calculation of the quantitative ratio of the different phases in the mixture was carried out according to the Rietveld method [71, 72] using dedicated Bruker Topas 4.2 software. The positions of the peaks were compared with the positions of reference reflections from the powder diffraction database [73].

Zeiss AURIGA Laser and Zeiss Supra 40VP electron microscopes from MRC Nanotechnologies were used for SEM. Acceleration voltages ranging from 5 to 30 kV were used during the studies. Different detectors were used for image registration. The secondary electron (SE) detectors used were the In-Lens SE and Everhart-Thornley (SE2). Micrographs of magnesium hydride samples were used to determine the size of the powder particles and to characterise the morphology of the particle surface before and after the effects applied to investigate the mechanisms of hydrogen desorption from magnesium hydride.

DSC measurements were carried out using a Netzsch STA 449 F1 Jupiter synchronous thermal analysis instrument at the RC Thermogravimetric and Calorimetric Research Centre. The DSC results obtained were heat flow curves as a function of temperature. The method allows the determination of phase transition parameters. For example, the enthalpy of reaction is calculated by integrating the peak corresponding to the given transition. [74]. Samples with a typical mass of 2-3 mg were studied; controlled heating in the range of 25 - 350 °C was carried out at a rate of 20 °C/min, followed by a rate of 5 °C/min up to 550 °C. The technique was used to investigate the effect of hydraulic press force on the activation of hydrogen desorption from the MgH_2.

2.3 MgH_2 synthesis

In this work, samples of magnesium hydride obtained by direct hydrogenation of magnesium powder grade MPF-40 with a particle size of 50-100 microns and a purity of 99.92% were used for the experiments. A high pressure bench was used

for the synthesis, the scheme of which is shown in Figure 2.3. The maximum hydrogen content in the synthesised samples is approximately 7.5 wt%.

Pure magnesium powder is charged into the V_A autoclave. The autoclave with the powder is pumped out by a force pump and 'purged' with hydrogen: the gas is pumped to a pressure of 0.5 to 1 MPa and then pumped out to remove the remaining air and adsorbed water. Hydrogen is injected from a cylinder at a pressure of 10 to 12 MPa. Similar conditions were used in the [75]

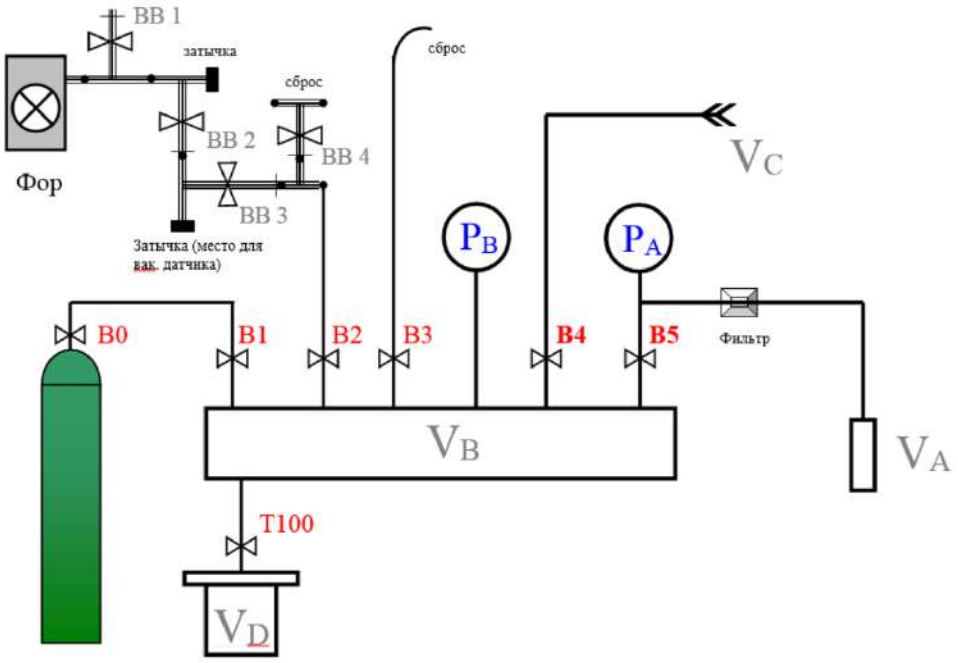

Figure 2.3 – Schematic diagram of a high pressure bench for direct hydrogenation of magnesium powder.

The autoclave is then heated to 450 °C, with a thermal stabilisation of 0.5 °C. The uniformity of the autoclave heating is achieved by the small volume V_A = 1.5 cm^3. Figure 2.4 shows a typical dependence of the pressure in the volume V_A on the time during the synthesis of magnesium hydride. Approximately 250 mg of magnesium hydride is obtained for one synthesis on this unit.

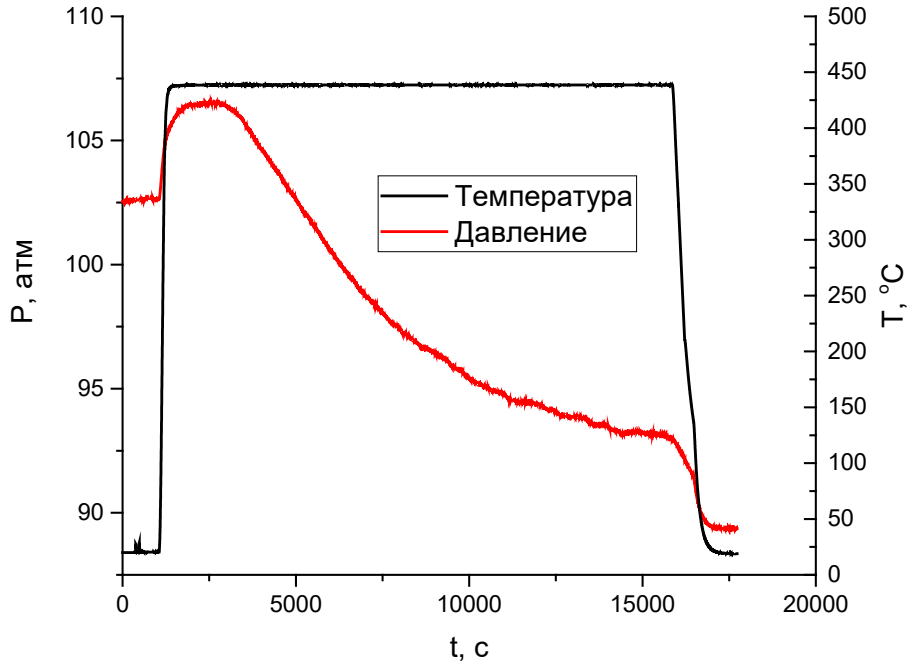

Figure 2.4 – Time dependence of pressure during hydrogenation of magnesium powder

During the hydrogenation process, the pressure measured by the P_A sensor decreases. The powder remains in this state for approximately one day. The synthesis process ends when the pressure reaches a steady state. The certification of the obtained MgH_2 samples was carried out by TDS results on the setup described in section 2.1 (Figure 2.1) and X-ray phase analysis (example in Figure 2.6).

For the MgH_x samples obtained in this plant, $x \approx 1.80$-1.96, corresponding to approximately 7.5 wt% hydrogen content in the hydride. For complete hydrogenation, the dispersity of the magnesium powder is an important parameter. Large particles are not fully hydrogenated because diffusion ceases as the hydride crust grows around the metal core.

After synthesis, the flask of magnesium hydride is opened in a glove box in an inert gas environment, usually nitrogen, and packed in small portions (10-20 mg) into airtight containers. The containers are then placed in a desiccator and stored at room temperature. Small doses of the resulting powder allow one container to be used in

each experiment, i.e. all experiments are performed with powder stored under identical conditions.

2.4 Description of MgH_2 synthesised samples

Magnesium hydride samples are light grey dull powder. Under mechanical stress, MgH_2 is more brittle than metallic magnesium. Figure 2.5 shows a typical micrograph of the synthesised magnesium hydride powder. The particle dispersity ranges from 5 to 100 μm.

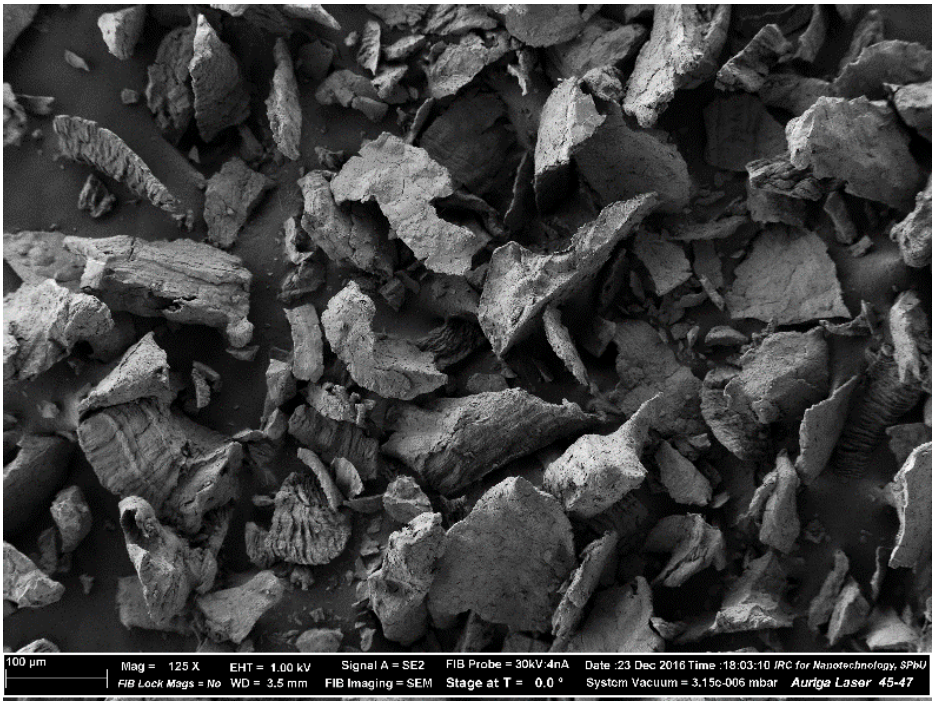

Figure 2.5 – SEM of the synthesised powder MgH_2

Quantitative X-ray phase analysis (Figure 2.6) shows that the powder contains ~90% α-MgH2 main phase and ~5% metallic Mg phase, which is consistent with the results of the metallic magnesium hydrogenation process described in Section 2.3. In addition, ~3.5% - $Mg(OH)_2$ and ~1.5% - MgO are present, which is also acceptable due to the influence of oxygen and water from the atmosphere when moving the samples for the diffractometer study.

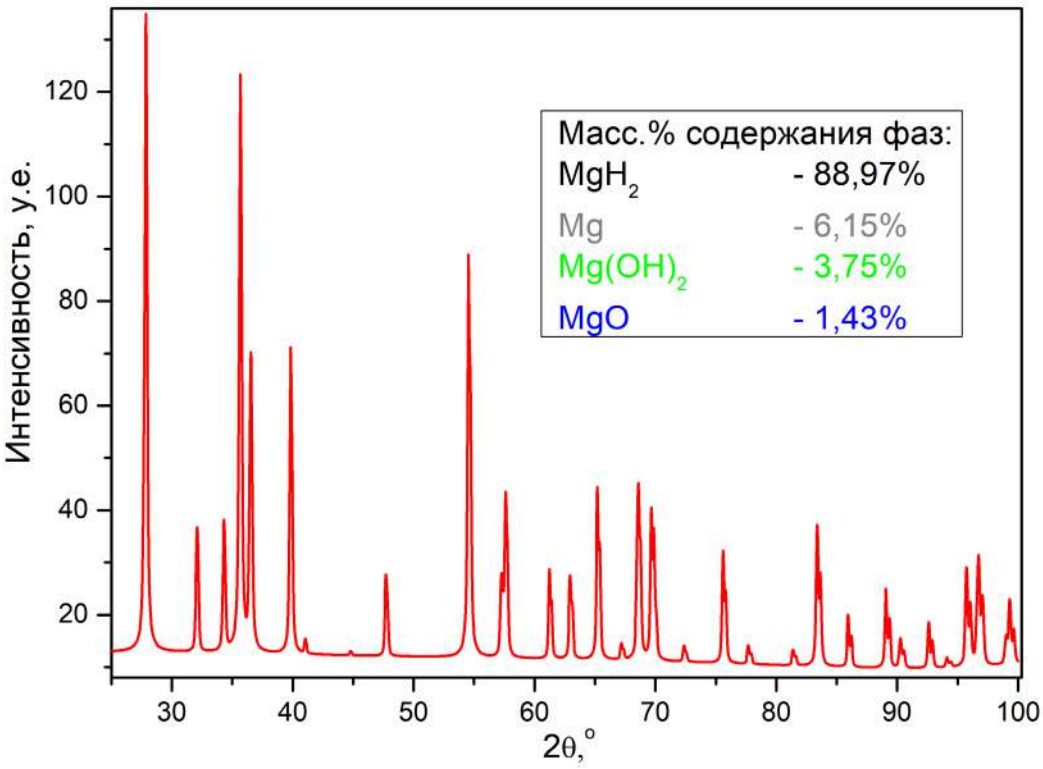

Figure 2.6 – XRD of the synthesised powder MgH_2

Chapter 3

Chemical and mechanical activation

3.1 Mixing MgH_2 with catalytic additives

A catalytic additive is a substance that increases the rate of reaction without being consumed in the reaction. The reaction here means the thermal decomposition of MgH_2, which in an isothermal experiment starts faster in the presence of a catalytic additive.

The following materials were chosen as catalytic additives:

- Nickel as the most promising catalyst [76], PNK-UT3 powder was used;
- Magnesium, MPF-4 powder, as the material from which the hydride under investigation was synthesised.;
- Aluminium, often used as a catalytic additive [76], A5 aluminium powder was used;
- Activated carbon, OU-A grade, because there are applications of carbon as a catalytic additive: graphene and graphite nanotubes [77], and graphite in ball milling [78].

All catalytic additives were mixed with the initial magnesium hydride in a 1:1 molar ratio. A series of isothermal dehydrogenation experiments with magnesium hydride were carried out on an uncompressed mixture of different substances. The samples were heated to 380 °C at a rate of 0.2 °C/s. Figure 3.1 shows the thermodesorption results of the mixtures and the original MgH_2. In the mixtures with magnesium and aluminium, the active desorption of hydrogen starts earlier, at 3000-3500 s, in contrast to the original magnesium hydride, from which the active desorption starts around 5000 s. Activated carbon, from the point of view of reducing the incubation time, does not lead to activation of the desorption, but influences the rate of this process. At the beginning of the active decomposition phase, the rate is slightly higher compared to the decomposition of the initial magnesium hydride, but

then the rate decreases sharply and during the observation time of ~11000 s it is not possible to reach the full hydrogen yield. This is probably due to the formation of hydrocarbons.

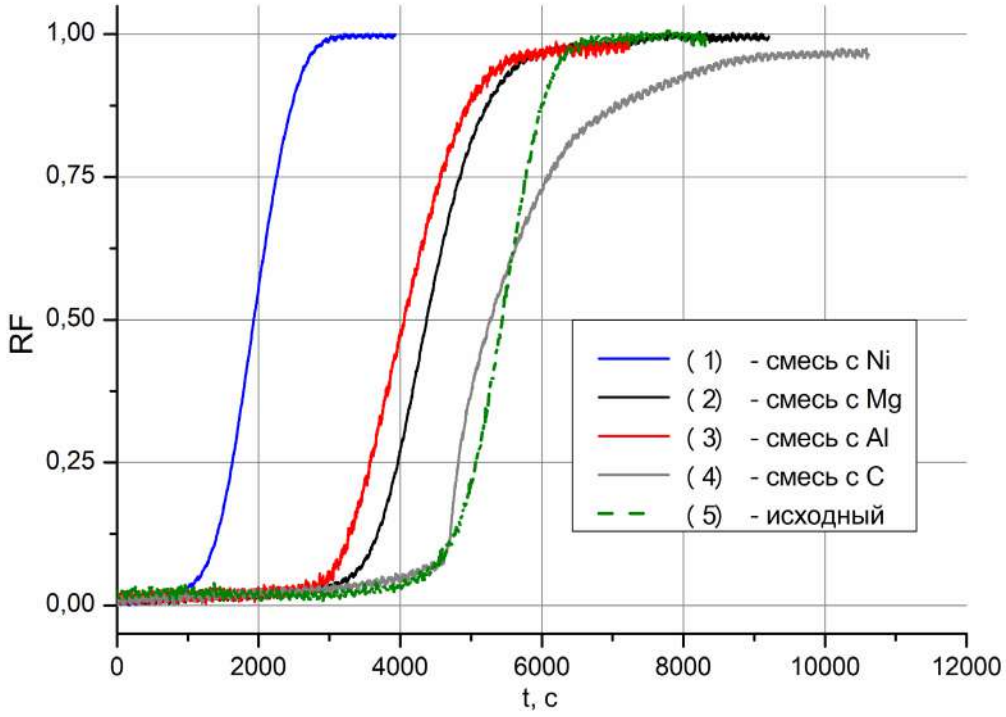

Figure 3.1 – RF as a function of time for isothermal (380 °C) decomposition of MgH_2 in different mixtures

Figure 3.1 shows that the best additive for activation is nickel. The incubation time in this mixture is just over 1000 s and the rate is slightly higher compared to desorption from other mixtures. The desorption rates are compared solely on the basis of the slope of the curves with respect to the vertical. The high quality of nickel as a catalyst is well known [79]. Nickel is a d-metal with an unfilled d-shell, so the desorption (adsorption) rate of hydrogen from nickel is far superior to that from the metal magnesium, which is an s-metal [80]. It's worth noting that under certain conditions [81], Nickel and magnesium can form an intermetallic compound Mg_2Ni, which can react with hydrogen to form hydride Mg_2NiH_4, meaning that nickel can act not only as a catalyst but also as a reagent in this reaction.

It is shown that the mixing with catalytic additives leads to an increase in the rate of desorption of the hydrogen.

3.2 Uniaxial air pressing

Uniaxial pressing is a mechanical method of activating the thermal decomposition of metal hydrides by applying a mechanical load to a sample of hydride powder using a press. In our case, a hydraulic press was used. The free bulk hydride powder with typical suspensions of 5-20 mg was pressed with a force ranging from 2 to 9.5 tons according to the pressure gauge of the press. After pressing, a solid disc of 10-25 mm diameter and 0.1 to 0.5 mm thickness was obtained, which was then broken into fragments for loading into the autoclave. The method is simple and serves as an excellent alternative to other mechanical and mechanochemical methods for activating hydrogen desorption from metal hydrides.

The effect of the magnitude of the pressure applied on the incubation time was investigated. Figure 3.2 shows the TDS results for MgH_2 samples subjected to different pressures. The initial sample is magnesium hydride powder which was not subjected to any pressure.

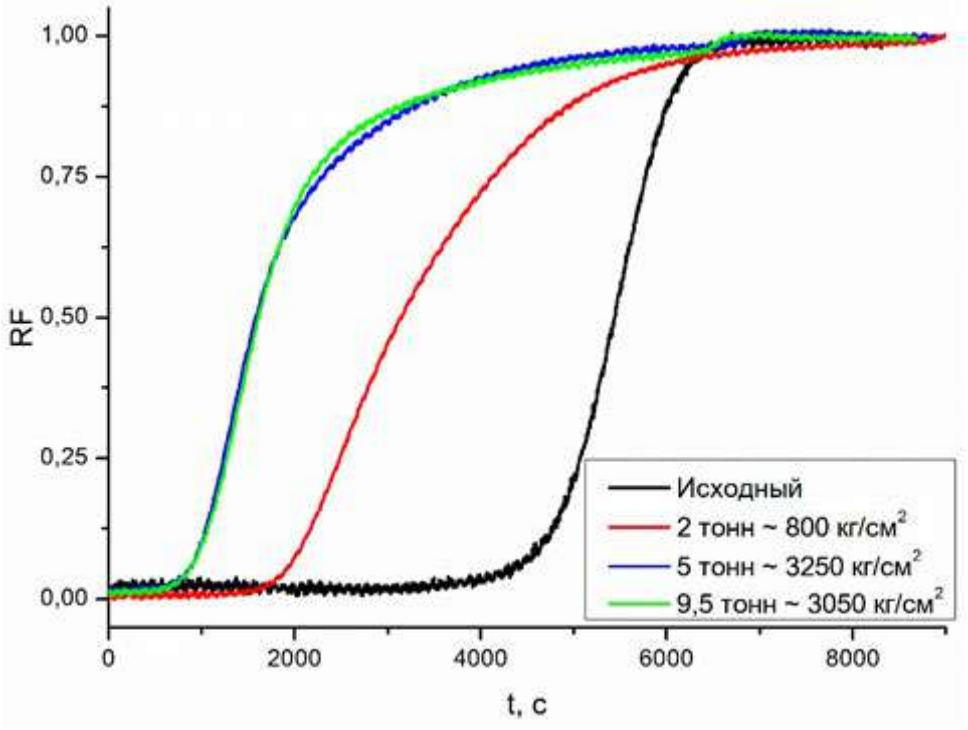

Figure 3.2 – RF as a function of time for the isothermal (380 °C) decomposition of MgH_2 at different hydraulic press forces.

Figure 3.2 shows that when pressing with a force of 5 tons according to the press gauge and above, the incubation times are practically the same and are of the order of 800 s. This is due to the fact that when normalized by the area of the disc obtained by pressing, the specific forces at 5 and 9.5 tons are close in value. The result obtained shows good reproducibility when pressing at the same pressure.

The dependence of the hydrogen desorption activation on the applied pressure was further investigated by differential scanning calorimetry (Figure 3.3). The presence of DSC peaks in the negative region indicates an endothermic phase transition, and the shift of the peaks to the left with increasing applied force indicates a decrease in the hydrogen desorption temperature. Also, as in the case of the TDS studies (Figure 3.2), the incubation time decreases as the magnitude of the press force increases. The reasons for this dependence are discussed below.

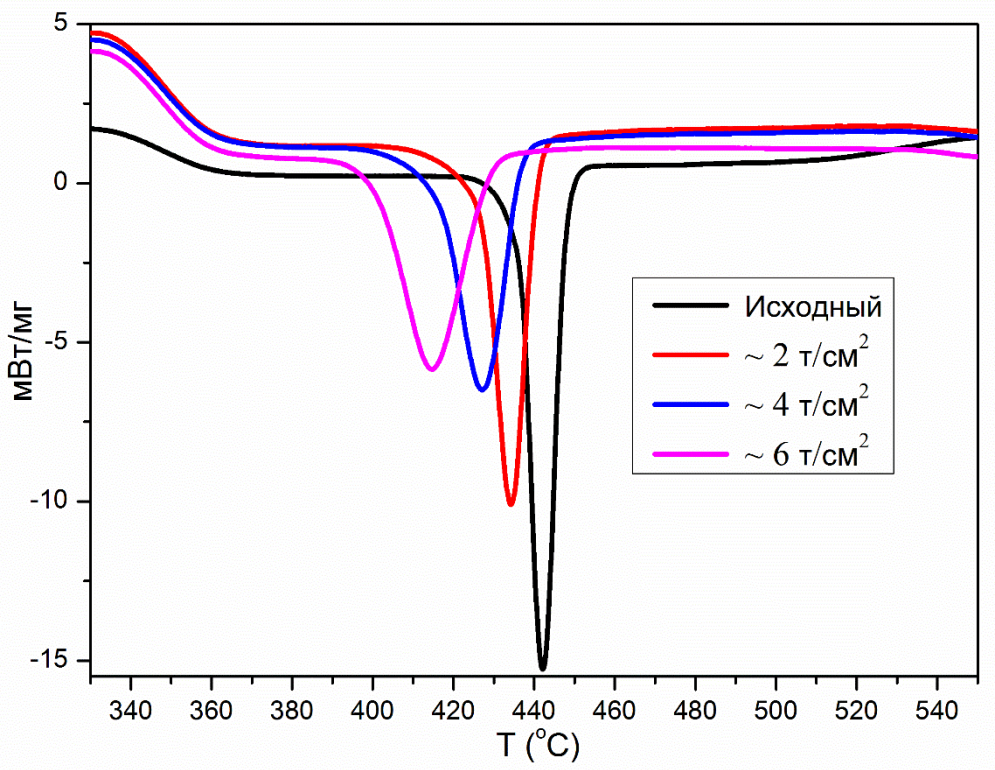

Figure 3.3 – DSC at a heating rate of 5 °C/min for magnesium hydride samples pressed at different forces.

On the basis of the results obtained, a force of 5 tons was chosen for further experiments.

Experiments on mixing magnesium hydride with metals show that such catalytic additives reduce the temperature at which hydrogen desorption begins, so it is necessary to exclude the influence of the die material on the activation of decomposition in the production of pressed magnesium hydride. Steel (st.20) and glass plates (SiO_2) were considered as materials. Glass is obviously a completely passive material and served as a punch passivity check. The test results of the selected punch materials showed no effect on the activation of hydrogen desorption from MgH_2. However, it is obvious that glass is not practical as it splits under the pressure of the press. Therefore, hardened high hardness St.20 steel plates were used for all further uniaxial pressing experiments.

Figure 3.4 shows SEM micrographs of the pressed magnesium hydride powder. These are surface and cross sectional images taken at the disc fracture after pressing. It can be seen that it consists of fragments of different sizes, with the larger fragments showing cracks.

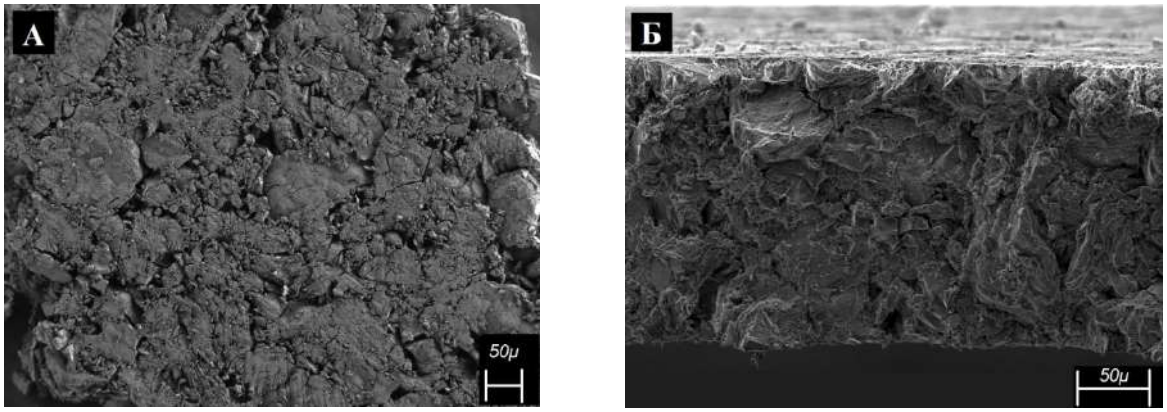

Figure 3.4 – SEM of pressed MgH_2: A - Top view; B - Cross section

Pressing experiments reduce the incubation time from 4500 to 1000 s in an isothermal experiment at 380 °C. Let us consider three possible mechanisms leading to the activation of thermodesorption during the pressing of MgH_2:

1) The direct synthesis of magnesium hydride is incomplete, leaving a core of magnesium metal in the centre of each particle. Pressing can split the particle and open a channel for easy desorption of hydrogen from the parent metal.

2) Pressing leads to the formation of a large number of defects in the crystal structure, which can be centres of accelerated formation of metallic phase nuclei. [82, 83].
3) Some hydrogen may be released during pressing, resulting in the appearance of metallic magnesium nuclei.

Simultaneous action of these factors is also possible. In order to verify the assumptions made, X-ray phase analysis was carried out on initial and pressed samples.

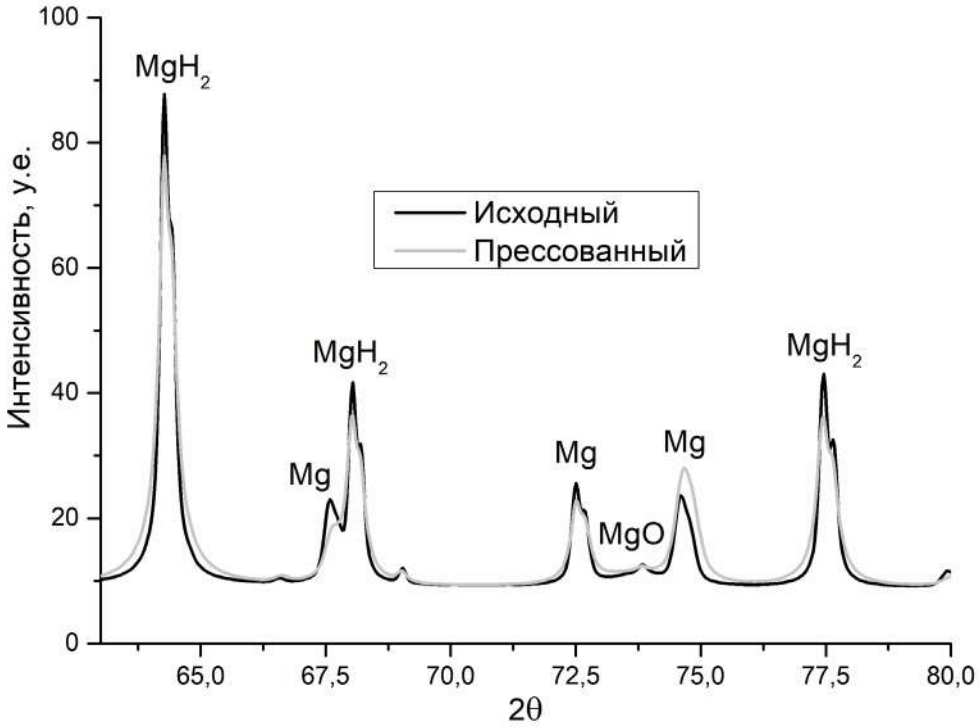

Figure 3.5 – Fragment of XRD for magnesium hydride (result of approximation of experimental data by TOPAS software): original (black); pressed (grey)

Figure 3.5 shows a fragment of the diffractogram for the initial and compacted samples of MgH_2 powder. In addition to MgH_2, the analysis shows that the material contains 5.34% metallic magnesium and 2.02% magnesium oxide. PCA of the pressed sample shows a slight decrease in the amount of hydride phase. Quantitative analysis of the phase content showed a slight decrease in the magnesium hydride phase ~1% of the mass, indirectly indicating the release of some hydrogen during the pressing process.

In addition, the same fragment of the diffractogram shows that the peaks for the pressed magnesium hydride are slightly broader than for the original sample. The broadening of the peaks indicates a relative increase in the number of microstructural defects and a decrease in grain size. In addition, for the pressed sample, the parameter indirectly indicating the magnitude of microstrains in the crystal lattice (parameter 'e0' in the TOPAS programme) increases significantly (original - 0.000128(13); pressed - 0.0005(10)). This may be due to the appearance of new defects in the crystal structure such as vacancies, dislocations, etc. during pressing. This assumption is supported by the work of [54], in which the accelerating effect of hydrogen vacancies on the rate of hydrogen desorption from AlH_3 was investigated. It is possible that structural defects that appear after pressing of MgH_2 also accelerate hydrogen desorption.

The results shown in Figure 3.5 were obtained on different samples and the changes are small, but it is possible that pressing releases some hydrogen, leaving fragments of metallic magnesium on the surface which become channels for rapid desorption when the samples are heated.

3.3 Uniaxial vacuum pressing

In order to clarify the question of whether hydrogen is released when magnesium hydride is pressed under vacuum, an additional module was constructed to the setup described in section 2.1. The vacuum module is shown schematically in Figure 3.6. It allows pressing with registration of possible desorption products by mass spectrometer (MS) and measurement of their amount.

The sample was pressed between two steel dies, Ø52 mm. The sample was poured as a circular layer of free bulk, Ø20 mm and 0.5 mm high. After pressing, a solid disc Ø21-22 mm with irregular edges and a thickness of ≈0.15-0.20 mm was obtained; the disc thickness irregularity at opposite edges did not exceed 0.02 mm. The primary compression of the specimen occurred already during the process of vacuumisation: due to the atmospheric pressure, the shells of the punch were compressed with a force of about 10 to 30 kgf [84].

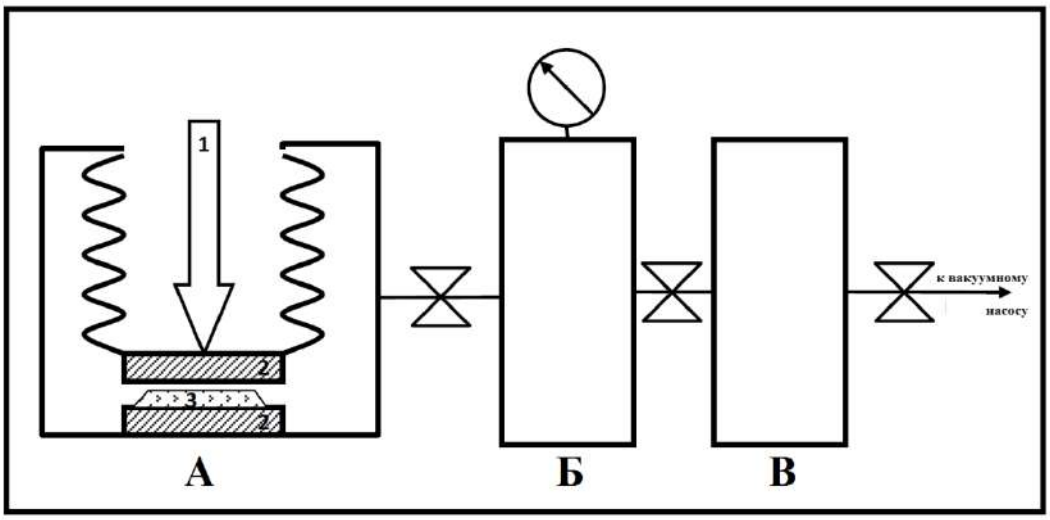

Figure 3.6 – Vacuum module consisting of chambers: A) Pressing chamber; B) Measuring and calibration chamber; C) Mass spectrometry chamber. 1 - Hydraulic press rod; 2 - Steel die; 3 - Sample

Figure 3.7 shows the comparison of the thermal decomposition of two samples: original and activated by uniaxial pressing at a force of 2 t/cm^2. The isothermal desorption curves at 380 ^{o}C are shown on the left side of Figure 3.7. It can be seen that for the pressed magnesium hydride the decomposition starts about 1000 s after heating to 380 ^{o}C, while for the original sample the incubation time is about 2500 s. On the right side of Figure 3.7 are the hydrogen desorption curves of the hydride, which show that under linear heating at a rate of 0.05 ^{o}C/s the decomposition of the pressed magnesium hydride sample starts at about 390 ^{o}C, while that of the original sample starts at about 420 ^{o}C. The onset times of hydrogen desorption from the vacuum-pressed samples during the isothermal experiment and the onset temperature of desorption during linear heating are similar to the experiments in air.

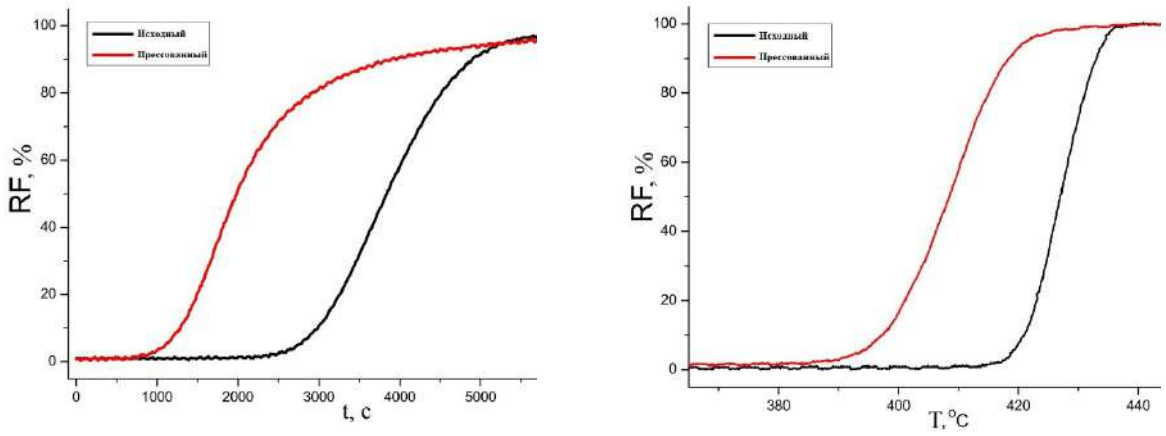

Figure 3.7 – Comparison of hydrogen desorption kinetics from the initial MgH_2 powder and pressed at 2 t/cm^2 under the following conditions: isothermal experiment at 380 °C (left) and linear heating at a rate of 3 °C/min (right).

Figure 3.7 shows that the application of force during uniaxial pressing results in a marked activation of hydrogen desorption from magnesium hydride. Pump mode pressing experiments with MS measurement of the release products showed that hydrogen is released with each successive increase in load. Figure 3.8 shows the dynamics of the MS signal proportional to the hydrogen release flux from the sample. The numbers in the graph correspond to the magnitude of compression during the stepwise increase in force. The resulting magnitude of compression at each step was achieved by several acts of press loading, resulting in the appearance of several peaks of hydrogen release.

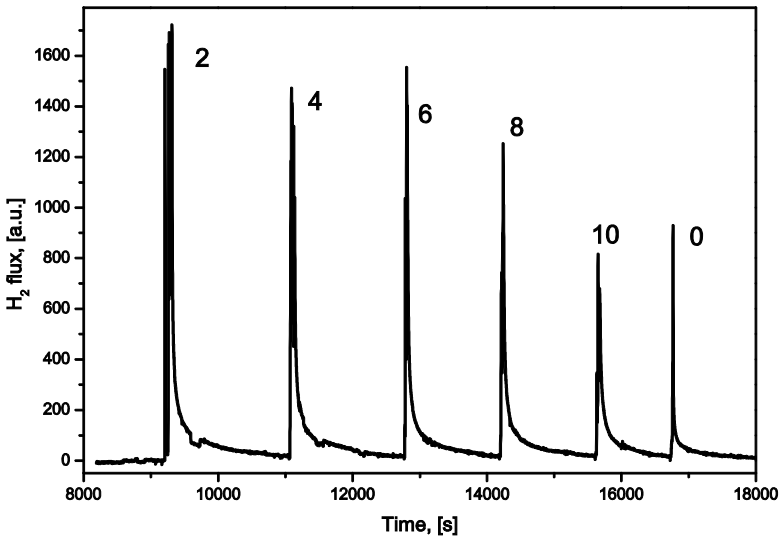

Figure 3.8 – Hydrogen release dynamics during pressing in 'stepwise pressing' mode

It can be seen that each increase in compression pressure results in the release of some hydrogen from the magnesium hydride. This is the main part, but there is also a small but prolonged release in the pause between the steps of pressure increase. There was also a small peak of release at the time of complete depressurisation (labelled 0 in the figure).

In order to assess the effect of the boosting procedure on the total amount of hydrogen released, a further series of experiments was carried out in which a complete depressurisation was performed after the required pressure was reached at each step. Figure 3.9 shows that holding or releasing pressure between stages has no significant effect on the amount and type of hydrogen released. It should be noted that hydrogen release is also observed on depressurisation as well as at the end of the previous series (peak 0 in Figure 3.8), albeit in smaller quantities.

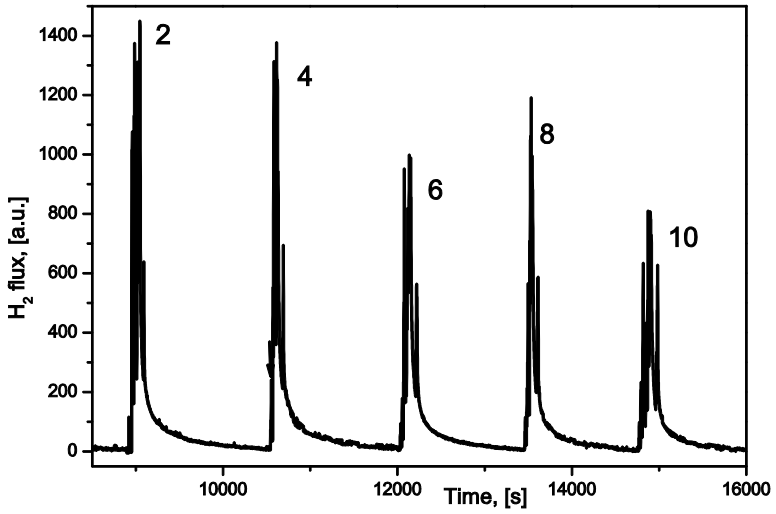

Figure 3.9 – Hydrogen release dynamics during pressing in 'load shedding' mode

Figure 3.10 shows one of the emission peaks (peak 4 in Figure 3.9) magnified. A small emission can be seen when the load is increased to the previous level, the main emission when the load is increased to a new level and a small emission when the load is returned to zero. The non-monotonicity of the dependence of the hydrogen emission on the application of force is related to the gradual application of force by pressing the lever of the hydraulic press four times.

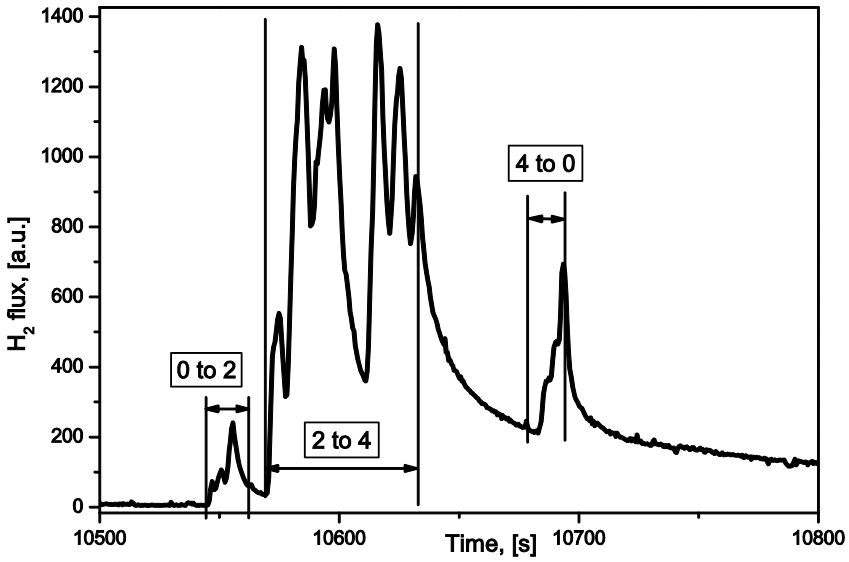

Figure 3.10 – Peak 4, shown in Figure 3.10, on an enlarged time scale. The time of increase and decrease of the compressive force is marked

The total hydrogen released during pressing to a pressure of 2.4 t/cm^2 was about 10^{-4} mass fractions, which in turn is about 10^{-3} of the initial hydrogen content in the sample.

In addition, it was observed that the magnesium hydride sample did not release the same proportions of hydrogen at the same steps of increasing force, and that the proportions decreased as the pressure increased. Figure 3.11 clearly shows this effect.

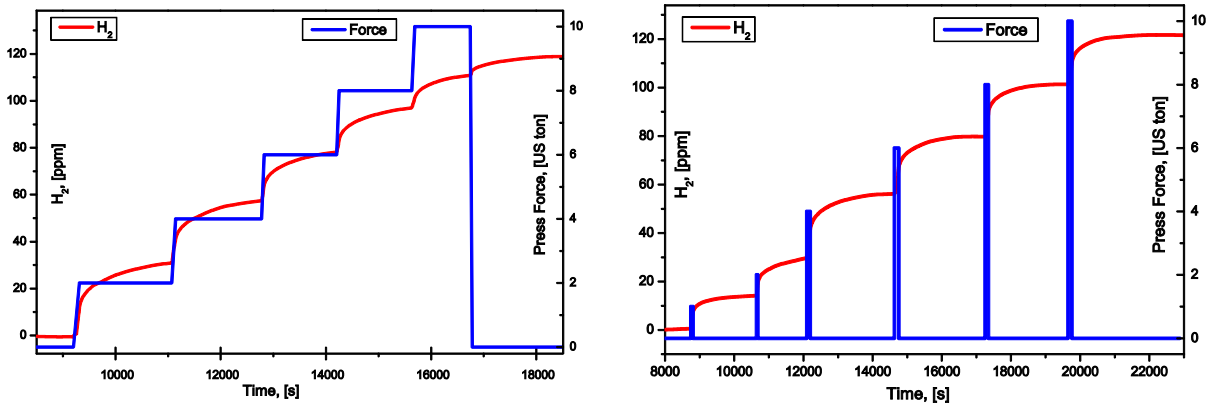

Figure 3.11 – The amount of hydrogen released during successive increases in press force in two modes: with load held (left); with intermediate load release (right)

The data obtained for several samples of magnesium hydride show that the amount of hydrogen released is directly proportional to the pressure applied. This relationship is shown in Figure 3.12, the slope of the line is $5 \cdot 10^{-3}$ $\frac{\text{масс\%}\cdot\text{см}^2}{\text{т}}$. The

graphs are plotted taking into account the variation in the dimensions of the pressed disc for different specimens and different force generation procedures. Figure 3.11 shows that maintaining the compression force during the stepwise pressure increase or releasing it between steps does not affect the total amount of hydrogen released. This result is explained by the release of hydrogen at the moment of deformation into the micropores formed during this process, which corresponds to the sharp increase in the mass spectrometer signal in Figure 3.11. The subsequent relatively slow decrease in this signal corresponds to the release of hydrogen from the pores of the sample.

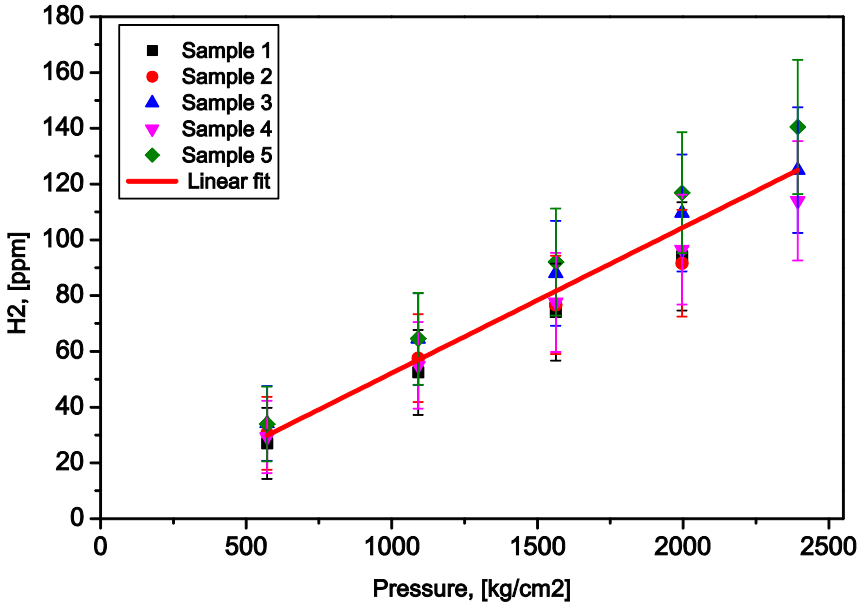

Figure 3.12 – Amount of hydrogen released as a function of press force for a stepwise increase in pressure

The main result of the experiments carried out is the detected release of hydrogen with increasing press load. Hydrogen desorption inevitably leads to the appearance or increase of metallic magnesium on the surface of the hydride particles. Thus, the partial desorption of hydrogen during the pressing process affects the activation of hydrogen release during subsequent degassing.

The effect of uniaxial pressing used in this study appears to be significantly more 'gentle' than the effect on the material of ball milling. It can therefore be assumed that partial hydrogen release, i.e. the activation effect, also occurs during ball milling and during the production of industrial samples [84, 85].

The amount of hydrogen released in these experiments is small - $(1,2\pm0,2)\cdot10^{-4}$ wt% at compression to pressures of 2.4 t/cm^2. However, the mere presence of metal nuclei is sufficient to activate decomposition, and the more nuclei there are, the higher the activation efficiency and the rate of hydrogen desorption - as shown in [42, 43, 54]. Partial hydrogen desorption during pressing is sufficient to activate the subsequent thermal decomposition, but further in section 3.3 it will be shown that the activation effect can be increased by mixing the catalyst with magnesium hydride powder.

3.4 Pressing of magnesium hydride with catalytic additives

The same materials were chosen as catalytic additives as those used for mixing in section 3.1. The results of the isothermal thermodesorption of the pressed mixes in comparison with the original sample are shown in Figure 3.13.

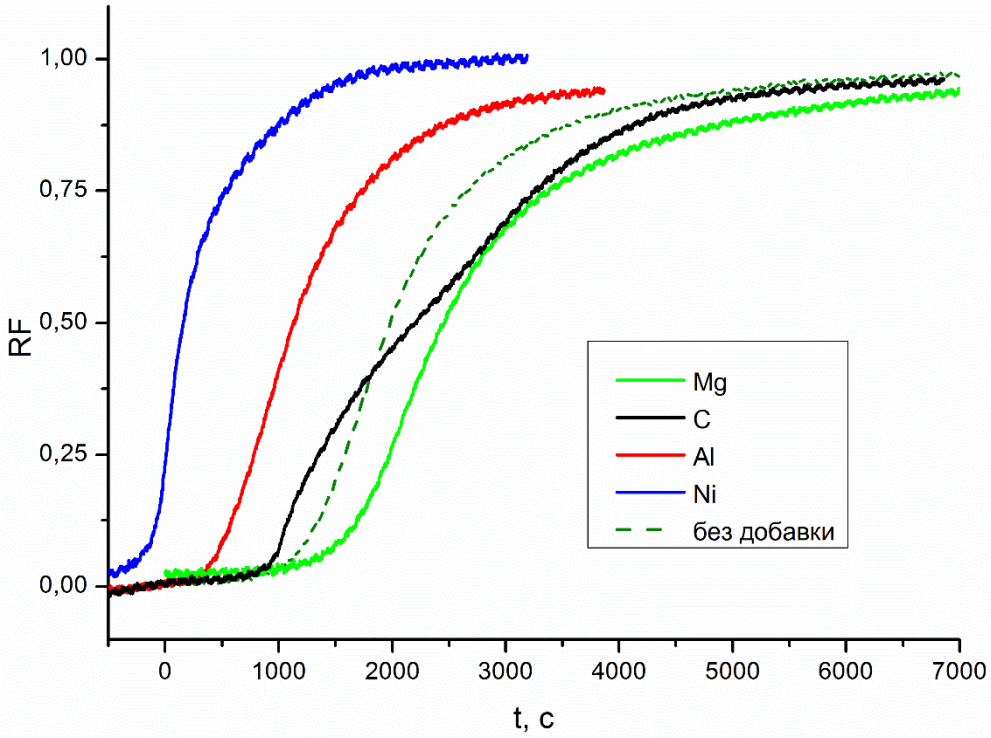

Figure 3.13 – RF as a function of time for isothermal (380ºC) decomposition of pressed mixtures of magnesium hydride with: magnesium, aluminium, nickel, carbon and magnesium hydride without additive

The graph shows that the addition of different catalysts to magnesium hydride during pressing leads to an earlier onset of hydrogen desorption from the samples.

The only exception was the mixture with magnesium, from which active desorption started later than from the pure pressed hydride, but there is an explanation for this. The particles of metallic magnesium in the prepared mixture are larger or similar in size to the particles of hydride powder, while the metal particles are plastic, unlike the brittle hydride, and therefore take up most of the load when force is applied, reducing the deformation of the magnesium hydride.

The behaviour of the compacted carbon mixture is also unusual. Compared to the unpressed mixture, hydrogen desorption from the pressed mixture can be divided into two phases: a short, high rate phase and a long, low rate phase. In this case, the hydrogen release starts earlier, although it is slower. The mixture pressed with aluminium shows active decomposition already after 500 s after heating. And judging by the slope of the curve, the decomposition rate is similar to that of the magnesium hydride sample pressed without additives. However, the best result in terms of activation was shown by the pressed mixture with nickel, from which hydrogen desorption began before the isothermal point of 380 ^{o}C was reached.

Figure 3.14 shows SEM micrographs of the unpressed and pressed mixtures of magnesium hydride and nickel hydride at a molar ratio of 1:1. From Figure 3.14 it can be seen that the finer particles of nickel powder, of the order of 3-5 μm, surround the larger hydride particles on all sides. The photo of the pressed mixture also shows the cracking of the magnesium hydride particles. The hydrogen release from the pressed mixture of magnesium hydride and nickel starts earlier than the others and has a steeper front compared to the unpressed mixture of magnesium hydride and nickel. It is concluded that the addition of different catalysts, especially nickel, leads to the activation of magnesium hydride and that pressing with nickel leads to a significant acceleration of hydrogen evolution from magnesium hydride.

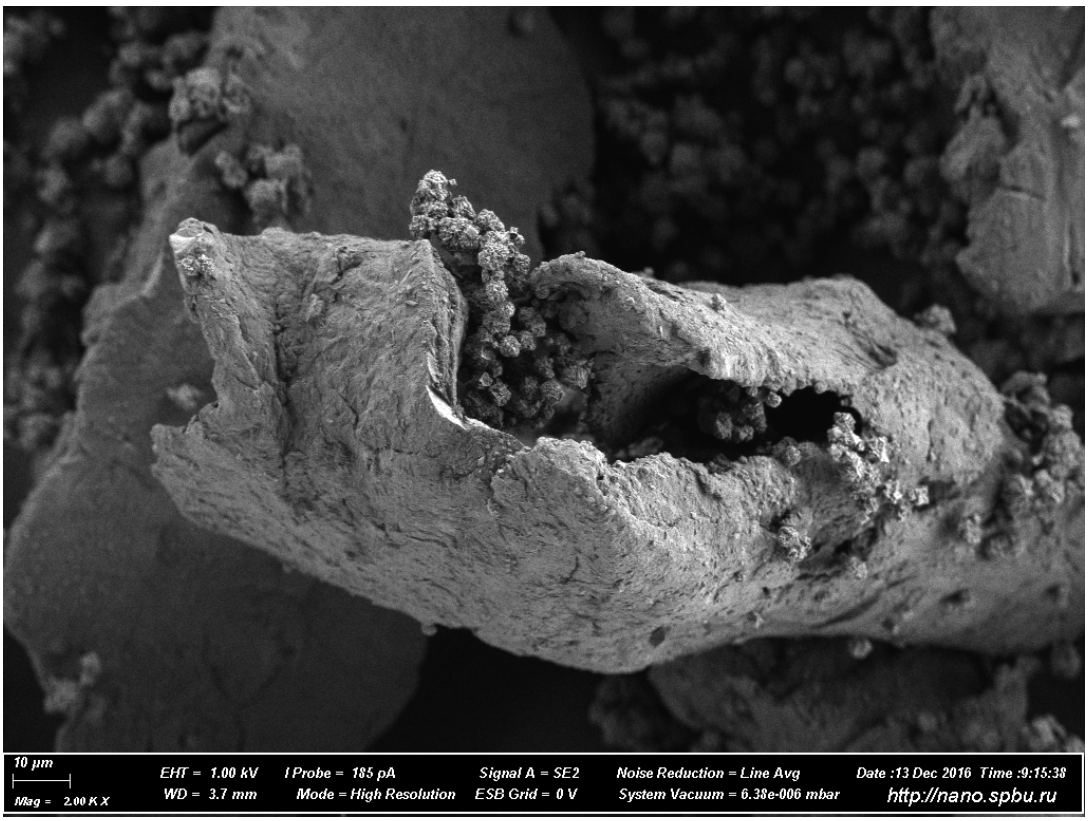

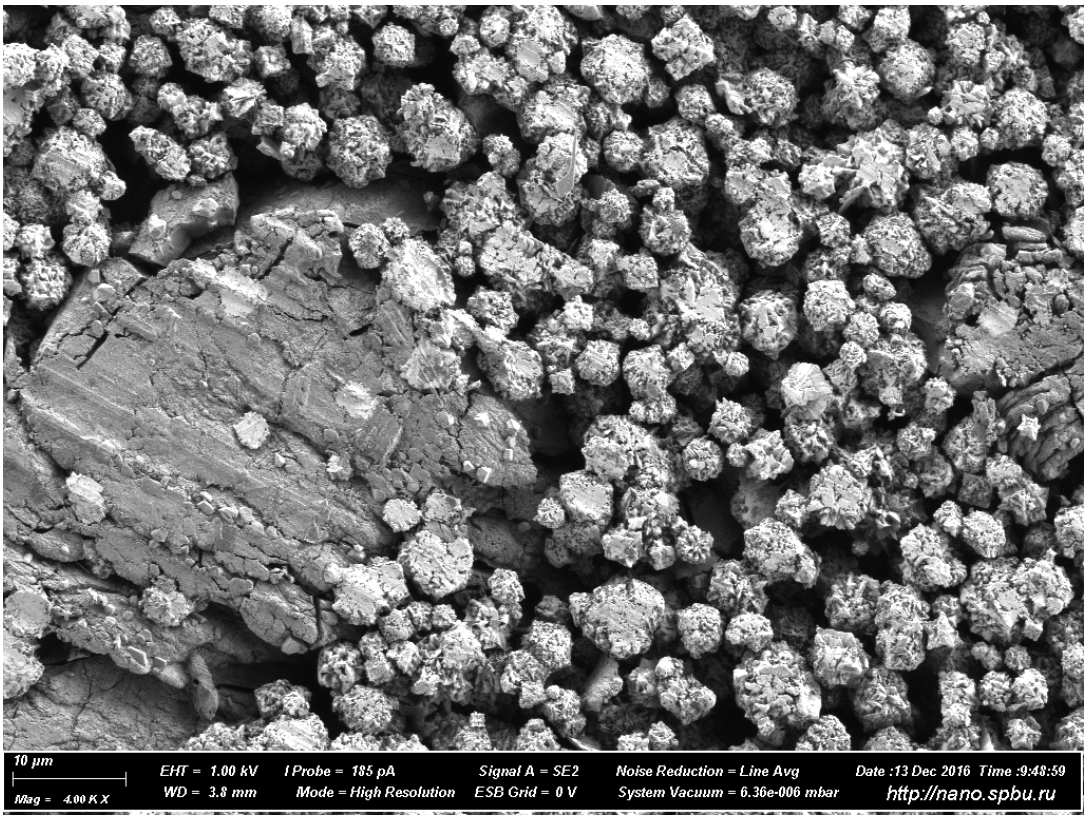

Figure 3.14 – SEM of unpressed and pressed 1:1 molar ratio magnesium and nickel hydride mixtures

The results of the dehydrogenation experiments for the samples of MgH_2, compressed magnesium hydride, magnesium hydride-nickel mixture and compressed magnesium hydride-nickel mixture in the linear heating experiment are shown in Figure 3.15. Heating was carried out from 20 to 280 ºC at a rate of 0.5 ºC/s to optimise the experimental time and from 280 to 470 ºC at a rate of 0.05 ºC/s. This separation was made because of the early onset of hydrogen evolution from the pressed magnesium-nickel hydride samples. [87].

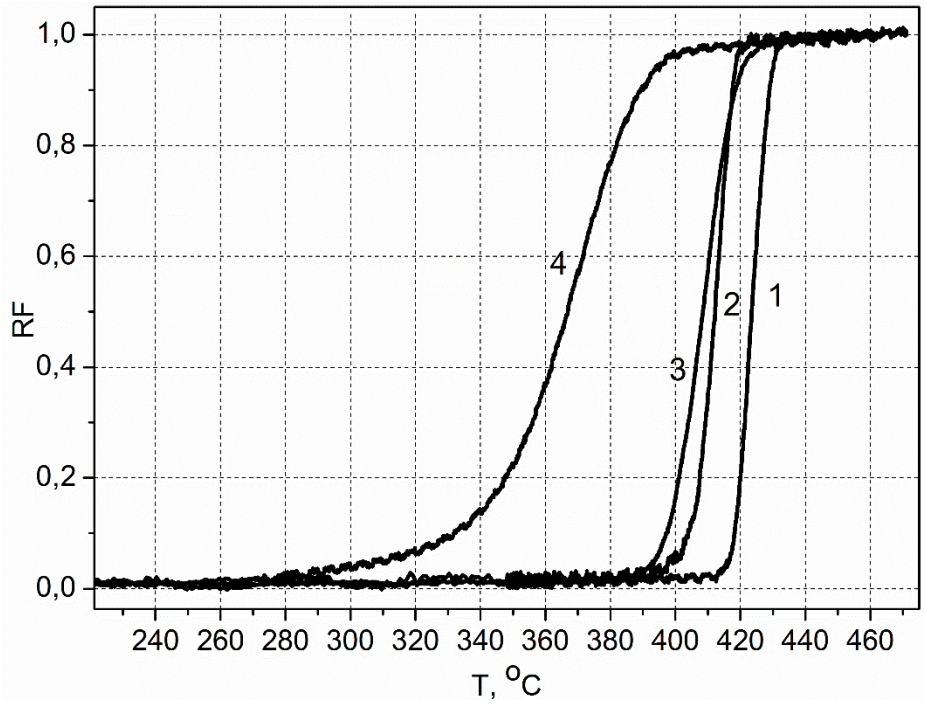

Figure 3.15 –Proportion of reacted substance during hydrogen evolution from unpressed and pressed magnesium hydride with Ni during linear heating up to 470 ºC
1 - initial MgH_2; 2 - mixture of MgH_2 with Ni
3 - compressed MgH_2; 4 - compressed MgH_2 with Ni
[87]

The results show that mechanical activation (using a hydraulic press) and the addition of a catalyst (nickel) leads to a decrease in the temperature threshold for the onset of hydrogen desorption from magnesium hydride.

Thus, it is shown that pressing with catalysts is an effective method of mechanical activation of magnesium hydride, which does not require large energy and time costs. Nickel leads to activation of hydrogen desorption from magnesium hydride. The pressing of magnesium hydride results in the formation of metallic

nuclei which help to lower the temperature threshold for the onset of hydrogen release, and the addition of nickel during pressing increases the activation effect required for practical applications.

The pressing of magnesium hydride with and without nickel is an excellent alternative to the known mechanical and mechanochemical methods of activating metal hydrides. The influence of nickel on the activation of hydrogen desorption from magnesium hydride samples during pressing will be considered in more detail.

3.5 Uniaxial air pressing of magnesium hydride with nickel

In the course of this research, uniaxial pressing was found to be a reliable, simple and inexpensive method for activating hydrogen desorption from magnesium hydride. Ni powder with a purity of 99.92% (PNK-UT3) and a particle size of 1-5 μm was used for uniaxial pressing in air. Heating was carried out from 20 to 280 ºC at a rate of 0.5 ºC/s. Figure 3.16 shows the results of thermodesorption experiments on pressed mixtures of magnesium hydride with nickel at different concentrations. The figure shows that the rate of hydrogen desorption increases as the amount of nickel in the mixture increases. Curve 6 describes the result of hydrogen extraction from pressed magnesium hydride without catalyst. It should be noted that for curves 1-5, hydrogen starts to be released before the set temperature of 280 °C is reached. The chosen temperature allows us to compare in one figure the hydrogen desorption kinetics for pressed MgH_2 without catalyst with samples pressed with different amounts of nickel catalyst.

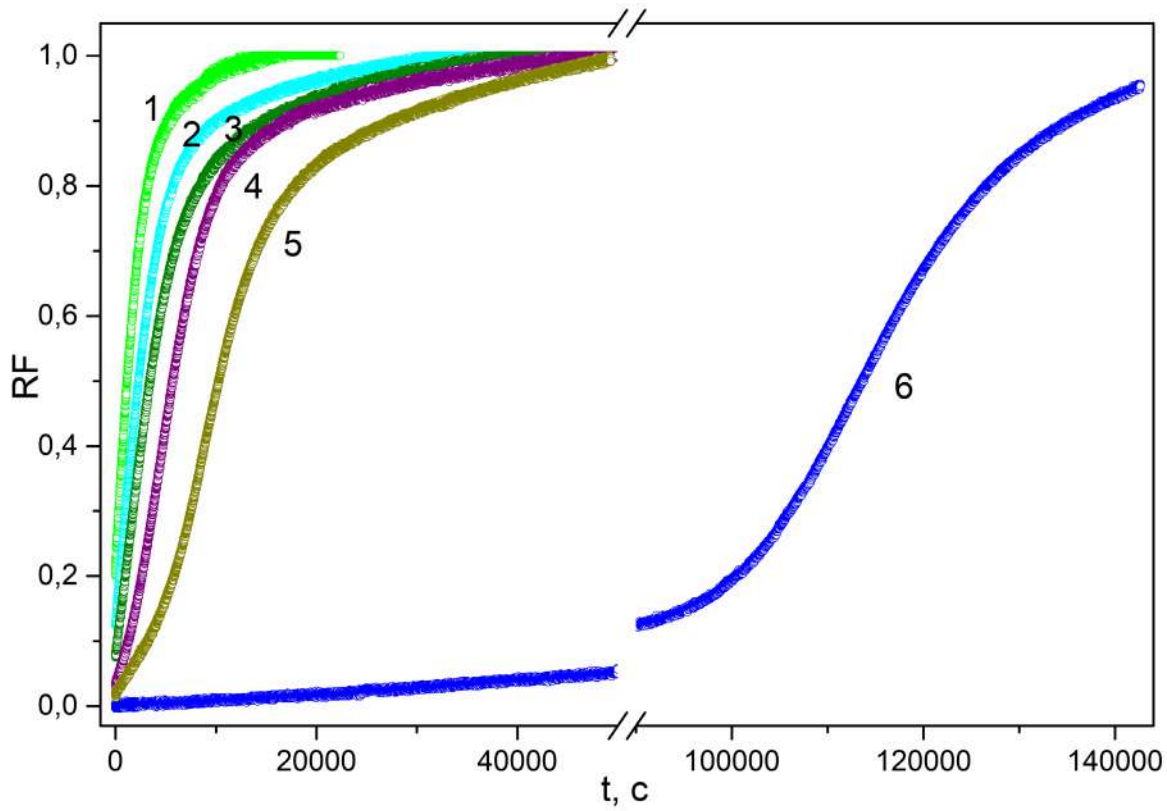

Figure 3.16 – Hydrogen desorption at 280 °C for different amounts of nickel catalyst;
MgH_2:Ni molar ratio: 1) 1:1, 2) 2:1, 3) 5:1, 4) 10:1, 5) 20:1, 6) 1:0

During pressing, nickel particles are attached to the surface of the MgH_2 particles, allowing hydrogen atoms to move more easily from the bound state in MgH_2 to solid solution in the nickel lattice. The diffusion pathways to the nickel surface are small (about 1 μm), so hydrogen can reach and desorb relatively quickly, even at low temperatures, as the catalytically active metal promotes rapid recombination of hydrogen atoms. Further release of hydrogen transforms MgH_2 into metallic magnesium. As a result of the desorption of H_2 through the nickel channel initially formed on the surface of the hydride particle during pressing, a nucleus of metallic magnesium appears at the site of attachment of the nickel particle. The desorption flux density of magnesium is much lower than that of nickel, but the area of metallic magnesium increases, resulting in the formation of a metallic crust of Mg, while the area of nickel remains constant. Therefore, more nickel in the mixture means more metallic areas and earlier formation of metallic crust on the surface.

After the formation of the metallic crust, the phase of movement of the metallic boundary deep into the sample begins with the possible merging of nickel and magnesium desorption channels. This is a shrinking core model represented by a sphere with magnesium hydride in the centre and metallic magnesium on the surface. However, desorption from the brightened channels (nickel) can still be much faster than from the formed areas of metallic magnesium.

In the case of nickel-free pressing, the long incubation time is similar to the results of the magnesium hydride studies in [43], where metallic magnesium nuclei act as a channel for rapid hydrogen desorption.

The mathematical description of the hydrogen desorption process during hydride decomposition should be based on conservation laws and take into account the most important elementary reactions (not necessarily a limiting reaction). Based on the approach used in [43, 54, 86] In order to describe the kinetics of hydrogen desorption, a probable mechanism of decomposition of pressed MgH_2 has been described.

The description of the mechanism of hydrogen desorption from magnesium hydride during pressing with nickel is based on two important facts:

- Hydrogen desorption from ionic covalent metal hydrides (MgH_2 is one of these) is much slower than from metals.
- Nickel, which is a d-metal with an unfilled d-shell, activates hydrogen adsorption and desorption better than magnesium, which is an s-metal.

3.6 Mathematical modelling of hydrogen release from samples with different nickel content

A model for the thermal decomposition of metal hydride powders in the single particle approximation is described in detail for aluminium hydride, e.g. in [54]. The model presented here is very similar: only the shape of the powder particles differs.

Such models can be applied to other ionic-covalent metal hydrides to describe the mechanism of hydrogen desorption from them.

The following simplifying assumptions are used in the model The following simplifying assumptions are used in the model:

- All powder particles have the same size and spherical shape of radius L, which does not change after hydrogen release;
- Metal nuclei growing in tangential directions form a metal shell, which is a spherical layer (ρ, L) with a thickness of $h = L - \rho$;
- This shell thickens further in a shrinking core scenario as the core shrinks $\rho(t)$ (phase morphology is similar to that described in the [89]);
- The resulting shell is spherically symmetric and is completely described by its thickness h and the external surface area of the particle $S(t)$;
- Hydrogen is desorbed from the surface of the catalyst, whose particles are smaller than the hydride particles, but provide a total flux equal to or greater than the flux from the magnesium surface due to the high flux density of desorption from nickel J_{Ni};
- Hydrogen is also desorbed from the magnesium surface, producing a flux density of I, however, this desorption is limited by the rate of hydride decomposition.;
- The flux density I includes both the hydrogen released by the shrinking nucleus $1-v$, and released from the expanding layer v; then assume that the flux density due to shell expansion is equal to $v \cdot I$, and the rest of $(1-v) \cdot I$ is caused by a shrinking nucleus.
- The concentration of hydrogen dissolved in the metal is small compared to the constant concentration of hydrogen. c_h in hydride.

Figure 3.17 shows the stages of the model of thermal decomposition of magnesium hydride after pressing with nickel. The nickel powder particles adhere

closely to the surface of the magnesium hydride and the area of such contacts increases with the concentration of Ni in the mixture. When the sample is heated, the Ni particles on the surface of the hydride act as channels for easy hydrogen desorption and the first nuclei of metallic Mg appear on the surface of MgH_2 at the points of contact with nickel (stage A). The main contribution to the desorption is given by the hydrogen flux from the nickel. The metal nucleates then proliferate in the near surface region and the desorption fluxes of Ni and Mg are almost comparable (stage B). In the final stage C, the Mg nucleates coalesce into a continuous crust. Now, due to the increased surface area of metallic magnesium, the main contribution to desorption is given by the hydrogen flux from Mg. The process continues until the complete decomposition of MgH_2 and in the final stage has the character of a 'shrinking core'.

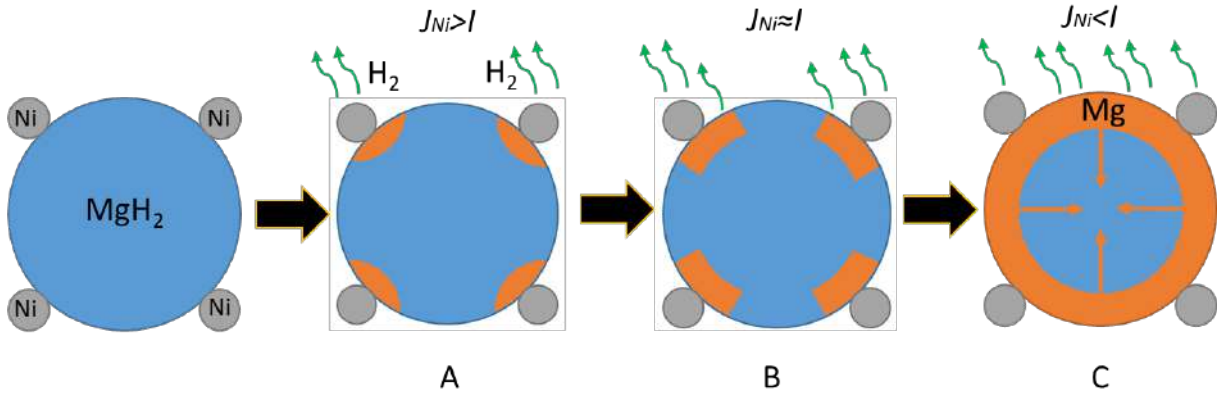

Figure 3.17 – Stages of the decomposition model of MgH_2 pressed with Ni: A - Appearance of Mg nuclei; B - Growth of Mg nuclei in the near-surface region; C - Coalescence of nuclei into a continuous crust and 'shrinking core'.

The notations used in the model are summarised in Table 3.1.

Table 3.1 – Model parameters

L	Particle radius	ρ	Hydride core radius
h	Thickness of spherical metal layer $(L-\rho)$	I	Hydrogen flux density from the magnesium surface

RF	Percentage of reacted fraction (proportional to the volume of metal phase formed)	v	Shrinking core parameter (fraction of hydrogen coming from behind the shrinking hydride core)
W	Geometric factor for spherical particles $(L^3 - \rho^3)/3$	c_h	Hydrogen concentration in hydride
S	Specific area of magnesium nucleation on the surface	S_0, ρ_0, RF_0	Initial values$S$, ρ, RF
J_{Ni}	Hydrogen flux density from catalyst	t_λ	Incubation period
Δt	Time shift (not take into account the initial part of the curve)	V_λ	Percentage of reacted fraction in the incubation

The local equilibrium near the phase boundary is described by equation (3.1):

$$c_h\dot{\rho} = -(1 - \nu(S))I \qquad (3.1)$$

This equation is valid for $S < 1$; and obviously $\nu = 0$ when the layer has formed, $S = 1$.

According to the law of the conservation of mass:

$$-c_h\rho^2\dot{\rho}S + c_hW\dot{S} = I\rho^2S + J_{Ni}L^2(1 - S) \qquad (3.2)$$

where $W = (L^3 - \rho^3)/3$. Substituting (3.1) into (3.2) we get:

$$c_hW\dot{S} = \nu I\rho^2S + J_{Ni}L^2(1 - S) \qquad (3.3)$$

The measured quantity RF(t) is the fraction of the reacted substance as a function of time. It is dimensionless and is equal to the relative volume of the new phase with respect to the volume of the whole particle:

$$RF(t) = (1 - \frac{\rho^3}{L^3})S \qquad (3.4)$$

The initial conditions for equations (3.1) and (3.3) are as follows $S(0) = S_0$ and $\rho(0) = \rho_0$, values ρ_0 и S_0 are parameters. The experimental curves are shifted to the right by the time Δt, in order to exclude the incubation phase from consideration.

This model describes the experimental results well, as shown in Figure 3.18, where the thin black line shows the result of the approximation of the thermodesorption spectra by this mathematical model.

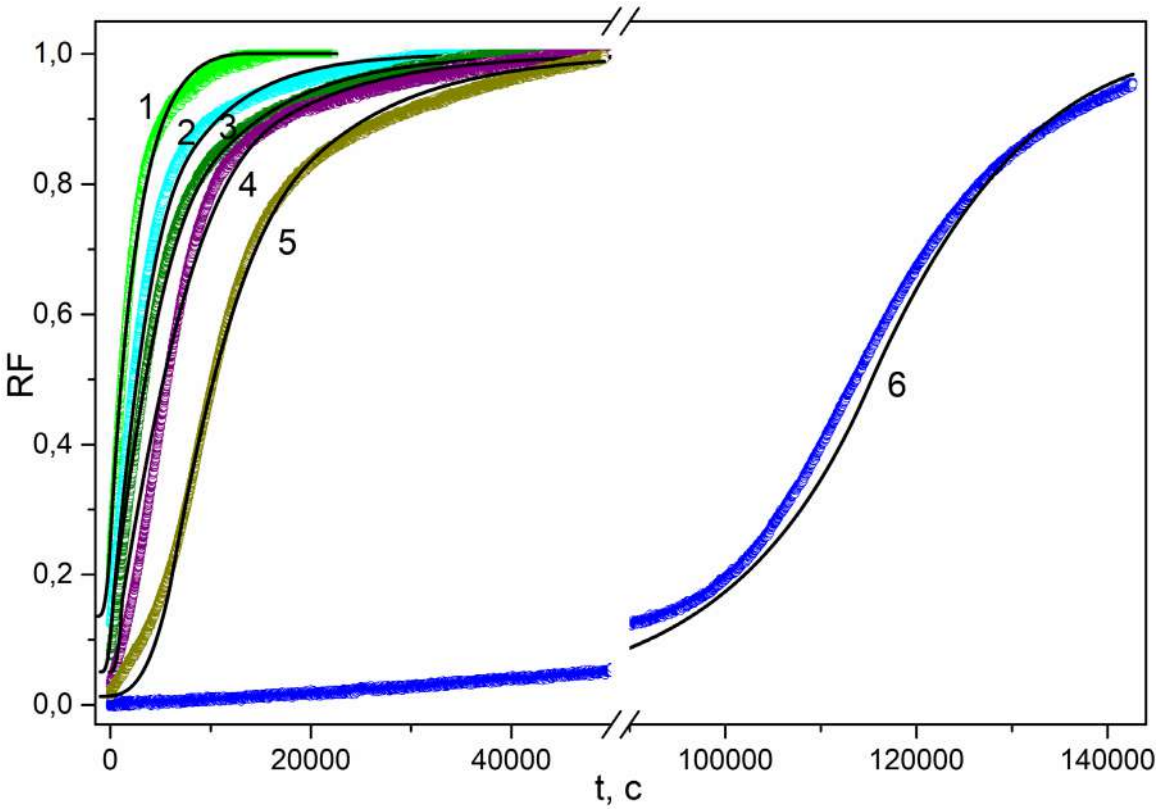

Figure 3.18 – Hydrogen desorption at 280 °C for different amounts of nickel catalyst;
The black line corresponds to the approximation of the experimental curves by the chosen model;
MgH_2:Ni molar ratio: 1) 1:1, 2) 2:1, 3) 5:1, 4) 10:1, 5) 20:1, 6) 1:0

Table 3.2 shows the approximation parameters used to fit the experimental data according to the described model. The rows in the table correspond to the experimental curves with the corresponding number in Figure 3.18. Curves with a higher number correspond to a lower nickel content. The second column of the table is the density of hydrogen desorption J_{Ni} from nickel particles on the magnesium hydride surface. It is lower with a lower amount of catalyst, which seems reasonable.

The next column shows the decomposition rate of hydride *I*. It is the same for all particles with catalyst and more than 4 times lower for curve 6, which corresponds to pressed magnesium hydride without nickel addition. This is also reasonable as the main function of the catalyst is to increase the reaction rate.

Table 3.2 – Approximation parameters

Desorption curve	J_{Ni}, 10^{-9} 1cm^2·sec	I, 10^{-9} 1/cm^2·sec	v	ρ_0	S_0	RF_0, %	Δt, sec	t_λ, sec
1	6,125	3,75	0,1	0,45	0,15	13,6	1300	1300
2	2,50	3,75	0,1	0,77	0,20	10,9	1000	1300
3	1,81	3,75	0,1	0,79	0,10	5,1	1000	1300
4	1,69	3,75	0,2	0,79	0,10	5,1	0	1000
5	1,50	3,75	0,1	0,70	0,02	1,3	1000	7000
6	0,0	0,875	1,0	0,80	0,09	4,4	$-8\cdot10^4$	0

The parameter v, which describes the shrinking of the nucleus, is quite stable. The metal layer on the particle surface thickens due to the intensive growth of nuclei in the presence of a catalyst. In the absence of a catalyst, the particle nuclei do not shrink to form a continuous shell. This is explained by the formation of nuclei on the surface. The initial area of metallic phase S_0 is larger the more catalyst is present and then grows due to the metal nuclei appearing under the nickel particles. The initial fraction of the metallic phase RF_0 increases with increasing amount of nickel, except for the sample without catalyst. The appearance of the metallic phase is due to the long incubation time. It is important to note that the sensitivity of curve 6 (without catalyst) to parameter variations is much higher than that of any of the other curves.

The model is used to describe the desorption of hydrogen from pressed magnesium hydride in the presence of a catalyst such as nickel. Curve 6 in Figure

3.18 refers to a sample without a catalyst and is also well approximated by the model. For this curve (see Table 3.2) J_{Ni} = 0. The dimensionless density of the hydride decomposition rate was significantly lower compared to curves 1-5: $I = 0{,}0875 \cdot 10^{-8}$. For the pressed magnesium-nickel hydride mixtures, the hydrogen desorption rate is high. The limiting process for hydrogen desorption is the movement of the interfacial boundary in the presence of the catalyst. In the case of decomposition of the pressed hydride without nickel addition, the limiting factor is the hydrogen desorption rate as it is much lower here.

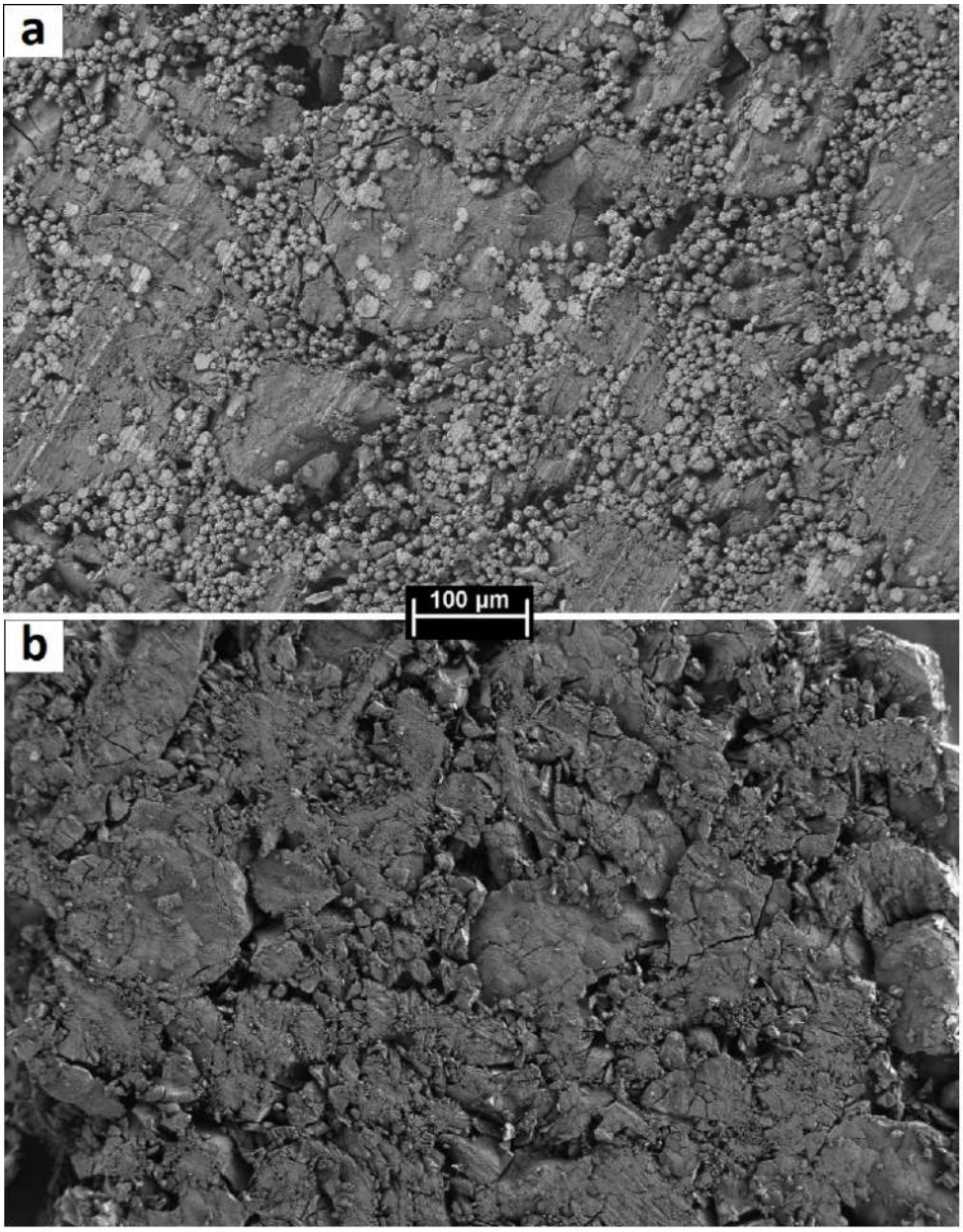

Figure 3.19 – SEM of magnesium hydride sample pressed in the presence of nickel (a) and without nickel (b)

Figure 3.19 shows the SEM micrograph for a sample of magnesium hydride pressed in the presence of nickel (a) and without nickel (b).At the active stage of magnesium hydride decomposition, the area of the hydride-metal interface is comparable to the outer surface of the powder particle. A rough estimate of the average powder particle size (Figure 3.19b) after pressing without nickel is in the order of 1 μm ($L = 0{,}5 \cdot 10^{-4}$ cm). To estimate the hydrogen desorption flux density for curve 6 of Figure 3.18, after curve fitting, we multiply the dimensionless value of I by the hydrogen concentration in magnesium hydride, which is $0{,}33 \cdot 10^{23}$ cm^{-3} and obtain $2{,}8875 \cdot 10^{13}$ cm^{-2} s^{-1}.

This estimate of the hydrogen desorption flux density can be compared with the estimate in [43]. In our case, magnesium hydride was compressed, whereas in the cited paper it was not, but the hydride decomposition parameters should be quite similar. Using the desorption kinetic parameters obtained in [43] nd extrapolating the results to 280 °C, we can estimate the hydrogen desorption flux density to be $0{,}81 \cdot 10^{13}$ cm^{-2} s^{-1}. The obtained result is in good agreement with the literature data, the discrepancy being less than one order of magnitude. Thus, the parameters describing the motion of the MgH_2-Mg, interface obtained in this work do not contradict the previously obtained results.

The obtained result proves that hydrogen desorption from magnesium hydride follows the same scenario in the case with and without catalyst, namely associative hydrogen desorption from the surface of metal phase nucleates, regardless of the nature of its occurrence.

3.7 Comparison of uniaxial pressing with other mechanical activation methods

The results obtained show that pressing with nickel catalyst makes it possible to reduce the hydrogen desorption temperature and improve the dehydrogenation kinetics. Compared to the decomposition temperature of the initial hydride, the

activation temperature is reduced by more than 100 °C. The efficiency of this method can be evaluated by comparing it with other mechanical activation methods, in particular with a method such as ball mill grinding.

The paper [90] presents the results of DSC of magnesium hydride heated at a rate of 10 °C/min after 20-hour grinding in a ball mill. The desorption peak is at a temperature of about 370 °C. The results in Fig. 3.3 show the peak at 420 °C for a sample pressed with a force of 6 t/cm^2 and heated at a rate of °C/min. The paper [91] also presents DSC results of magnesium hydride after different grinding times in a ball mill and subsequently heated at a rate of 6 °C/min. Samples milled for 35-50 h had a desorption peak at 430 °C, while samples treated for 60-100 h showed the best result at 480 °C. This shows that the activation effect of ball milling for 35-50 h and 6 t/cm^2 pressing is similar.

It can therefore be concluded that activation by pressing is similar or slightly less effective than ball mill grinding of hydride, but this method is much simpler, requires less processing time and does not require expensive equipment. In addition, the material obtained by pressing does not spontaneously combust in air, unlike samples prepared by ball milling.

The paper [8] presents DSC results of magnesium hydride heated at a rate of 10 °C/min after cold rolling. The desorption peak is around 430 °C, which is comparable to our result of 420 °C at a heating rate of 5 °C/min. This coincidence is to be expected as the actual rolling is a pressing of the material between the rollers.

The addition of nickel catalyst and pressing dramatically increases the rate of hydrogen desorption from magnesium hydride. This is confirmed by the described mechanism of hydride decomposition and the mathematical model of this process. The experimental curves are well approximated by this mathematical model.

Conclusions:

- *Mixing magnesium hydride with metals results in shorter incubation times and increases the rate of hydrogen desorption. The best effect is achieved by adding nickel, which reduces the incubation time to about 1000 s.*
- *A mechanical method of magnesium hydride activation, uniaxial pressing, has been developed as an effective alternative to other mechanical methods.*
- *Mechanical impact on magnesium hydride powder leads to cracking of particles and formation of a large number of defects in the crystal structure, which are centres of accelerated formation of metallic phase nuclei and consequently channels for rapid desorption of hydrogen, leading to active decomposition of magnesium hydride.*
- *During uniaxial pressing, a small amount of hydrogen is released, resulting in the appearance of metallic magnesium nuclei. At a force 2400 kg/cm^2, the amount of hydrogen released is 1,4·10^{-3} wt%.*
- *Even without a catalyst, pressing accelerates hydrogen desorption, but with the use of a catalyst such as nickel, a more significant effect can be achieved, comparable to other mechanical and mechanochemical methods of activating magnesium hydride decomposition.*
- *The mathematical model used describes the experimental results well and confirms the proposed mechanism of H_2 desorption from MgH_2, which is as follows: nickel attached to the surface of the hydride particle allows hydrogen to desorb even at rather low temperatures. The desorption of hydrogen through the nickel channel is high, so the rate of hydride decomposition is rate limiting. Metallic magnesium appears on the surface of the particle, the area of which increases until a metallic shell is formed: the hydride core then begins to shrink.*
- *The desorption kinetic parameters obtained by mathematical modelling are in satisfactory agreement with those of unpressed magnesium hydride.*

– *Metal phase nucleations on the surface of MgH_2, regardless of the nature of appearance: its own metal (Mg) or a foreign metal desorption catalyst (Ni), are channels for rapid hydrogen desorption.*

The properties described above, which occur in magnesium hydride samples during mixing and uniaxial pressing with nickel, undoubtedly have a positive effect on the kinetics of hydrogen desorption, but in the course of experimental work another important fact was found and studied, namely the formation of intermetallides $MgNi_2$ and Mg_2Ni in such mixtures. From the literature it is known that the former does not form hydride under our conditions, while the latter reacts with hydrogen to form hydride Mg_2NiH_4. It has suitable hydrogen uptake/release kinetics for use under mild conditions and is therefore considered more suitable for hydrogen storage systems [90, 91]. Realisation in the field of application implies solving a number of problems, such as increasing the rate of hydrogen sorption-desorption processes and improving the cycling stability of the adsorbent material, so that in-depth studies of the physicochemical processes of formation and decomposition of intermetallic hydrides are required.

Chapter 4

Intermetallic hydrides based on Mg and Ni

4.1 Synthesis of intermetallide hydride Mg_2NiH_4

To investigate the properties of hydride intermetallide Mg2NiH4, samples of films on nickel substrate were synthesised. The synthesis was carried out on a high-pressure bench, the scheme of which is shown in Figure 2.3 (Chapter 2), by interaction of the nickel plate with magnesium hydride powder at a temperature of 450 °C and pressures exceeding the equilibrium pressures for hydride formation: both MgH_2 (≈4.6 MPa) and Mg_2NiH_4 (≈5.4-5.5 MPa) [94]. These values were obtained in hydride synthesis experiments, and they correspond to the middle of the absorption branch of the P-C diagram. The synthesis temperature of 450 °C proved to be the most suitable under these conditions, because at lower values the synthesis rate decreases sharply, and higher temperatures require higher pressures exceeding the capabilities of the bench.

The substrate used was technical rolled nickel with a thickness of 150 μm and a purity of 99.93%. The plate was cut into strips of 5x80 mm, these strips were washed with alcohol and then annealed in vacuum at 600 °C for 30 min. The properties of the magnesium hydride powder used are described in Chapter 2. It should be noted that for the synthesis of the intermetallic hydride, the MgH_2 powder was additionally ground by hand in a laboratory mortar to provide a larger contact surface between the powder particles and the nickel plate. After grinding, the particle size ranged from 1 to 50 μm. To produce the films, the nickel strips were placed in an autoclave and covered with magnesium hydride powder so that they did not touch the walls of the autoclave. In this way, the nickel strips were surrounded by magnesium hydride powder at all times during the synthesis of the Mg_2NiH_4 film.

The autoclave was evacuated and 'washed' three times with hydrogen: the gas was pumped to a pressure of 0.5-1 MPa and then pumped out to remove residual air

and adsorbed water. Hydrogen was then injected to working pressure and the sample was heated to the working temperature of 450 °C. The hydrogen pressure during the synthesis was above 6 MPa, so that the hydrides (MgH_2 and Mg_2NiH_4) could not decompose. The time is counted from the moment 450 °C was reached. This method allows hydride films of different thicknesses to be obtained in a reproducible manner. Possible synthesis mechanisms are discussed in section 3.2.

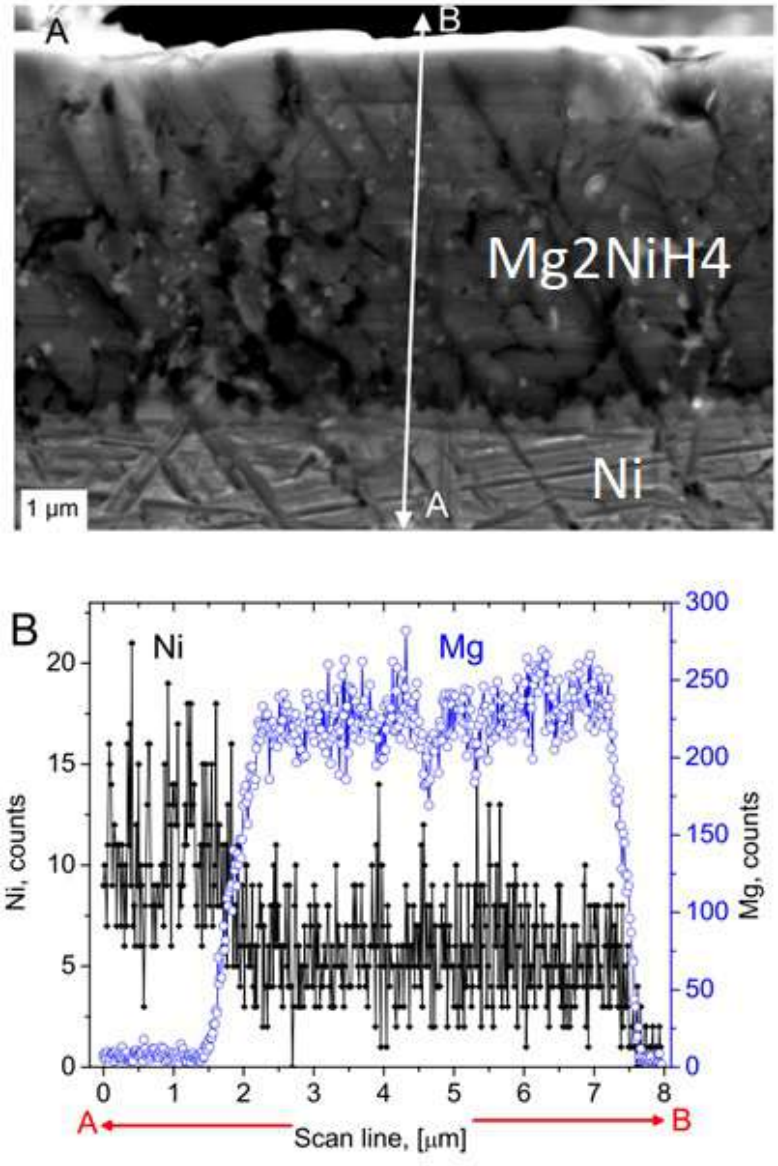

Figure 4.1 – (A) SEM cross section of the coating on the nickel substrate. (B) EDS scan results along the 'A-B' line in Fig. A

Several methods have been used to study the composition and crystal structure of the films obtained. Figure 4.1 shows the SEM (A) and elemental analysis (energy dispersive X-ray spectroscopy - EDS) (B) of a cross-section of a film with a nickel

substrate. The sample is oriented with the nickel substrate at the bottom and the hydride at the top. The white line 'A-B' shows where the EDS scan was performed. The synthesis time is four hours. From Figure 4.1 it can be seen that the nickel concentration decreases from the substrate to the film, while the magnesium concentration increases at this interface and remains almost constant with increasing film thickness. The extent of the transition region of the Mg signal is approximately 1 μm, which is comparable to the resolution of the EDS method.

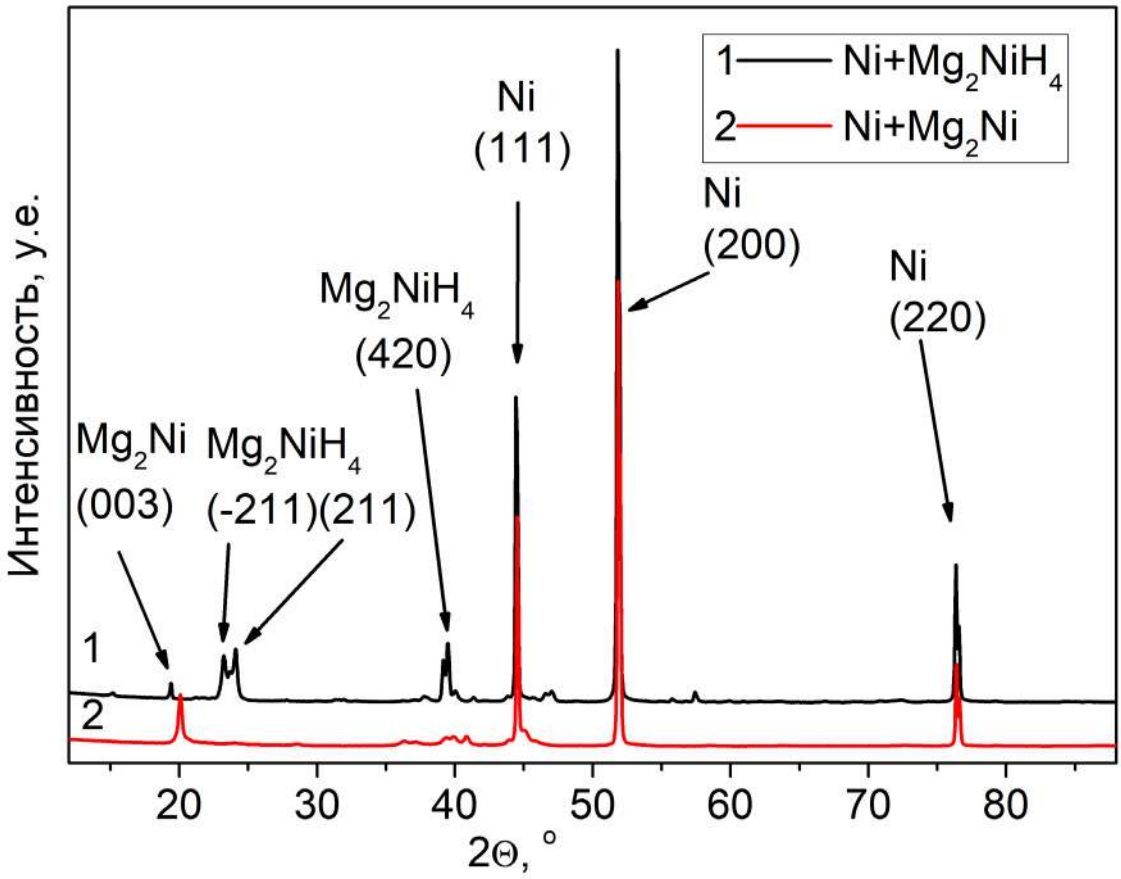

Figure 4.2 – XRD of polycrystalline Mg_2NiH_4 film on nickel substrate before and after hydrogen desorption

Figure 4.2 shows the X-ray diffraction pattern of a sample with a thickness of about 5 μm. Curve 1 corresponds to the original sample and contains, in addition to the most intense peaks of the nickel substrate, peaks characteristic of the hydride intermetallide Mg_2NiH_4 at angles *2θ*: 23°, 24° и 39,5°. Curve 2 was obtained on the same sample after heating in vacuum at 220 °C. During heating, hydrogen was released and, as can be seen from the figure, the Mg_2NiH_4 peak disappears and the

Mg_2Ni peak appears at 20° (*2θ*), hydride decomposition occurred and the Mg2Ni intermetallide was obtained. Figure 4.3 shows parts of the X-ray diagrams, which clearly show the presence of the hydride reflection of Mg_2NiH_4 after synthesis, but later, after desorption of hydrogen, it was replaced by the reflection of Mg_2Ni.

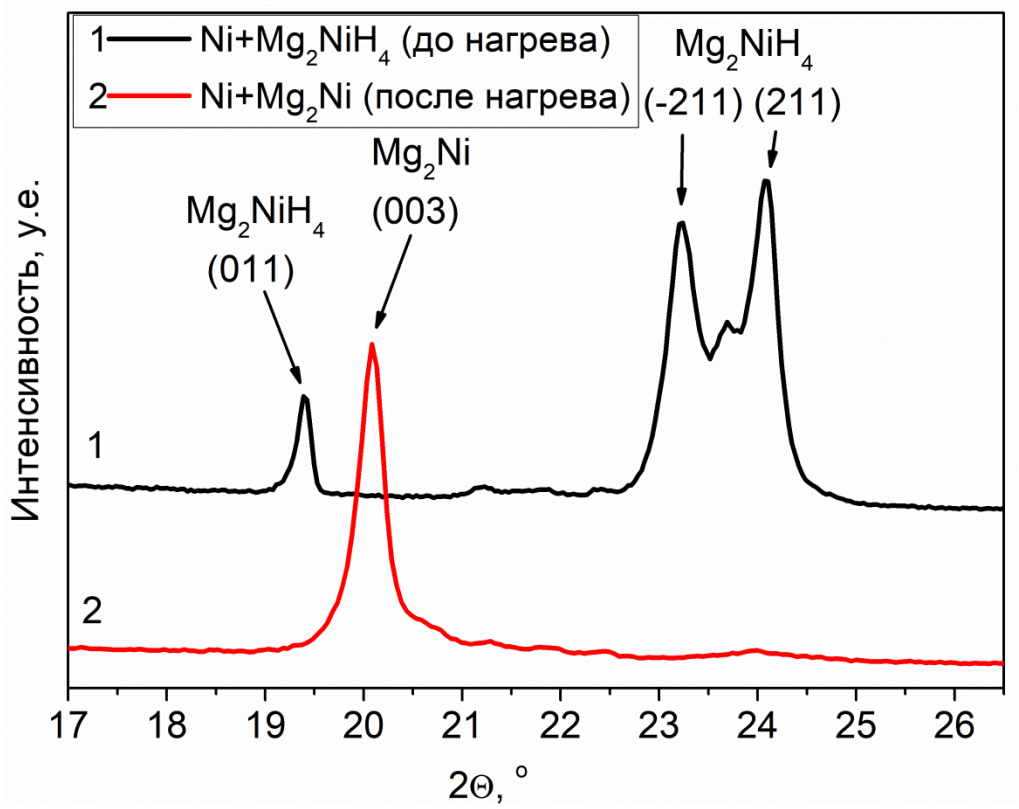

Figure 4.3 – Enlarged fragment of radiograph in Figure 4.2

The films obtained are quite thin, so the signal from the nickel substrate is much stronger, making accurate quantitative XRD of such results difficult. There is also a noticeable texture on the films. This is natural as the substrate is a polycrystalline nickel foil. In addition, many peaks corresponding to the film material are masked by the intense peaks of the nickel substrate. This is particularly the case for the two main peaks of $MgNi_2$ (43,9° и 44,8°), which are not labelled in Figure 4.3 because they are close to the Ni (111) peak (44,5°).

Table 4.1 – Phase content in wt% for samples before and after hydrogen desorption

wt.%	Mg_2NiH_4	Mg_2Ni	$MgNi_2$	Ni	Mg
before	36,6	-	5,9	57,6	-
after	-	23,3	16,6	59,2	0,94

Table 4.1 shows the results of X-ray diffraction analysis of the reaction products (wt%) for samples before and after hydrogen desorption. The data were obtained by full Rietveld analysis [95]. These data also confirm the presence of Mg_2NiH_4 after synthesis and its transformation into Mg_2Ni after hydrogen release. It should be noted that the intermetallic compound $MgNi_2$ is also present. This phase always appears during the synthesis of Mg_2NiH_4, but it does not form hydride.

The TDS method was used to evaluate the hydrogen content of the synthesised films. For this purpose, the coated nickel plates were cut into pieces with an area of 0.2 to 2 cm^2 (smaller area corresponds to longer synthesis time). Figure 4.4 shows a family of hydrogen desorption curves for films with different synthesis times (in hours) at a heating rate of 0.05 ºC/sec. The thicknesses corresponding to this family of curves are given in the legend.

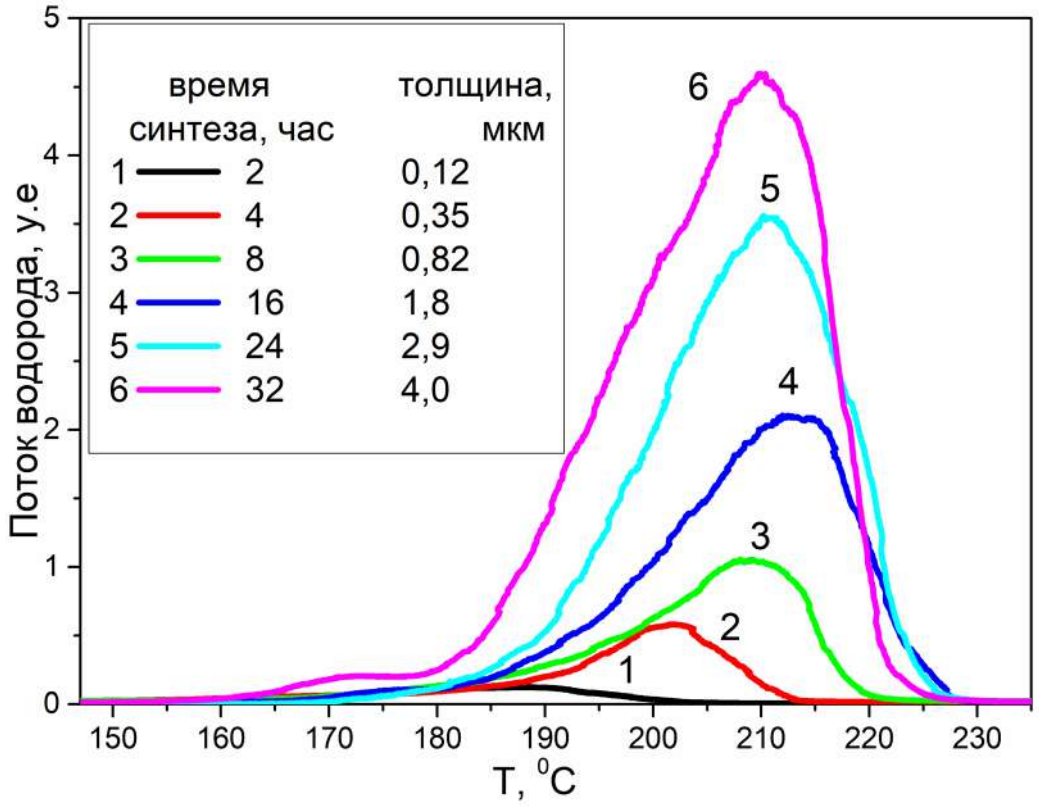

Figure 4.4 – Family of hydrogen desorption curves of Mg_2NiH_4 films of different thicknesses

The film thickness was calculated from the amount of desorbed hydrogen and the sample area, assuming the film is dense and homogeneous, and its density is 2.57 g/cm^3 [64]. The film thickness estimated in this way is similar to that obtained from the SEM cross section. For example, the cross section of the most coloured film (as shown in Figure 4.1) gives a thickness estimate of 4.8 μm of the volume, whereas the estimate based on the desorption of hydrogen gives 4.1 μm. The discrepancy between these values can be explained by the error of the RTD in constant pumping mode and by the inhomogeneity of the film thickness.

The hydrogen desorption temperature range of 180-220 °C for the Mg_2NiH_4 film at a heating rate of 3 °C/min is very close to the results for powder samples at similar heating rates: 220-350 °C at 2-8 °C/min in [96], 230–260 °C at 3 °C/min in [97], 220–260 °C at 5 °C/min in [98], 220–280 °C at 5 °C/min in [99]. The difference is explained by the fact that the results were obtained by differential scanning

calorimetry, i.e. in a gas flow, whereas when using an TDS there was constant pumping.

Thus, all the results obtained for the characterization of the films allow us to conclude that the synthesis described leads to the formation of polycrystalline Mg_2NiH_4 films on a nickel substrate.

4.2 Kinetics of Mg_2NiH_4 hydride film formation

Let us consider the region of the reaction flux. The source of nickel atoms is the substrate and hydrogen atoms at a pressure of 6 MPa can easily get here. Magnesium atoms from MgH_2 can only enter the reaction zone via the gas phase, since the decomposition of magnesium hydride does not take place. The synthesis experiment shows that Mg_2NiH_4 films are formed, so we can assume that at the synthesis temperature of 450 °C, magnesium hydride contains many hydrogen vacancies. As a result, clusters of metallic magnesium can form on the hydride particles and be transferred atom by atom from the MgH_2 particles through the gas to the growing Mg_2NiH_4 film.

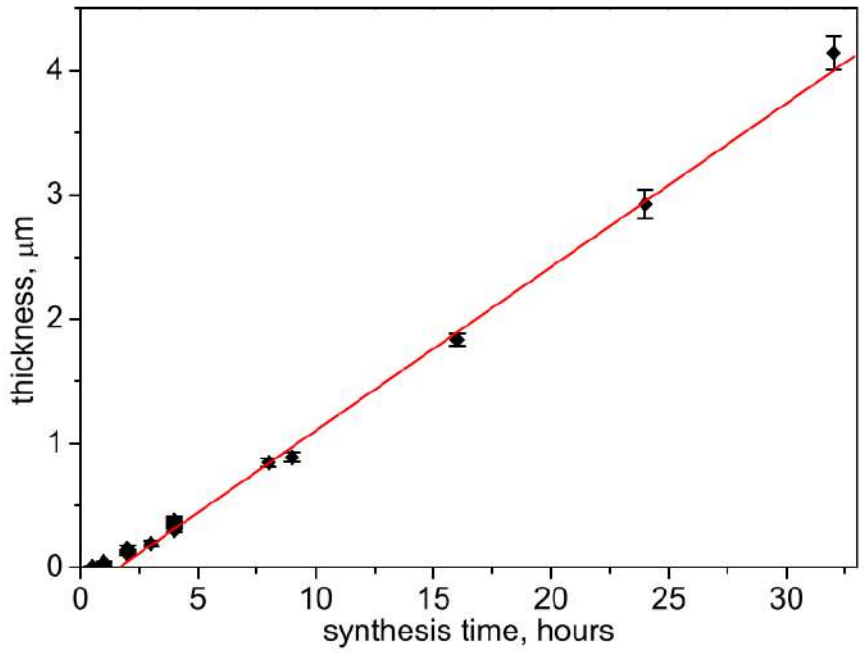

Figure 4.5 – Film thickness as a function of synthesis time

To evaluate the kinetics of film formation, a series of experiments with different synthesis times were carried out. Figure 4.5 shows the dependence of the film thickness on the synthesis time. The film thickness was estimated from the amount of hydrogen desorbed, as in the previous section. Figure 4.5 shows that the thickness of the Mg_2NiH_4 film grows almost linearly from about 2 h after the start of synthesis, as indicated by the red line in the figure, and that the linear approximation of the points does not cross the origin. This means that the Mg_2NiH_4 film starts to grow with a delay of at least one hour.

Figure 4.6 shows the X-ray images obtained for the film samples after synthesis for 1, 3 and 9 hours. Figure 4.6B shows the peaks corresponding to Mg_2NiH_4 and $MgNi_2$. They show that the Mg_2NiH_4 hydride is not yet present during the first hour, while the $MgNi_2$ intermetallide is already present in significant amounts. After three and nine hours we see almost the same amount of intermetallide, with the hydride layer increasing significantly. All the data obtained from the analysis of the radiographs, the TDS results and the $MgNi_2$ density of 6.03 g/cm^3 give an estimated thickness of 0.09 ± 0.02 μm.

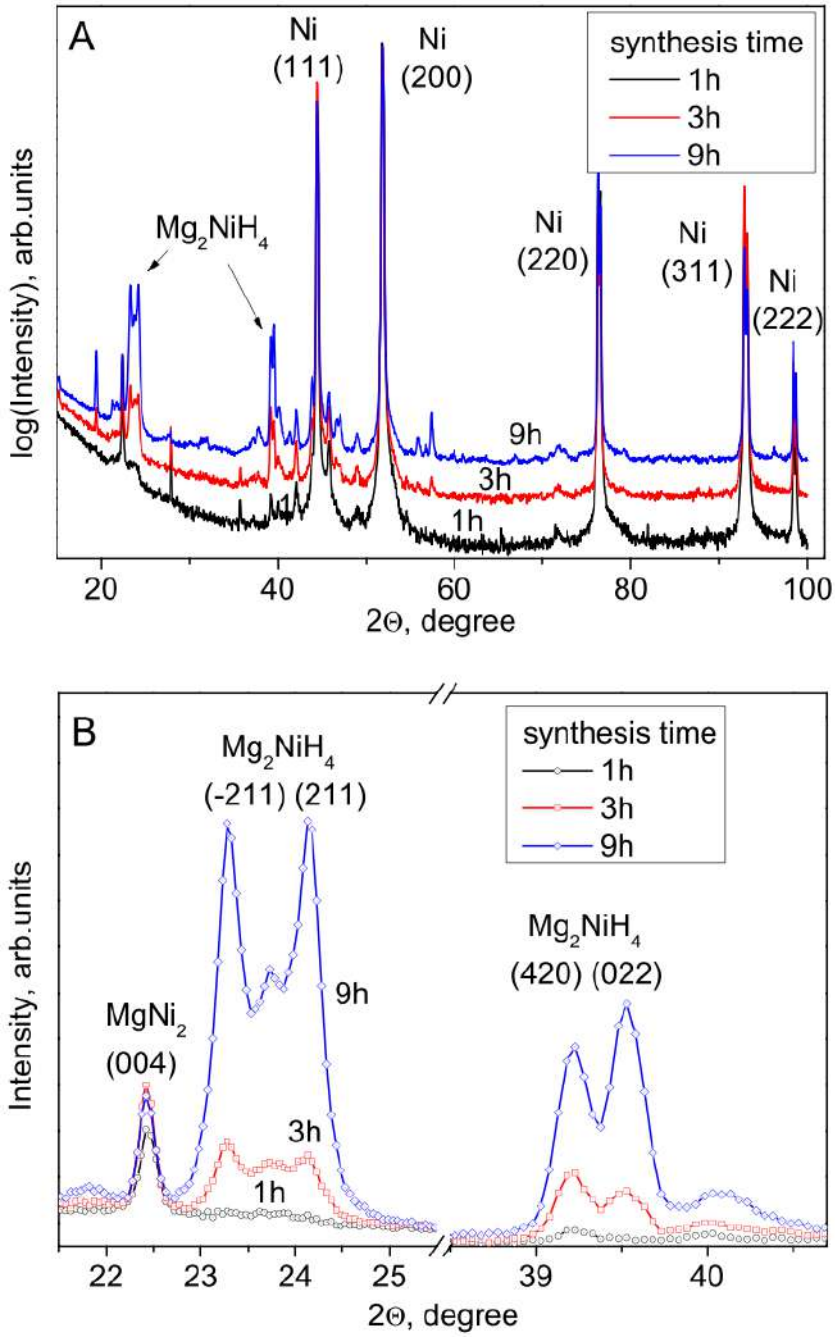

Figure 4.6 – (A) XRD of samples taken after synthesis for 1, 3 and 9 h, (B) enlarged sections of the XRD

It can be concluded that the $MgNi_2$ layer grows first on the nickel substrate and then the Mg_2NiH_4 hydride starts to grow on top of it. To achieve such film growth, the flow of nickel atoms into the reaction area is necessary. $MgNi_2$ is then synthesised on its outer surface, facing the gas phase, where MgH_2 hydride is initially present. At the same time, nickel atoms are transferred through this layer from the nickel substrate by diffusion. The $MgNi_2$ layer grows until the flux of nickel atoms becomes

too low due to the increase in diffusion length. After the formation of the hydride forming phase, Mg_2Ni becomes more efficient.

Thus, in the early stages of the reaction, when the $MgNi_2$ layer is thin, the flux of nickel into the reaction zone is large and a nickel-rich layer is formed. Then, when the $MgNi_2$ layer is thick enough, a Mg_2Ni layer with a lower nickel content begins to grow. This intermetallide, being hydride-forming, reacts with hydrogen to form the hydride Mg_2NiH_4. All this is possible at elevated temperature and pressure.

The slope of the red line in Figure 4.5 characterises the growth rate of Mg_2NiH_4, which is 0.13 μm/h. We can estimate how many nickel and magnesium atoms react in an area of 1 cm^2 per second: 10^{14} and $5 \cdot 10^{13}$ atoms/second respectively. These values are quite high if we consider that one of the reactants must be introduced into the reaction zone by diffusion, probably by a vacancy mechanism.

4.3 Mechanism of Mg_2NiH_4 hydride film formation on Ni substrate

A number of simplifications are made to describe the mechanism of hydride film and interface formation. The mechanism is based on the following physical assumptions:

- The films are planar, i.e. all model variables depend on a single spatial coordinate.
- The flux density of magnesium from the gas phase to the film-gas interface is constant.
- A layer of $MgNi_2$ is first formed on the nickel plate. After some time, about 2 hours under our conditions (see Fig. 4.5), the intermetallide Mg_2Ni is formed on top. This compound reacts with hydrogen to form the hydride Mg_2NiH_4. The thickness of the $MgNi_2$ layer remains unchanged.
- The growth of the Mg2NiH4 layer is time dependent and linear over 32 hours.

- There is always enough hydrogen in the film formation zone due to the high hydrogen pressure during the reaction and its high diffusion rate. The dissociation of hydrogen molecules is promoted by clusters (or possibly even a film) of metallic magnesium on the Mg_2NiH_4 layer. Mg is present in the reaction zone due to influx from the gas phase.

Let us therefore consider the formation of a Mg_2NiH_4 film on a nickel plate with an intermediate layer of $MgNi_2$. The magnesium atoms come from the gas phase at a constant temperature and a sufficiently high hydrogen pressure, so that the Mg_2NiH_4 hydride does not decompose.

It is now necessary to consider the assumed limits of the hydride film synthesis reaction:

1) Boundary $MgNi_2$-Mg_2NiH_4.
2) Boundary Mg_2NiH_4-gas.

We assume that the transport of magnesium and nickel atoms in the films is possible due to the vacancy mechanism. If we denote the concentrations of nickel atoms and vacancies as C_{Ni} and $C_{V(Ni)}$ respectively, then their sum is equal to the stoichiometric nickel concentration:

$$C_{Ni} + C_{V(Ni)} = C_{st(Ni)} = \text{const}(x, t).$$

The same applies to magnesium. We will use similar notation:

$$C_{Mg} + C_{V(Mg)} = C_{st(Mg)} = \text{const}(x, t).$$

Figure 4.7 shows the spatial concentrations of magnesium and nickel. The red line marks the reaction boundary. In both cases, the $MgNi_2$ film has already formed (it occupies the region from 0 to l_1) and a new Mg_2NiH_4 film is in the process of forming (from 0 to $l_2(t)$).

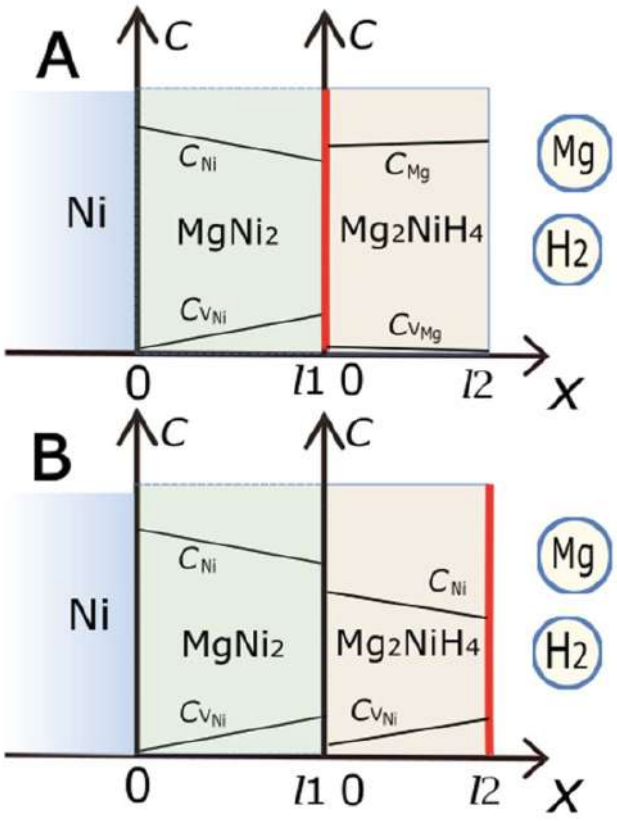

Figure 4.7 – Scheme of the spatial distribution of the Mg and Ni concentrations. Synthesis takes place at the interface:

(A) $MgNi_2$-Mg_2NiH_4 interface,

(B) Mg_2NiH_4-gas interface.

Obviously, the film growth rate can only be constant if one of the following conditions is met:

• Option 1: Reagent flow densities are constant and in the required ratio to fully utilise the components entering the reaction zone.

• Option 2. One of the reagents is added at a constant rate and the other is in excess and its high concentration is constant.

Let us consider two scenarios for hydride film synthesis. Suppose that a film of Mg_2NiH_4 is formed at the $MgNi_2$ - Mg_2NiH_4 interface. Transients are not considered. The schematic concentration distribution is shown in Figure 4.7A. Taking into account the constancy of the $MgNi_2$ film thickness, we have the following constant flux density of nickel J_{Ni} into the reaction zone:

$$J_{Ni}(l_1) = -D_{Ni}\frac{C_{Ni}(0) - C_{Ni}(l_1)}{l_1}$$

where D_{Ni} is the diffusion coefficient of nickel in $MgNi_2$. At first sight, this supports the possibility of variant 1, but the constancy of the flux density of magnesium atoms is impossible if their diffusive transport in the growing layer of Mg_2NiH_4 is limited. Similar formula for magnesium:

$$J_{Mg}(0) = -D_{Mg}\frac{C_{Mg}(l_2) - C_{Mg}(0)}{l_2}$$

where D_{Mg} is the diffusion coefficient of magnesium in $MgNi_2$, shows that the flux density decreases with increasing thickness l_2.

Option 2 requires a quasi-equilibrium concentration of magnesium from the gas phase. The concentration decreases because the reaction is slow compared to the exchange from the gas phase. In this case, the high diffusion rate ensures that the Mg concentration is spatially constant throughout the thickness of the Mg_2NiH_4 film.

It can therefore be assumed that the magnesium concentration in the Mg_2NiH_4 layer is constant along the entire boundary: $C_{Mg}(x)$=const, $x \in (0;l_2)$, and the thickness of the film formed ensures the constancy of the reaction rate over the times considered. Obviously, further growth of the thickness and consequently of the diffusion coefficient of the magnesium atoms will at some point make quasi-equilibrium impossible and the film growth rate will decrease. However, linear film growth was observed in the experiments carried out.

Another scenario for film formation suggests that the reaction takes place at the Mg_2NiH_4-gas interface. Figure 5.7B shows the schematic concentration distribution. Magnesium atoms exchange rapidly with this surface and the gas phase. Consequently, there are always sufficient magnesium atoms available, so only option 2 should be considered.

The diffusion flux density of nickel atoms into the reaction zone is equal to

$$J_{Ni}(l_2) = -D^*_{Ni}\frac{C_{Ni}(0) - C_{Ni}(l_2)}{l_2(t)}$$

similar formula, but with a different diffusion coefficient D_{Ni}^* (Ni atoms in Mg_2NiH_4). The flux density cannot be constant due to the growth of the film thickness, and the second possibility seems unlikely. It is also difficult to assume a quasi-equilibrium nickel concentration, as we did for magnesium when considering the first scenario, because of the slow transport of nickel through the $MgNi_2$ film. The impossibility of this scenario is confirmed by the structure of the Mg_2NiH_4 hydride, which represents NiH_4 tetrahedra in the lattice of Mg atoms. Analysis of the corresponding total density of states shows that the Ni-H bonds are strongly covalent [100]. A similar conclusion follows from the analysis of the overlap populations obtained from density functional theory calculations in [101]. This means that for each jump the nickel atom must simultaneously break bonds with four hydrogen atoms. The probability of such a break seems low, so this transport must be slow.

Given all this, the first scenario seems the most likely: the formation of a Mg_2NiH_4 film at the $MgNi_2$-Mg_2NiH_4 interface. Nickel atoms flow through the $MgNi_2$ intermetallic layer and the density of this flow determines the growth rate of the film.

Conclusions:

- *The technique of synthesizing Mg_2NiH_4 film on the surface of nickel plate surrounded by magnesium hydride in hydrogen atmosphere was proposed. The synthesis temperature was 450 °C, the hydrogen pressure was high enough, not less than 6 MPa, to prevent the decomposition of Mg_2NiH_4 and MgH_2 hydrides.*
- *The study of the films obtained showed that a dense polycrystalline film of Mg_2NiH_4 hydride appears on a thin sublayer of $MgNi_2$ intermetallide with a thickness of about 0.09 μm.*
- *By changing the synthesis time from 2 to 32 hours, films with thicknesses from 0.2 to 4 μm could be produced.*

- *The analysis of the growth kinetics of the crystalline structure of the material allowed the synthesis reaction at the interface of $MgNi_2$ and Mg_2NiH_4 layers to be adequately described. The mechanism of film formation at the $MgNi_2$-Mg_2NiH_4 interface with a constant growth rate is described.*
- *For the synthesis conditions presented above, the film growth rate was constant and was 0.13 μm/h. This value corresponds to flux densities of 10^{14} and $5 \cdot 10^{13}$ atoms/(s·cm^2) for magnesium and nickel, respectively.*

Summary

- The activation of the thermal decomposition of magnesium hydride by the addition of catalyst powders with and without pressing corresponds to the previously established mechanisms: rapid desorption of hydrogen through the metal channel of the foreign metal particles and subsequent expansion of this channel.
- An effective mechanical method of uniaxial pressing to activate the desorption of magnesium hydride has been developed and tested. The method is quite simple to use and comparable in efficiency to other known mechanical methods (ball mill grinding, cold forging and rolling), reducing the decomposition temperature to 280°C.
- During the uniaxial pressing of magnesium hydride, the following processes take place which lead to the activation of thermodesorption:
  1) Splitting of magnesium hydride particles reveals the metallic core left over from direct synthesis;
  2) Formation of a large number of defects in the crystal structure, which can be centres of accelerated formation of metallic phase nuclei;
  3) When the force is applied and released, some hydrogen is released, resulting in the appearance of metallic magnesium nuclei. At a force of 2400 kg/cm^2, the amount of hydrogen released is $1.4 \cdot 10^{-3}$ wt%.

- A probable mechanism of hydrogen thermodesorption from magnesium hydride pressed with nickel powder is proposed and confirmed by a valid mathematical model. The approximation results obtained are in good agreement with the experimental data.
- - The technique of synthesis of Mg_2NiH_4 film on the surface of nickel plate surrounded by magnesium hydride in hydrogen atmosphere at pressure exceeding the decomposition pressure of Mg_2NiH_4 has been developed, which allowed to create dense crystalline films with thickness from 0.2 to 4 μm by increasing the synthesis time from 2 to 32 hours.

- The mechanism of film formation at the $MgNi_2$-Mg_2NiH_4 interface is described. The limiting factor is the diffusion of nickel through a thin sublayer of $MgNi_2$ intermetallide. The growth rate of the film thickness was found to be 0.13 μm/h.

Acknowledgements

I would like to express my sincere gratitude to my supervisor Professor Igor Evgenyevich Gabis, for setting the research problem, assistance in planning experiments and interpreting the results obtained, invaluable contribution to the writing of the thesis. Thanks to Igor Evgenyevich I have gained valuable knowledge and scientific experience.

I express my gratitude to Evgeny Alexandrovich Denisov, who was my supervisor in the Master's programme. With him I got acquainted with a new direction of science: "Hydrogen interaction with solid state" and learnt the peculiarities of working in a scientific environment.

I would like to express my special gratitude to Voyt Alexey Petrovich, for his help in mastering the technique of thermal desorption spectroscopy, preparing the experiments, and interpreting and discussing the results.

I would like to express my deep gratitude to the co-authors of the scientific publications: Professor Baraban Alexander Petrovich; Chernov Ilya Alexandrovich;. Dmitriev Valentin Alexandrovich; Dobrotvorsky Mstislav Alexandrovich; Shikin Ilya Viktorovich, Kuznetsov Vladimir Georgievich.

I would like to thank my colleagues from Laser Diagnostics of Plasma and Plasma-Surface Interaction Laboratory (Ioffe Institute) for the time they spent reading my thesis and for their critical comments, which helped to improve the text of the work: Mukhin Evgeny Evgenyevich, Razdobarin Alexey Gennadievich, Medvedev Oleg Sergeyevich, Dmitriev Artem Mikhailovich; and I would like to thank Zalavutdinov Rinad Harisovich from IPCE RAS for help in proofreading the text of the thesis.

I would like to thank the entire staff of the MRC 'Nanotechnologies' of SPbU for the preparation and execution of additional research, and I would like to express my special thanks to Anton Loshachenko and Denis Danilov.

To my relatives and friends, I am grateful for their boundless support, patience and belief in me. I cannot imagine my scientific path without my parents - Elets Tatiana Vasilievna and Elets Igor Gennadievich. Special thanks for the support of my

brother Elets Mikhail Igorevich. I am immensely grateful to my wife Elets Alisa Sergeevna and my son Elets Maxim Denisovich for all the care and love they give me on a daily basis.

References

1. Chen D. et al. Alloying effects of transition metals on chemical bonding in magnesium hydride MgH 2. 2004. Vol. 52. P. 521–528.

2. Ali N.A., Ismail M. Advanced hydrogen storage of the Mg – Na – Al system : A review // J. Magnes. Alloy. Elsevier B.V., 2021. Vol. 9, № 4. P. 1111–1122.

3. Gabis I.E. et al. Thermal and Photoactivation of Aluminum Hydride Decomposition // Russ. J. Phys. Chem. A. 2012. Vol. 86, № 11. P. 1736–1741.

4. Johnson S.R. et al. Chemical activation of MgH2: a new route to superior hydrogen storage materials // Chem. Commun. 2005. Vol. 22. P. 2823–2825.

5. Webb C.J. Journal of Physics and Chemistry of Solids A review of catalyst-enhanced magnesium hydride as a hydrogen storage material // J. Phys. Chem. Solids. Elsevier, 2015. Vol. 84. P. 96–106.

6. Varin, R. A., Zbroniec, L., Polanski, M., & Bystrzycki J. A Review of Recent Advances on the Effects of Microstructural Refinement and Nano-Catalytic Additives on the Hydrogen Storage Properties of Metal and Complex Hydrides // Energies. 2011. Vol. 4, № 1. P. 1–25.

7. Zhou C., Peng Y., Zhang Q. Journal of Materials Science & Technology Growth kinetics of MgH 2 nanocrystallites prepared by ball milling // J. Mater. Sci. Technol. The editorial office of Journal of Materials Science & Technology, 2020. Vol. 50. P. 178–183.

8. Leiva D.R. et al. Nanostructured MgH 2 prepared by cold rolling and cold forging // J. Alloys Compd. Elsevier B.V., 2011. Vol. 509. P. S444–S448.

9. Skryabina N. et al. Impact of Severe Plastic Deformation on the stability of MgH 2 // J. Alloys Compd. Elsevier B.V., 2015. Vol. 645. P. S14–S17.

10. Botta W.J. et al. Metallurgical processing of Mg alloys and MgH2 for hydrogen storage // J. Alloys Compd. Elsevier, 2022. Vol. 897. P. 162798.

11. Yu H., Bennici S., Auroux A. Hydrogen storage and release : Kinetic and thermodynamic studies of MgH 2 activated by transition metal nanoparticles // Int. J. Hydrogen Energy. Elsevier Ltd, 2014. Vol. 39, № 22. P. 11633–11641.

12. Gialanella S. et al. CALPHAD : Computer Coupling of Phase Diagrams and Thermochemistry Microstructural refinement using ball-milling and spark-plasma sintering of MgH 2 based materials for hydrogen storage // CALPHAD Comput. Coupling Phase Diagrams\ Thermochem. Elsevier Ltd, 2009. Vol. 33, № 1. P. 82–88.

13. R. Martínez-Coronado, M. Retuerto, B. Torres, M.J. Martínez-Lope, M.T. Fernández-Díaz J.A.A. High-pressure synthesis , crystal structure and cyclability of the Mg 2 NiH 4 hydride // Int. J. Hydrogen Energy. 2013. Vol. 8, № 14. P. 5738–5745.

14. Yartys V.A. et al. ScienceDirect Magnesium based materials for hydrogen based energy storage : Past , present and future // Int. J. Hydrogen Energy. Elsevier Ltd, 2019. Vol. 44, № 15. P. 7809–7859.

15. Yong H. et al. Hydrogen storage behavior of Mg-based alloy catalyzed by carbon-cobalt composites // J. Magnes. Alloy. Elsevier B.V., 2021. Vol. 9, № 6. P. 1977–1988.

16. Oumellal Y. et al. Metal hydrides for lithium-ion batteries. 2008. Vol. 7, № November.

17. Chem J.M. Magnesium hydride as a high capacity negative electrode for lithium ion. 2012. P. 14531–14537.

18. Sougrati M.T., Jumas J., Aymard L. Reactivity of complex hydrides Mg 2

FeH 6 , Mg 2 CoH 5 and Mg 2 NiH 4 with lithium ion : Far from equilibrium electrochemically driven conversion reactions. 2013. Vol. 8. P. 0–10.

19. Aymard L., Oumellal Y., Bonnet J.P. Metal hydrides: An innovative and challenging conversion reaction anode for lithium-ion batteries // Beilstein J. Nanotechnol. 2015. Vol. 6, № 1. P. 1821–1839.

20. Zeng L., Kawahito K., Ichikawa T. Metal Hydride-Based Materials as Negative Electrode for All- Solid-State Lithium-Ion Batteries // Alkali-ion Batter. 2016.

21. Qian Z. et al. Atomistic Modeling of Various Doped Mg2NiH4 as Conversion Electrode Materials for Lithium Storage // Crystals. 2019. Vol. 9, № 5. P. 254.

22. S T.G.F.R. Magazine and Journal of Science LXIX . On the absorption and dialytic separation of gases by colloid septa. 2009. Vol. 5982, № May.

23. Гебхардт Е., Фромм Е. Газы и углерод в металлах. 1980. 710 p.

24. Габис И.Е., Чернов И.А. Кинетика разложения гидридов металлов. 2014. 138 p.

25. Aguey-Zinsou K.F., Ares-Fernández J.R. Hydrogen in magnesium: New perspectives toward functional stores // Energy Environ. Sci. 2010. Vol. 3, № 5. P. 526–543.

26. Sandrock G. A panoramic overview of hydrogen storage alloys from a gas reaction point of view // J. Alloys Compd. 1999. Vol. 295. P. 877–888.

27. Beyer W. Diffusion and evolution of hydrogen in hydrogenated amorphous and microcrystalline silicon. 2003. Vol. 78. P. 235–267.

28. Nordlander P. Hydrogen adsorption on metal surfaces p. nordlander. 1984. Vol. 136. P. 59–81.

29. Science E.S., Physics A.M., Technology A. Electronic factors determining the reactivity of metal surfaces. 1995. Vol. 343. P. 211–220.

30. Schlapbach L., Schlapbach L., Züttel A. L. Schlapbach and A. Züttel, Nature, 2001, 414, 353. // Nature. 2001. Vol. 414, № May 2016. P. 353–358.

31. Zachariasen W.H., Holley C.E., Stamper J.F. Neutron diffraction study of magnesium deuteride // Acta Crystallogr. International Union of Crystallography, 1963. Vol. 16, № 5. P. 352–353.

32. Bortz M. et al. Structure of the high pressure phase λ-MgH2 by neutron powder diffraction // J. Alloys Compd. 1999. Vol. 287, № 1–2. P. 4–6.

33. Shantilal Gangrade A. et al. The dehydrogenation mechanism during the incubation period in nanocrystalline MgH2 // Phys. Chem. Chem. Phys. 2017. Vol. 19, № 9. P. 6677–6687.

34. Vajeeston P. et al. Structural stability and pressure-induced phase transitions in MgH2 // Phys. Rev. B - Condens. Matter Mater. Phys. 2006. Vol. 73, № 22. P. 1–8.

35. Jolibois M.P. Hydrolysis of magnesium hydride in the presence of ammonium salts // Compt. Rend. Acad. Sci. 1912. Vol. 155, № 5. P. 353–355.

36. Wiberg E., Goelttzer H. B.R. Notizen: Synthese von Magnesiumhydrid aus den Elementen // Z. Naturforsch. 1951. Vol. 6b, № 7. P. 394–395.

37. Дымова Т. Н., Стерлядкина З. К. Е.Н.Г. О некоторых свойствах гидрида магния // Журнал неорганической химии. 1961. Vol. 6, № 4. P. 768–773.

38. Bogdanovic B., Liac S., Schwickardi M., Sikorsky P. S.B. Katalitiche Synthese von Magnesiumhydrid unter milden Bedingungen // Angew. Chem. 1980. Vol. 92, № 10. P. 1980.

39. Vigeholm B., Kjøller J., Larsen B. Magnesium for hydrogen storage // J. Less

Common Met. 1980. Vol. 74, № 2. P. 341–350.

40. F. H. Ellinger, C. E. Holley Jr., B. B. McInteer, D. Pavone, R. M. Potter, E. Staritzky W.H.Z. The Preparation and Some Properties of Magnesium Hydride // J. Am. Chem. Soc. 1955. Vol. 77, № 9. P. 2648–2648.

41. A. Zaluska, L. Zaluski J.O.S. Nanocrystalline magnesium for hydrogen storage // J. Alloys Compd. 1999. Vol. 288, № 1–2. P. 217–225.

42. Gabis I.E. et al. A mechanism of ultraviolet activation of the α-AlH3 decomposition // Int. J. Hydrogen Energy. 2014. Vol. 39, № 28. P. 15844–15850.

43. Evard E., Gabis I., Yartys V.A. Kinetics of hydrogen evolution from MgH 2 : Experimental studies , mechanism and modelling // Int. J. Hydrogen Energy. Elsevier Ltd, 2010. Vol. 35, № 17. P. 9060–9069.

44. Sanchez C.R., Fernandez J.F. R ate determining step in the absorption and desorption of hydrogen by magnesium * , // J. Alloy. Compd. Alloy. Compd. 2002. Vol. 340. P. 189–198.

45. Vigeholm B. et al. Elements of hydride formation mechanisms in nearly spherical magnesium powder particles // B. Vigeholm, K. Jensen, B. Larsen, A.Schrøder. 1987. Vol. 131, № 1–2. P. 133–141.

46. Cheng H. et al. ScienceDirect performances of MgH 2 with Pd-Ni bimetallic nanoparticles supported by mesoporous carbon // Int. J. Hydrogen Energy. Elsevier Ltd, 2019. Vol. 44, № 21. P. 10777–10787.

47. Hjort P., Krozer A., Kasemo B. Hydrogen sorption kinetics in partly oxidized Mg films // J. Alloy. Compd. Alloy. Compd. 1996. Vol. 237. P. 74–80.

48. J. F. Stampfer Jr., C. E. Holley Jr. J.F.S. The Magnesium-Hydrogen System // J. Am. Chem. Soc. 1960. Vol. 82, № 14. P. 3504–3508.

49. Габис И.Е., Чернов И.А. Кинетика разложения бинарных гидридов

металлов. Москва: Ай Пи Ар Медиа, 2023. 140 p.

50. Pedersen A., Andreasen A. Preparation and characterization of new metals and alloys for hydrogen storage // Presentation at NORSTORE conference/workshop, Stavern, Norway. 2004.

51. Bloch J., Mintz M.H. Kinetics and mechanisms of metal hydrides formation—a review // J. Alloys Compd. 1997. Vol. 253–254. P. 529–541.

52. Ke X., Kuwabara A., Tanaka I. Cubic and orthorhombic structures of aluminum hydride AlH 3 predicted by a first-principles study // Phys. Rev. B. 2005. Vol. 71, № 18. P. 184107.

53. Van Setten M.J. et al. Electronic structure and optical properties of lightweight metal hydrides // Phys. Rev. B - Condens. Matter Mater. Phys. 2007. Vol. 75, № 3. P. 1–13.

54. Gabis I.E. et al. Ultraviolet activation of thermal decomposition of α-alane // Int. J. Hydrogen Energy. Elsevier, 2012. Vol. 37, № 19. P. 14405–14412.

55. Liang G. et al. Catalytic effect of transition metals on hydrogen sorption in nanocrystalline ball milled MgH 2 –Tm (Tm 5 Ti, V, Mn, Fe and Ni) systems // J. Alloys Compd. 1999. Vol. 292. P. 247–252.

56. Zaluska A., Zaluski L. New catalytic complexes for metal hydride systems // J. Alloys Compd. 2005. Vol. 406. P. 706–711.

57. Bobet J., Akiba E., Darriet B. Study of Mg-M (M = Co , Ni and Fe) mixture elaborated by reactive mechanical alloying : hydrogen sorption properties // Int. J. Hydrogen Energy. 2001. Vol. 26. P. 493–501.

58. Oelerich W., Klassen T., Bormann R. Metal oxides as catalysts for improved hydrogen sorption in nanocrystalline Mg-based materials. 2001. Vol. 315. P. 237–242.

59. Blomqvist H. et al. Competing stabilisation mechanisms in Mg 2NiH 4 // J.

Alloys Compd. 2002. Vol. 330–332. P. 268–270.

60. Zolliker P., Yvon K., Baerlocher C.J. Structural Studies of the Hydrogen Storage Material Mg2NiH4. Part 2. Monoclinic Low-Temperature Structure // Inorg. Chem. 1986. Vol. 25, № 20. P. 3590–3593.

61. Zolliker P., Yvon K., Baerlocher C.J. Low-temperature structure of Mg2NiH4: Evidence for microtwinning // J. Less Common Met. 1986. Vol. 115, № 1. P. 65–78.

62. Noréus D., Kihlborg L. Twinning at the unit cell level in the low temperature phase of Mg2NiH4 studied by electron microscopy // J. Less-Common Met. 1986. Vol. 123, № 1–2. P. 233–239.

63. Massalski T. B. et al. Binary alloy diagrams // Am. Soc. Met. Met. Park OH. 1986. Vol. 44073, № 1. P. 2.

64. Reilly J.J., Wiswall R.H. The Reaction of Hydrogen with Alloys of Magnesium and Nickel and the Formation of Mg2NiH4 // Inorg. Chem. 1968. Vol. 7, № 11. P. 2254–2256.

65. Hatano Y., Watanabe K. Hydrogenation of MgNi2 by atomic hydrogen at elevated temperatures // Mater. Trans. 2002. Vol. 43, № 5. P. 1105–1109.

66. Simchi H., Kaflou A., Simchi A. Synergetic effect of Ni and Nb2O5 on dehydrogenation properties of nanostructured MgH2 synthesized by high-energy mechanical alloying // Int. J. Hydrogen Energy. Elsevier Ltd, 2009. Vol. 34, № 18. P. 7724–7730.

67. Gajdics M. et al. Characterization of a nanocrystalline Mg–Ni alloy processed by high-pressure torsion during hydrogenation and dehydrogenation // Int. J. Hydrogen Energy. 2016. Vol. 41, № 23. P. 9803–9809.

68. Révész Á., Gajdics M., Spassov T. Microstructural evolution of ball-milled

Mg-Ni powder during hydrogen sorption // Int. J. Hydrogen Energy. 2013. Vol. 38, № 20. P. 8342–8349.

69. Shao H. et al. Preparation and hydrogen storage properties of nanostructured Mg-Ni BCC alloys // J. Alloys Compd. 2009. Vol. 477, № 1–2. P. 301–306.

70. Sheppard D.A. et al. Methods for accurate high-temperature Sieverts-type hydrogen measurements of metal hydrides // J. Alloys Compd. Elsevier B.V, 2019. Vol. 787. P. 1225–1237.

71. Rietveld H.M. A profile refinement method for nuclear and magnetic structures // J. Appl. Crystallogr. International Union of Crystallography, 1969. Vol. 2, № 2. P. 65–71.

72. McCusker, L. B., Von Dreele, R. B., Cox, D. E., Louër, D., & Scardi P. Rietveld refinement guidelines // J. Appl. Crystallogr. 1999. Vol. 32, № 1. P. 36–50.

73. The International Centre for Diffraction Data. База данных по порошковой дифракции ICDD-2011-PDF-2 [Electronic resource] // icdd.com. 2024. URL: url: http://www.icdd.com.

74. Haines P.J., Reading M., Wilburn F.W. Differential Thermal Analysis and Differential Scanning Calorimetry // Handbook of Thermal Analysis and Calorimetry. Elsevier Masson SAS, 1998. Vol. 1. 279–361 p.

75. Zhang S. et al. The synthesis and hydrogen storage properties of a MgH 2 incorporated carbon aerogel scaffold // Nanotechnology. 2009. Vol. 20, № 20. P. 204027.

76. Crivello J.C. et al. Review of magnesium hydride-based materials: development and optimisation // Appl. Phys. A Mater. Sci. Process. 2016. Vol. 122, № 2. P. 1–20.

77. Chin S. Recent progress in the development and properties of novel metal

matrix nanocomposites reinforced with carbon nanotubes and graphene nanosheets // Mater. Sci. Eng. R. Elsevier B.V., 2013. Vol. 74, № 10. P. 281–350.

78. Lototskyy M. Magnesium – carbon hydrogen storage hybrid materials produced by reactive ball milling in hydrogen // Carbon N. Y. Elsevier Ltd, 2013. Vol. 57. P. 146–160.

79. Jensen T.R. et al. Dehydrogenation kinetics of pure and nickel-doped magnesium hydride investigated by in situ time-resolved powder X-ray diffraction // Int. J. Hydrogen Energy. 2006. Vol. 31. P. 2052–2062.

80. Elets D. et al. Influence of uniaxial pressing and nickel catalytic additive on activation of magnesium hydride thermal decomposition // Int. J. Hydrogen Energy. Elsevier Ltd, 2017. Vol. 42, № 39. P. 24877–24884.

81. Baraban A.P. et al. Synthesis of a Thin Metal Hydride Mg 2 NiH 4 Film on a Nickel Substrate // Crystallogr. Reports. 2024. Vol. 69, № 1. P. 93–101.

82. Zhang J. et al. The effects of crystalline defects on hydrogen absorption kinetics of catalyzed MgH2 at ambient conditions // J. Alloys Compd. Elsevier, 2022. Vol. 927. P. 167090.

83. Duan C. et al. Journal of Materials Science & Technology The impact of vacancy defective MgH 2 (001)/(110) surface on the dehydrogenation of MgH 2 @ Ni-CNTs : A mechanistic investigation // J. Mater. Sci. Technol. 2024. Vol. 189. P. 77–85.

84. Voyt A.P. et al. Hydrogen Release from Magnesium Hydride Subjected to Uniaxial Pressing // Mater. Sci. 2019. Vol. 54, № 6. P. 810–818.

85. de Rango P. et al. Nanostructured magnesium hydride for pilot tank development // J. Alloys Compd. 2007. Vol. 446–447. P. 52–57.

86. Chaise A. et al. Experimental and numerical study of a magnesium hydride

tank // Int. J. Hydrogen Energy. Elsevier Ltd, 2010. Vol. 35, № 12. P. 6311–6322.

87. Shikin I. V. et al. Activation of magnesium hydride by pressing with catalytic additives // Tech. Phys. Lett. 2017. Vol. 43, № 2. P. 190–193.

88. Gabis I.E., Chernov I.A., Voyt A.P. Decomposition kinetics of metal hydrides : Experiments and modeling // J. Alloys Compd. Elsevier B.V., 2013. Vol. 580. P. S243–S246.

89. Chernov I.A., Bloch J., Gabis I.E. Mathematical modelling of UH 3 formation // Int. J. Hydrogen Energy. Elsevier Ltd, 2008. Vol. 33, № 20. P. 5589–5595.

90. Huot J. et al. Structural study and hydrogen sorption kinetics of ball-milled magnesium hydride // J. Alloys Compd. 1999. Vol. 295. P. 495–500.

91. Gennari F.C., Castro F.J., Urretavizcaya G. Hydrogen desorption behavior from magnesium hydrides synthesized by reactive mechanical alloying // J. Alloys Compd. 2001. Vol. 321. P. 46–53.

92. Семененко К.Н., Вербецкий В.Н., Кочуков А.В. Взаимодействие с водородом сплавов системы магний - лантан // Доклады Ан СССР. 1981. Vol. 258. P. 362.

93. Вербецкий В.Н., Митрохин С.В. Гидриды интерметаллических соединений-синтез, свойства и применение для аккумулирования водорода // Альтернативная энергетика и экология. Альтернативная энергетика и экология. 2005. № 10. P. 41–61.

94. Baraban A.P. et al. The Mg2NiH4 film on nickel substrate: synthesis, properties and kinetics of formation // Thin Solid Films. Elsevier B.V., 2022. Vol. 762, № October. P. 139556.

95. Vaitkus A., Merkys A., Graz S. cif applications Validation of the

Crystallography Open Database using the Crystallographic Information Framework cif applications // J. Appl. Crystallogr. 2021. Vol. 54, № 2. P. 661–672.

96. Gajdics M. et al. Dehydrogenation-hydrogenation characteristics of nanocrystalline Mg 2 Ni powders compacted by high-pressure torsion a v e // ournal Alloy. Compd. 2017. Vol. 702. P. 84–91.

97. Atias-adrian I.C. et al. Development of nanostructured Mg 2 Ni alloys for hydrogen storage applications // Int. J. Hydrogen Energy. Elsevier Ltd, 2011. Vol. 36, № 13. P. 7897–7901.

98. Chen J. et al. High pressure experiments on the Mg2Ni and Mg2NiH4-H systems // J. Alloys Compd. 2002. Vol. 330–332. P. 162–165.

99. M. Polanski, T.K. Nielsen, I. Kunce, M. Norek, T. Płociński, L.R. Jaroszewicz, C. Gundlach, T.R. Jensen J.B. et al. Mg 2 NiH 4 synthesis and decomposition reactions // Int. J. Hydrogen Energy. 2013. Vol. 8. P. 2–9.

100. Ao B. et al. Semiconducting ground-state of three polymorphs of Mg 2 NiH 4 from first-principles calculations // Int. J. Hydrogen Energy. Elsevier Ltd, 2013. Vol. 38, № 36. P. 16471–16476.

101. Haussermann U., Blomqvist H., Noréus D. Bonding and stability of the hydrogen storage material Mg2NiH4 // Inorg. Chem. 2002. Vol. 41, № 14. P. 3684–3692.